Conformal Symmetry in Topological States of Matter

Dottorando   **Tutori**

Dott. Maffi Lorenzo   Prof. Andrea Cappelli

Prof. Domenico Seminara

Coordinatore

Prof. Raffaello D'Alessandro

Overview

One of the main goals in the study of physical systems, is the understanding of their phases and their low-energy universal features. The different phases are characterized by properties such as a mass gap in the spectrum or a non-vanishing local order parameter. Their description is provided by quantum field theory thanks to spontaneous symmetry breaking and the renormalization group. In particular, the Landau-Ginzburg approach consists in identifying the global symmetries of the system, the local order parameter and the effective action. When the order parameter vanishes the symmetry is preserved, otherwise the symmetry is spontaneously broken. This approach is extremely useful in a large number of cases, from magnetic systems through superfluidity to particle physics.

In the eighties, new condensed matter systems were discovered whose properties are not explained by a local order parameter: the so called *Topological Phases of Matter*. These are many body states giving rise to fascinating macroscopic quantum phenomena. For example, the collective behaviour depends on the topology of space. This fact led to the introduction of a new kind of order, called *topological order*.

The best known example of a topological phase is the quantum Hall effect (QHE). A two-dimensional system of electrons subjected to a strong orthogonal magnetic field, and placed at very low temperatures, shows constant plateaus in the transverse conductivity σ_H, called Hall conductivity. This quantity takes very precise values in units of e^2/h that are independent of details of the sample and can be integer or fractional, corresponding to the integer and fractional QHE respectively. The electrons form a droplet of incompressible fluid with a gap for bulk excitations. In the integer case, the exact quantization of the Hall conductivity is formulated in terms of a topological invariant derived from the electron band theory. In the fractional case, the ground state is non-trivial, because it displays a finite degeneracy for topological non-trivial spaces, while the excitations possess fractional exchange statistics and fractional charge.

Furthermore, the quantum Hall states exhibit massless chiral excitations at the edge of the system. The existence of boundary dynamical degrees of freedom is a general aspect of topological states.

Recently many other topological phases of matter have been discovered; these are also gapped in the bulk and possess boundary excitations. A classification of topological phases in ten universality classes has been achieved for free electron (band) systems in any space dimensions. This follows from the analysis of general free-fermion quadratic Hamiltonians and their symmetry under time reversal and charge conjugation. Each class is characterized by a topological invariant integer number.

The present challenge is to understand topological states made by interacting electrons. In this case, the low-energy effective theory approach is again useful, but it involves new kinds of field theories. These are the topological gauge theories that do not have any local dynamics but reproduce the global properties of ground states. The gauge fields are physically interpreted as hydrodynamic degrees of freedom. In presence of boundaries,

massless bosonsic degrees of freedom arise at the edge and their dynamics is described by conformal invariant field theories (CFT). The relation between CFT and topological bulk is called *bulk-boundary correspondence.*

The aim of this thesis is to characterize topological phases of matter by looking at the properties of their boundary conformal theories. In many cases, this approach allows to discuss universal features of the bulk that are robust and independent of microscopic details.

Furthermore, the theoretical methods are facing the problem of bosonization, namely that of finding correspondences between two seemingly different approaches:

- that of fermionic theories and band structures leading to the ten-fold classification of non-interacting topological phases;

- that of bosonic theories, derived from the topological gauge theories.

In this thesis, we develop this analysis for two different topological phases: the quantum Hall state in $(2 + 1)$ dimensions and the time-reversal invariant topological insulators in $(3 + 1)$ dimensions.

In Chapter 1, we begin this thesis by reviewing the effective field theory description of the QHE. This involves the Chern-Simons theory, a topological gauge theory that accounts for the responses of the system, such as the Hall conductivity, and the fractional charge and statistics of anyonic excitations. In presence of a boundary, the Chern-Simons theory is not gauge invariant and needs additional massless degrees of freedom located at the boundary. These are described by a conformal field theory (CFT) in (1+1) dimensions, whose relation with the bulk theory is well established.

We review the edge theory of quantum Hall states, the compactified chiral boson. This theory describes the *bosonization* of free and interacting fermions in $(1 + 1)$ dimensions. Moreover, this chiral theory is affected by anomalies, i.e. classical symmetries broken by quantum effects. Actually, the Hall current is orthogonal to the edge and corresponds to the non-conservation of the boundary charge, i.e. the integral of the $(1 + 1)$-dimensional chiral anomaly. Being an universal quantity related to a topological invariant, the anomaly allows us to recover the exactness of the Hall current also in the interacting case.

One of the goals of this thesis is to understand the universality of other responses for quantum Hall states. These have been extensively investigated in the recent literature by adding the coupling to the background metric in the Chern-Simons theory, leading to the so called Wen-Zee action.

In this thesis we analyze the response involving the electron's 'intrinsic orbital spin' s that parameterizes the Hall viscosity of bulk incompressible fluids. Recently it was shown that in geometries with boundary, the Wen-Zee action does not correspond to any anomaly in the edge theory. This fact raises dubts on the universality of s and the Hall viscosity and it motivates a deeper analysis of the role of this parameter in the conformal theory at the edge.

In Chapter 2, we first build the theory of edge excitations for general integer Hall effect, by taking a straightforward limit of the microscopic states near the edge. Next we discuss the edge spectrum and show that the orbital spin causes a shift in the dispersion relation of excitations: this can be included in the Hamiltonian of the conformal theory, by

a redefinition of the chemical potential. For particular boundary conditions, we find non-vanishing ground-state values of the edge charge and conformal spin that are parameterized by the orbital spin, and are in agreement with the results of the bulk Wen-Zee action. We explain that these Casimir-like effects at the edge are indeed universal.

We also show how to generalize these results to fractional Hall states by using the symmetry of incompressible Hall fluids. Namely, we describe the edge excitations as deformations of the density by area preserving diffeomorphisms of the plane, the so-called W_∞ symmetry. Finally, we briefly discuss the possibility of measuring the values of the orbital spin by a tunneling experiment in the Coulomb blockade regime and by quadrupole deformations of the incompressible Hall fluid.

In Chapter 3, we investigate the time-reversal invariant topological insulators in $(3+1)$ dimensions. In free fermion systems, they are classified by a $\mathbb{Z}_2$ topological index. They have a bulk energy gap and surface states, consisting of one free massless Dirac fermions in $(2+1)$ dimensions. In the literature, systems like these are called *symmetry protected topological phases*, due to the central role played by symmetry. In particular, time-reversal symmetry forbids a mass for a Dirac fermions in $(2+1)$ dimensions, while pairs of fermions can become massive and disappear from the low-energy theory. The $\mathbb{Z}_2$ index is again related to an anomaly of the surface fermion, the so called parity anomaly in $(2+1)$ dimensions.

Recently, interacting three-dimensional topological insulators were also introduced and theoretically analyzed, showing that they possess fractional charge and vortex excitations. The final part of this thesis is dedicated to the effective field theory description of interacting topological insulators provided by the BF topological gauge theory. This is a time-reversal invariant theory depending on two hydrodynamic fields, describing particles and vortex excitations.

In presence of a boundary, an additional surface action should be introduced to compensate for the gauge non-invariance of the BF bulk theory, in analogy to what happens in the quantum Hall effect. We thus study the corresponding bosonic surface theory and the dynamics it can support, respecting time-reversal invariance.

First we discuss a quadratic non-conformal theory already known in literature. We review the canonical quantization and the calculation of the partition function. We find that this theory is not satisfactory because it does not reproduce the dynamics of free fermions described earlier for non-interacting topological insulators.

In our original work described in Chapter 4, we propose a non-trivial conformal dynamics for the bosonic surface degrees of freedom. This amounts to a non-local, scale invariant version of the Abelian gauge theory in $(2+1)$ dimensions, also called *loop model*. This theory has appeared in a number of recent research topics such as the duality transformations in $(2+1)$ dimensions. Dualities map different descriptions of the same system in terms of particles or vortices as well as bosonic versus fermionic degrees of freedom. The loop model provides a neat example of a calculable self-dual massless theory. Moreover, this model is equal to electrodynamics in mixed dimensions $(QED_{4,3})$, in the limit of large number of fermion fields $N_F \to \infty$.

The loop model gives a conformal field theory in $(2+1)$ dimensions possessing a critical line parameterized by the coupling constant g. Its solitonic excitations correspond to order-disorder fields with fermionic or anyonic statistical phases depending on the value of g.

These features remind of the compactified boson theory in $(1 + 1)$ dimensions and makes the loop model a good candidate for bosonization of free and interacting fermions in $(2+1)$ dimensions.

We thus quantize the loop model and obtain the spectrum of excitations at the surface of three-dimensional topological insulators. In order to solve the issue of non-locality, we reformulate the model as a higher dimensional local theory with excitations in $(2+1)$ and in $(3+1)$ dimensions. We consider two different boundary spatial geometries, the torus $\mathbb{T}^2$ and the sphere S^2, and we evaluate the partition function of the theory by considering both the solitonic and oscillating spectra. In the sphere case, the geometry is conformally flat and the Hamiltonian maps into the dilatation operator. Therefore, the solitonic energies determine the spectrum of conformal dimensions of the fields in the theory. Our expression of the partition function in this geometry explicitly confirms the conformal invariance and self-duality of the loop model. We also find that the spectrum of conformal fields reproduces the expected fractional statistics of bulk excitations.

Finally, in Chapter 5, we conclude the thesis by presenting some interesting open problems.

Summarizing, the Chapters 2 and 4 contain the original part of this thesis.

List of publications

This thesis is based on the following publications

[1] A. Cappelli, L. Maffi,
     "Bulk-Boundary Correspondence in the Quantum Hall Effect",
     J. Phys. A: Math. Theor. **51** (2018) 365401.

[2] F. Andreucci, A. Cappelli, L. Maffi,
     "Quantization of a Self-dual Conformal Theory in $(2+1)$ Dimensions",
     JHEP **02** (2020) 116.

[3] A. Cappelli, L. Maffi,
     "W_∞ Symmetry in Quantum Hall Effect beyond the Edge Approximation",
     in preparation.

Other publications not included in this thesis

[4] A. Cappelli, L. Maffi, S. Okuda
     "Critical Ising Model in varying Dimension by Conformal Bootstrap"
     JHEP **01** (2019) 161.

Contents

Chapter 1

Conformal Field Theories of the Quantum Hall Effect

In this chapter we will give an introduction to the quantum Hall effect (QHE). In particular, after showing the main features of this phenomenon, we will focus on the effective field theory description. The QHE is a system of electrons in a planar geometry which is characterized by a gapped insulating bulk and conducting massless degrees of freedom living at the boundary.

In the first two sections, we will see that the incompressible fluid effective picture due to Laughlin, and the effective topological Chern-Simons gauge theory, describe the bulk physics of the system. These approaches explain the quantization of the Hall conductivity and the existence of excitations with fractional charge and fractional statistics.

Then we will analyze the dynamics of the boundary modes by using conformal field theory methods. We will show that these excitations have two field theory descriptions, one fermionic and one bosonic that is inherited by the Chern-Simons theory. These are equivalent owing to the bosonization map in $(1 + 1)$ dimensions. Furthermore, we will see that a quantum anomaly arises in the edge theory, but this violation of symmetry is cancelled by the bulk response leading to the mechanism called anomaly inflow.

In the final part of this chapter, we will present other transport properties of the quantum Hall state, in particular focusing on the mechanical strain response which is parameterized by the so-called Hall viscosity. The corresponding effect in the edge theory has been clarified in our work [1] and will be presented in Chapter 2.

1.1   Integer and fractional QHE

The best known example of a topological phase of matter is given by the quantum Hall effect. A two-dimensional electron system is realized in a layered semiconductor, e.g. Gallium Arsenide, and subjected to an orthogonal magnetic field B. At very low temperatures ($T \sim 10$ mK) and high magnetic field ($B \sim 10$ Tesla), the transverse (Hall) conductivity, as function of the magnetic field, shows constant plateaus at the values:

$$\sigma_H = \nu \frac{e^2}{h} \qquad \nu = 1, 2, \ldots, \frac{1}{3}, \frac{2}{5}, \ldots, \tag{1.1}$$

where h is the Plank constant and the value of ν, called *filling fraction*, turns out to be an integer or rational number. At the same time the longitudinal conductance vanishes and the system is insulating in the bulk (see Fig. 1.1). At the beginning, only integer values were observed in the experiments, but later fractions were measured, among which the so called Laughlin sequence, $\nu = 1/p$ with p odd are prominent. For both integer and fractional QHE cases, experimental results display a remarkable high precision of order $\Delta\nu \sim 10^{-9}$ in the quantized values, independently of the sample details. As will be more clear in the following, this universality is due to the invariance of σ_H under continuous deformations of the system and the dynamics; we say that this quantity is topological.
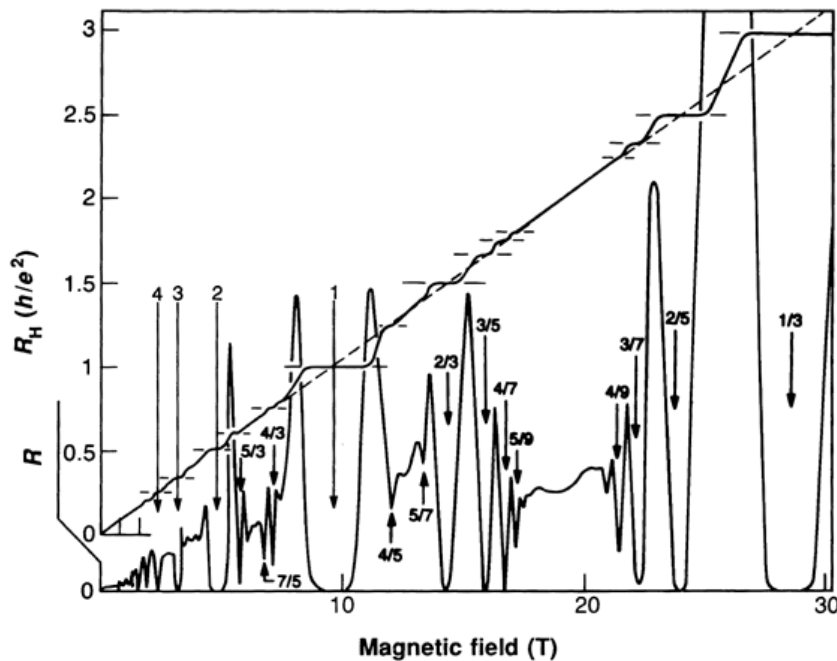
Figure 1.1: Longitudinal (R) and Hall (R_H) resistances as function of the applied magnetic field [5]. At the plateaus, the longitudinal and transverse conductivities, respectively σ_L and σ_H, obey to $\sigma_L = R = 0$ and $\sigma_H = 1/R_H$.

The main physical picture for the physics of the quantum Hall effect, due to Laughlin, is that the electrons form an incompressible quantum fluid, characterized by a constant density in the bulk and an energy gap that forbids density waves.

1.1.1 Integer Hall state: Landau levels

The Laughlin picture is easily understood in the integer case where the non-interacting electrons are organized in Landau levels. The gap between two consecutive levels is proportional to the cyclotron frequency $\omega_c = eB/Mc$, that is very large and higher than

thermal energies $k_B T$ (M the mass of the electron). Upon neglecting the Zeeman term for polarized electrons, the single particle Hamiltonian reads

$$\mathcal{H} = \frac{1}{2M}\left(\mathbf{p} - \frac{e}{c}\mathbf{A}\right)^2. \tag{1.2}$$

One can choose the symmetric gauge for the electromagnetic potential $\mathbf{A} = B/2(-y, x, 0)$. The Hamiltonian and the canonical angular momentum J can be easily rewritten in terms of two pairs of creation and annihilation operators $(a, a^\dagger)$ and $(b, b^\dagger)$, in the following way:

$$\mathcal{H} = \hbar\omega_c\left(a^\dagger a + \frac{1}{2}\right), \qquad J = \hbar\left(b^\dagger b - a^\dagger a\right), \tag{1.3}$$

satisfying the relations $[a, a^\dagger] = [b, b^\dagger] = \hbar$, while all the other commutators vanish. The single particle states are labelled by $|n, m\rangle$ where $n = 0, 1, \dots$ is the Landau level. Such states are degenerate with respect to the angular momentum $m = -n, -n+1, \dots$ as consequence of translation invariance of classical cyclotron orbits. The wave function $\psi_{n,m}(x, y)$ describes an electron in the n-th Landau level with angular momentum m and that is localized on the classical cyclotron orbit of radius $r_{n,m} = \ell_B\sqrt{n+m}$:

$$\psi_{n,m}(z, \bar{z}) = \frac{1}{\ell_B\sqrt{\pi}}\sqrt{\frac{n!}{(n+m)!}}\left(\frac{z}{\ell_B}\right)^m L_n^m\left(|z|^2/\ell_B^2\right)e^{-|z|^2/2\ell_B^2}, \tag{1.4}$$

where $z = x + iy$ and L_n^m are generalized Laguerre polynomials. The magnetic length $\ell_B = \sqrt{2\hbar c/eB}$ is the quantum unit of length: the cyclotron orbit encloses an integer number of quantum units of magnetic flux $\Phi_0 = B\pi\ell_B^2 = 2\pi$. In the following, we set units and constants $M = \hbar = c = e = \ell_B = 1$, which imply $\omega_c = B = 2$.

If the system lives on a disk of radius R, the angular momentum has an upper bound L corresponding to the largest orbit $r_{n,L} = R$. Thus, the degeneracy of each level is equal to the number of quantum fluxes passing through the disk: $N_d = BA/\Phi_0$ where A is the area of the disk. In order to realize an integer number n of filled Landau levels, the system should contain N electrons with $N = nN_d$. In this case, when the Fermi energy is placed between two subsequent Landau level the electrons cannot jump in the higher level due to the high energy gap $w_c \sim B$ and the system has vanishing longitudinal conductivity. Finally, by substituting the electron density $\rho = N/A$ in the classical Hall conductivity, i.e. $\sigma_H = \rho ec/B$, we get the relation (1.1) for the quantum Hall conductivity with $\nu = n$. Thus, a system of non-interacting electrons realizes the integer quantum Hall effect $\nu = n$ when the electrons fill an integer number n of Landau levels. The wave function Ψ is the Slater determinant of the single particle states (1.4). In particular, for $\nu = 1$, it takes the form of the Vandermonde determinant:

$$\Psi(z_1, z_2, \dots, z_N) = \prod_{i<j=1}^{N}(z_i - z_j)\,e^{-\sum_{i=1}^{N}|z_i|^2/2} \tag{1.5}$$

where z_i is the position[1] of the i-th electron in the lowest Landau level.

The second quantized Hamiltonian has the following form:

$$\hat{H} = \frac{1}{2}\int d^2x\,\left(D_i\hat{\Psi}\right)^\dagger\left(D_i\hat{\Psi}\right) + \int d^2x\,\hat{\Psi}^\dagger V_C(x)\,\hat{\Psi}, \tag{1.6}$$

---

[1]The coordinate z_i are dimensionless and expressed in unit of magnetic length ℓ_B.
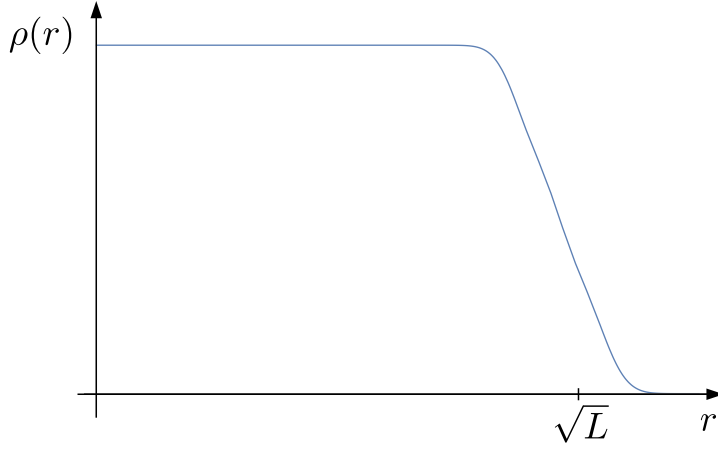
Figure 1.2: Density profile in a disk geometry of radius $R = \sqrt{L}$.

with $D_i = \partial_i + iA_i$ is the covariant derivative and $V_C(x)$ is a confining potential. In the lowest Landau level, the field operator $\hat{\Psi}$ can be written as a linear combination of single particle wave functions (1.4),

$$\Psi(\mathbf{x}, t) = \sum_{n=0}^{\infty} \sum_{m=0}^{\infty} \hat{c}_m \psi_{0,m}(\mathbf{x}) e^{-i\omega_c(n+1/2)t}. \tag{1.7}$$

The fermionic Fock space operators $\hat{c}_m$ satisfy the anticommutator relations

$$\{\hat{c}_m, \hat{c}_l\} = \delta_{m,l}, \tag{1.8}$$

while all the other anticommutators vanish. The ground state $|\Omega\rangle$ corresponding to filled lowest Landau level on the disk contains all the single particle states with angular momentum $0 \leq m \leq L = N - 1$,

$$|\Omega\rangle = \hat{c}_0^\dagger \hat{c}_1^\dagger \ldots \hat{c}_L^\dagger |0\rangle, \tag{1.9}$$

where $|0\rangle$ is the vacuum of the Fock space. The expectation value of the single particle density $\hat{\rho} = \hat{\Psi}^\dagger \hat{\Psi}$ is easily found to be

$$\langle\Omega| \hat{\rho}(r) |\Omega\rangle = \sum_{m=0}^{L} |\psi_{0,m}(x)|^2 = \frac{1}{\pi} e^{-r^2} \sum_{m=0}^{L} \frac{r^{2m}}{m!}. \tag{1.10}$$

This density has a constant profile in the bulk that rapidly drops to zero at the edge $r \sim \sqrt{L} = R$, see Fig. 1.2. The free electronic system is translational invariant and forms a fluid state. This is incompressible because transitions to higher Landau levels are suppressed for B large, as said. Finally the low lying excitations are described by the current that is different from zero only in the vicinity of the edge and longitudinal. This is the first hint about non-trivial dynamics at the edge of quantum Hall states.

1.1.2 Fractional Hall states: Laughlin wave-function

For fractional fillings, the free electron system is highly degenerate. This degeneracy is broken only by the interactions between particles, since the kinetic energy H in (1.2)

is simply a constant. Indeed, the incompressibility is due to the Coulomb interaction between electrons and the gap is a non-perturbative effect. This fact is confirmed by numerical simulations, but a microscopic description is still missing. Laughlin proposed a trial ground state wave function which describes very well the phenomenology of the sequence $\nu = 1/p$, with $p = 1, 3, 5, \ldots$:

$$\Psi(z_1, z_2, \ldots, z_N) = \prod_{i<j=1}^{N} (z_i - z_j)^p \, e^{-\sum_{i=1}^{N} z_i^2/2}. \tag{1.11}$$

Note, that p being odd, the antisimmetry under the exchange of two electronic coordinates z_i is satisfied. This wave function accurately approximates the numerical ground state for a large class of repulsive interactions. Haldane proposed a short-range potential for which the wave function (1.11) is the exact ground state.

Furthermore, the Laughlin probability distribution $|\Psi|^2$ can be interpreted as the classical Boltzmann distribution $\exp(-\beta V)$ of a two-dimensional Coulomb gas at temperature $\beta = 1/p$, with potential

$$V(\{z_i\}) = -p^2 \sum_{i<j}^{N_e} \ln|z_i - z_j|^2 + p \sum_{i=1}^{N_e} |z_i|^2. \tag{1.12}$$

This describes a system of particles of charge p in a uniform background with density $\rho_B = -1/\pi$. It is known that this plasma tends to form a neutral configuration with the background, realizing a uniform distribution. Therefore, the electrons form the fractional Hall state with constant density $\rho = 1/p\pi$.

Numerical and analytical analysis show that the charges in the plasma are dynamically screened (Debye screening) on length scales $\mathcal{O}(\ell_B)$. More precisely, this screening happens as long as the artificial temperature $\beta = 1/p$ is high enough that the plasma lies in the fluid phase and Debye screening can occur, namely when $p < \mathcal{O}(100)$. The screening provides an energy gap for excitations of the fluid which appear as 'holes' of dimension $\mathcal{O}(\ell_B)$ in the profile of the uniform density; the removed charge is fractional, $\Delta Q \sim \rho\pi\ell_B^2 = 1/p$. Furthermore, under an exchange of two identical excitations, the wave function acquires a phase $\Delta\theta = \pi/p$, which is different from bosonic, $\Delta\theta = 0$, or fermionic, $\Delta\theta = \pi$, statistics. These gapped excitations are called *anyons* and they have fractional charge and fractional quantum statistics [6, 7]. Indeed, fractional spin values are admitted in three space-time dimensions where, in general, unitary irreducible representations of spin group are labeled by a real number. The presence of these Aharonov-Bohm phases is related to global, topological properties hidden in the ground state that will be discussed in the following.

The fractional quantum Hall states are topological fluids made by strongly interacting electrons, that are different from standard crystals and liquids: they represent new states of matter that cannot be described by the Landau-Ginzburg effective theory and a local order parameter [8, 9, 10]. We shall see that one is led to introduce effective gauge field theories, that account for topological properties. For these reasons, these new states of matter were called *topologically ordered* by Wen [9].

The competing phase: the Wigner crystal

The Laughlin theory describes a liquid phase of electrons characterized by a kind of global order. There is a competing solid phase in which the electrons form a two-dimensional

triangular lattice, known as Wigner crystal. Before the discovery of the Quantum Hall effect, it was thought that this would be the preferred phase of electrons in high magnetic fields. Actually, the Wigner crystal does take place when electronic densities are low, for filling fractions $\nu < 1/7$.

Jain hierarchical states

Besides Laughlin's values $\nu = 1/p$, the most stable plateaus are observed at filling fractions $\nu = m/(2qm \pm 1)$, with m and q two positive integers. An attempt to find a systematic physical picture for all observed filling fractions is due to Jain and is called the composite fermion theory. The idea is that the fractional quantum Hall state $\nu \in \mathbb{Q}$, is essentially an integer quantum Hall state of composite particles, $\nu^* \in \mathbb{N}$. Such particles, called composite fermions, are made by attaching to each electron an even number $2q$ vortices carrying each a quantum unit of magnetic flux Φ_0. This composite states retain the fermionic character and leave a residual magnetic field $B^* = B - 2q\Phi_0\rho$ which realizes 'effective' Landau levels. Upon filling an integer number $\nu^* = m$ of such levels, the filling fraction becomes $\nu = \nu^*/(2q\nu^* + 1)$, known as Jain sequence, that reproduces the observed values.

However, the mechanism of flux-attachment is not explained by a microscopic theory, thus the Jain theory is another effective approach. Both Laughlin and Jain pictures can be easily obtained in the effective field theory framework, as we briefly present in the next sections.

1.2 Chern-Simons theory and Hall conductivity

We have seen that quantum Hall systems form states of incompressible quantum fluids that are characterized by universal and robust quantities; in such states, we expect that the physical properties can be deduced from general considerations of symmetries and conservation laws, that are independent of the detailed microscopic theory. It is then natural to formulate the problem in terms of the effective field theory for low-energy excitations. We shall show that this is given by the Chern-Simons (CS) gauge theory in $(2+1)$ dimension, a topological theory that cannot describe local dynamics but only global effects.

First of all we have to identify the effective degrees of freedom. The Hall electrons can be described by a conserved matter current j^μ, which, in $(2+1)$ dimensions, is dual to a gauge field a_μ,

$$j^\mu = \frac{1}{2\pi}\varepsilon^{\mu\nu\rho}\partial_\nu a_\rho, \tag{1.13}$$

where $\varepsilon^{\mu\nu\rho}$ is the completely antisymmetric tensor. Note that the continuity equation $\partial_\mu j^\mu = 0$ is satisfied. The $U(1)$ gauge field a_μ is said to be a hydrodynamic field, and its effective action should have the same global symmetries of the system. In $(2+1)$ dimensions, the Chern-Simons action,

$$S_{CS}[a] = -\frac{k}{4\pi}\int d^3x \, \varepsilon^{\mu\nu\rho}a_\mu\partial_\nu a_\rho. \tag{1.14}$$

is a $U(1)$ gauge theory which violates time-reversal and parity symmetries[2], just like in a quantum Hall state due to the presence of the external magnetic field. This action does not

---

[2]Note that in $d = 2+1$ dimensions the parity trasnformation is given by $x_0 \to x_0$; $x_1 \to -x_1$; $x_2 \to x_2$.

describe any local dynamics since it is independent of the metric tensor $g_{\mu\nu}$ and thus the Hamiltonian vanishes. Note that the usual Maxwell term would introduce dynamics but it contains two derivatives and is irrelevant in the low-energy limit. The coupling constant k in the Chern-Simons action takes integer values as will be explained later.

The electromagnetic response is described by adding to the Chern-Simons term a minimal coupling with the external electromagnetic field $j^\mu A_\mu$. The effective action becomes:

$$S_{eff}[a; A] = -\frac{k}{4\pi} \int_{\mathcal{M}} d^3x \, \varepsilon^{\mu\nu\rho} a_\mu \partial_\nu a_\rho + \frac{1}{2\pi} \int_{\mathcal{M}} d^3x \, A_\mu \varepsilon^{\mu\nu\rho} \partial_\nu a_\rho \tag{1.15}$$

Since a_μ appears quadratically in the effective action, it can be integrated out using the equations of motion. We obtain the induced action

$$S_{ind}[A] = \frac{1}{4\pi k} \int d^3x \, \varepsilon^{\mu\nu\rho} A_\mu \partial_\nu A_\rho. \tag{1.16}$$

By taking functional derivatives respect to A_μ, we get the induced current,

$$J^\mu = \frac{\delta S_{ind}[A]}{\delta A_\mu} = \frac{1}{2\pi k} \varepsilon^{\mu\nu\rho} \partial_\nu A_\rho, \tag{1.17}$$

from which one can easily read the quantized Hall conductivity (1.1):

$$\sigma_H = \frac{1}{2\pi k} \qquad \nu = 1/k, \tag{1.18}$$

corresponding to the Laughlin sequence.

The Chern-Simons theory also describes the existence of fractional charges in the system. The quasi-holes are the low-energy excitations of the incompressible fluid, whose world-lines can be represented by a set of currents $\mathcal{J}_\mu$, that couple to the hydrodynamic field a_μ. Including these sources, the effective action becomes:

$$S_{eff}[a; A, \mathcal{J}] = -\frac{k}{4\pi} \int d^3x \, \varepsilon^{\mu\nu\rho} a_\mu \partial_\nu a_\rho + \frac{1}{2\pi} \int d^3x \, \varepsilon^{\mu\nu\rho} A_\mu \partial_\nu a_\rho + \int d^3x \, \mathcal{J}^\mu a_\mu. \tag{1.19}$$

Integrating out the a-field, the induced action becomes

$$S_{ind}[A, \mathcal{J}] = \int d^3x \left(\frac{1}{4\pi k} \varepsilon^{\mu\nu\rho} A_\mu \partial_\nu A_\rho - \frac{1}{k} A_\mu \mathcal{J}^\mu - \frac{1}{4k} \int d^3y \, \mathcal{J}_\mu(x) \varepsilon^{\mu}{}_{\nu\rho} \frac{(x-y)_\nu}{\mid x-y \mid^3} \mathcal{J}_\rho(y) \right). \tag{1.20}$$

We can easily read the minimal fractional charge of quasi-holes $Q = -1/k$. Furthermore, the last term in (1.20) gives the winding number of quasi-holes and thus the fractional statistics. However, we can more easily show this effect from Hamiltonian formalism. In order to do that, we have to come back to the effective action (1.19) and consider $A_\mu = 0$. Taking a static source of quasi-holes $\mathcal{J}^\mu(x) = n\delta^{(2)}(x)\delta^{\mu 0}$, the equation of motion for a_μ,

$$\varepsilon^{0ij} \partial_i a_j = 2\pi \frac{n}{k} \delta^{(2)}(x) \tag{1.21}$$

shows that each excitation is equipped by n/k units of flux with respect to the field a_μ. Then the adiabatic process of carrying a quasi-hole around another one implies a non trivial Aharanov-Bohm phase:

$$\theta = 2\pi \frac{n_1 n_2}{k}, \tag{1.22}$$

where n_1 and n_2 are the charges respect to the a_μ field of the two excitations. For two identical particles $n_1 = n_2 = k$, with electromagnetic charge $Q = -1$, the exchange correspond to the statistical phase $\Delta\theta = \pi k$. If k is odd, such excitations are fermionic and can be identified with two electrons. Therefore, the integer k should take odd values. In conclusion, the Chern-Simons effective theory correctly describes Laughlin states with $\nu = 1/k = 1, 1/3, 1/5, \ldots$ and quasiparticles with fractional charge $Q_n = -n/k$ and fractional statistics $\Delta\theta_n = \pi n^2/k$.

1.2.1 Quantization of Chern-Simons theory on compact manifolds

Usually, at long distances, gapped systems become trivial, but topological phases are characterized by non-trivial gapped ground states with global effects, that are described by the Chern-Simons theory.

In order to see them, we consider the quantization of the topological theory on compact spatial manifolds, for instance on a torus $\mathbb{T}^2$. The quantum states are supposed to make up an Hilbert space which provides a representation of the algebra of quantum operators. In a gauge theory, the local gauge-invariant observables are polynomials in $f = da$ and its derivatives [3]. The equations of motion of the Chern-Simons theory (1.14)

$$S = -\frac{k}{4\pi} \int_{\mathbb{T}^2 \times \mathbb{R}} a\,da, \tag{1.23}$$

imply $f = 0$, thus there are no local gauge invariant classical observables. However, there are gauge invariant non local operators, the Wilson loops. In the case of the torus geometry, we have two non-trivial cycles γ_i with $i = 1, 2$, along which we construct operators

$$W^{(i)}[a] = \exp\left(i \oint_{\gamma_i} a\right). \tag{1.24}$$

A simple way to derive the algebra of Wilson loops is the following. In the $a_0 = 0$ gauge, the Chern-Simons action becomes

$$S = \frac{k}{4\pi} \int_{\mathbb{T}^2 \times \mathbb{R}} d^3x\, \varepsilon^{ij} a_i \partial_0 a_j\,, \qquad i, j = 1, 2\,. \tag{1.25}$$

Upon defining the holonomies

$$\bar{a}_1(x^0) = \oint_{\gamma_1} dx^1\, a_1(x^0, x^1), \qquad \bar{a}_2(x^0) = \oint_{\gamma_2} dx^2\, a_2(x^0, x^2), \tag{1.26}$$

the Chern-Simons action can be rewritten as

$$S = \frac{k}{4\pi} \int dx^0\, \bar{a}_1 \dot{\bar{a}}_2. \tag{1.27}$$

This is a problem of quantum mechanics with just the symplectic form in the action. The canonical commutation relations are given by

$$[\bar{a}_1, \bar{a}_2] = i\frac{2\pi}{k}, \tag{1.28}$$

---

[3]We are using the notation of differential forms, $a = a_\mu dx^\mu$ and d is the external derivative.

and by using the Baker-Campbell formula, we get the algebra for Wilson loops:

$$W^{(1)}W^{(2)} = W^{(2)}W^{(1)} \exp\left(-\frac{2\pi i}{k}\right). \tag{1.29}$$

Indeed, the algebra (1.29) describes the Aharonov-Bohm phases previously seen for anyons in (1.22) [7].

Now consider the expectation value of the Wilson operator for the loop $\gamma_1\gamma_2\gamma_1^{-1}\gamma_2^{-1}$ that can be shrunk to a point. On one side this should leave the ground state invariant, on the other side it amounts to the phase $\exp(-i2\pi/k)$. The solution is that the ground state is actually degenerate and the Wilson loop acts on this multiplet by a (necessarily finite) representation. Its minimal dimension is k, with k integer.

In conclusion, the ground state of the CS theory is k-fold degenerate on the torus geometry. The degeneracy extends to the k^g for a genus g Riemann surface. This argument also shows that the CS coupling constant k is integer.

One may think that a rational value of k would also realize a finite dimensional representation of the Wilson loop vevs. However, the Chern-Simons action is gauge invariant for integer k values only, due to the following argument. Suppose that the time direction is also periodic, i.e. the theory is defined on the compact space-time manifold $S^1 \times \mathbb{T}^2$, and evaluate the action for a spatial field configuration of a monopole of unit flux inside $\mathbb{T}^2$,

$$\oint_{\mathbb{T}^2} f = 2\pi. \tag{1.30}$$

Next, we consider a non-trivial time-dependent gauge transformation $\delta a_0 = \partial_0\Lambda$, $\delta a_i = 0$, with

$$\Lambda = 2\pi n\tau/\beta \qquad n \in \mathbb{Z}, \tag{1.31}$$

with τ the time coordinate with period β. This corresponds to non-trivial windings in the time direction that keep $e^{i\Lambda}$ periodic, The change in the action is non-vanishing:

$$\delta S_{CS} = -\frac{k}{2\pi}\left(\Lambda(\beta) - \Lambda(0)\right)\int_{\mathbb{T}^2} f = -kn2\pi. \tag{1.32}$$

This does not affect the phase $e^{iS_{CS}}$ in the path integral for integer values of k.

1.2.2 Multi-component theory

The effective theory just introduced in (1.15) is not able to describe other observed values of the filling fractions, most notably the Jain series $\nu = m/(2qm+1)$. It is necessary to consider a generalization involving m fluids, each branch being associated to an 'effective' Landau level of composite fermions. We consider m hydrodynamic fields, $a_{(i)}$, $i = 1,\ldots,m$, that are coupled by a general symmetric matrix $K_{(ij)}$. The effective action is:

$$S_{eff} = \frac{1}{4\pi}\int d^3x\, K_{(ij)}\varepsilon^{\mu\nu\rho}a_{(i)\mu}\partial_\nu a_{(j)\rho} + \frac{1}{2\pi}\int d^3x\, t_{(i)}\varepsilon^{\mu\nu\rho}A_\mu\partial_\nu a_{(i)\rho}, \tag{1.33}$$

where A_μ is the external electromagnetic field and $t_{(i)}$ is the electric charge of $a_{(i)\mu}$. In presence of a quasiparticle source of charges $l_{(i)}$ for $a_{(i)\mu}$, we read from the induced action
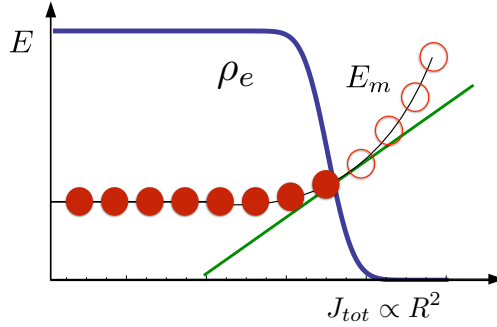
Figure 1.3: The confining potential modifies the Landau levels at the edge. The edge excitations (green line) are massless and chiral.

the filling fraction, the charge and statistics of the quasiparticle in terms of the parameters (K, t):

$$\nu = \sum_{i,j} t_{(i)} K_{(ij)}^{-1} t_{(j)}, \qquad Q = \sum_{i,j} t_{(i)} K_{(ij)}^{-1} l_{(j)} \quad \text{and} \quad \frac{\Delta\theta}{\pi} = \sum_{i,j} l_{(i)} K_{(ij)}^{-1} l_{(j)}. \qquad (1.34)$$

The analysis of fractional charges and statistics provided by these formulas implies that $t_{(i)}$ and $K_{(ij)}$ are integer-valued and that $K_{(ij)}^{-1}$ is the Gram matrix for the lattice of fractional statistics vectors $l_{(i)}$.

The Jain series are obtained by assuming m branches, or effective Landau levels as in the composite fermion picture. We also take the most symmetric form of $K_{(ij)}$, under exchanges of the fluids among themselves. This implies the expression

$$K_{ij} = \delta_{ij} + 2qC_{ij}, \qquad \text{with} \quad C_{ij} = 1 \; \forall i, j = 1, \dots, m, \qquad (1.35)$$

with electric charges normalized by $t_{(i)} = 1 \; \forall \; i$. Upon evaluating the expressions (1.34) for this K_{ij} one indeed obtains the filling fractions of the Jain series $\nu = m/(2qm + 1)$. The integer parameter $2q$ is again fixed by requiring the presence of electron excitations in the system with unit charge and fermionic statistics.

Although Jain theory has not been completely proven, analytic and numerical results confirm its predictions. The extensive phenomenology based on the composite fermion correspondence [11] between integer and hierarchical states let us argue that the structure of several branches is correct. The fractional charges of excitations (1.34) have also been confirmed experimentally [12, 13, 14],.

1.3 Edge States

In a finite geometry, like a disk or an annulus, the confining potential $V_C(|\mathbf{x}|)$ modifies the structure of Landau levels such that energy eigenvalues are not longer degenerate in angular momentum m, (see Fig. 1.3). Since the bulk is incompressible, a Fermi surface is

created at the boundary. We consider the QH system in the geometry of a spatial disk of radius R, whose boundary forms the space-time cylinder $\partial \mathcal{M} = S^1 \times \mathbb{R}$. The particle-hole excitations around such Fermi surface are massless and possess an approximate linear spectrum $E_{m'} \sim vm'/R$ with m' the rescaled boundary angular momentum $m = L + m'$, with $L = R^2$, as in Fig. 1.3. These excitations are chiral [15], i.e. propagate on the edge in one direction only, with velocity v. Furthermore, due to the bulk incompressibility, a quasi-hole excitation implies the transport of charge at the boundary, namely the formation of a charged edge excitation. Then the study of the boundary physics allows us to analyze both neutral particle-hole and charged excitations.

The edge dynamics is provided by the conformal field theory (CFT) of Weyl fermions. The low-energy approximation for excitations near the boundary can be carried out explicitly for the quantities of the second-quantized theory of electron in lowest Landau level [16]. The field operator $\hat{\Psi}$ reduces at the edge $z = Re^{i\theta}$ to the Weyl fermion field in the CFT, as follows

$$\hat{\Psi}\left(Re^{i\theta}, t\right) \sim \mathcal{N} e^{i(L+\mu)\theta} \hat{F}_R\left(\theta, t\right), \tag{1.36}$$

where $\mathcal{N}$ is a normalization constant and μ the chemical potential as explained later. In the thermodynamic limit $R \to \infty$ the dependence on the radial coordinate in $\mathcal{N}$ can be neglected, the momentum is rescaled $m \to L + m$, $m \leq \sqrt{L}$, and the energy can be linearized as previously said. It is then useful to redefine a fermionic Fock operator, $\hat{b}_m = \hat{c}_{m+L}$. The field operator reads

$$\hat{F}_R\left(\theta, t\right) = \sum_{m=-\infty}^{\infty} \frac{\hat{b}_m}{\sqrt{2\pi R}} \exp\left[i\left(m - \mu\right)\left(\theta - vt/R\right)\right], \tag{1.37}$$

and the second quantized hamiltonian

$$\hat{H}_R = \frac{v}{2} \int_0^{2\pi R} dx\, \hat{F}_R^\dagger\left(-i\partial_\theta\right) \hat{F}_R + \text{h.c.}, \tag{1.38}$$

define the non interacting $(1+1)$-d CFT of a Weyl fermion on the cylinder $S^1 \times \mathbb{R}$ with coordinates $(x = R\theta, t)$. Upon applying a Wick rotation to euclidean time $\tau = it$ and mapping the cylinder to the plane via the conformal map $\eta = e^{w/R}$ with $w = (v\tau - iR\theta)$, one can easily construct the following conformal generator L_n and current modes ρ_n [16],

$$L_n \equiv \frac{R}{iv} \oint d\eta\, \mathcal{H}_R\left(\eta\right) \eta^n = \sum_{k=-\infty}^{\infty} \left(k - \frac{n}{2} - \mu\right) : b_{k-n}^\dagger b_k :, \tag{1.39}$$

$$\rho_n \equiv \frac{R}{i} \oint d\eta\, \rho_R\left(\eta\right) \eta^{n-1} = \sum_{k=-\infty}^{\infty} : b_{k-n}^\dagger b_k :, \tag{1.40}$$

where we removed the hats on operators and $\mathcal{H}_R$ and ρ_R are the edge Hamiltonian density and particle density, respectively. The normal ordering : () : subtracts the infinite contribution of the filled Dirac sea given by the incompressible ground state in (1.9). Let us conventionally fill the sea up to the $k = 0$ state [16], i.e. define the conformal theory ground-state by the conditions:

$$b_k|\Omega, \mu\rangle = 0, \qquad k > 0,$$
$$b_k^\dagger|\Omega, \mu\rangle = 0, \qquad k \leq 0. \tag{1.41}$$

11

Thus, the normal ordering is defined by putting b_k to the right of $b_k^\dagger$ for $k > 0$ and viceversa for $k \leq 0$.

The modes ρ_n and L_n satisfy the following algebra

$$
\begin{aligned}
[\rho_n, \rho_m] &= n\delta_{n+m,0}\,, \\
[L_n, \rho_m] &= -m\rho_{n+m,0}\,, \\
[L_n, L_m] &= (n-m)L_{n+m,0} + \frac{1}{12}c(n^3 - n)\delta_{n+m,0}\,, \qquad c = 1\,.
\end{aligned}
\tag{1.42}
$$

The first relation is the $U(1)$ Kac-Moody algebra (current algebra) for the generators ρ_n; the third expression is the Virasoro algebra for the generators L_n of local conformal transformations. As is well known in the CFT literature [17, 18], the $c-$number term in the right-hand side of the last equation, comes from the conformal anomaly and defines the central charge c, that takes the value $c = 1$ for Weyl fermions. Finally, we can easily see from the first two relations in (1.42) that the oscillators ρ_{-n} with $n > 0$ create neutral edge excitations with momentum n/R.

As shown in Ref.[16], the chemical potential μ in the expression (1.39) plays a double role. First, it determines the boundary conditions of the Weyl fermion (1.37) on the edge, i.e. $\Psi(\theta = 2\pi) = \exp(i2\pi\mu)\Psi(0)$, distinguishing the Neveu-Schwarz sector ($\mu = 1/2 + \mathbb{Z}$) from the Ramond sector ($\mu = \mathbb{Z}$). Next, it parameterizes the ground-state expectation values, as follows:

$$
L_n \left|\Omega, \mu\right\rangle = \rho_n \left|\Omega, \mu\right\rangle = 0, \qquad n > 0,
\tag{1.43}
$$

$$
L_0 \left|\Omega, \mu\right\rangle = \frac{1}{2}\left(\frac{1}{2} - \mu\right)^2 \left|\Omega, \mu\right\rangle,
\tag{1.44}
$$

$$
\rho_0 \left|\Omega, \mu\right\rangle = \left(\frac{1}{2} - \mu\right) \left|\Omega, \mu\right\rangle.
\tag{1.45}
$$

These values of charge and Virasoro dimension amount to finite renormalization constants that should be added to the definitions of L_0 and ρ_0 in (1.39, 1.40). The two values are related among themselves by the current algebra (1.42), and can actually be computed by checking the commutation relations on the expectation values $\left\langle\Omega, \mu\right| L_n L_{-n} \left|\Omega, \mu\right\rangle$ and $\left\langle\Omega, \mu\right| L_n \rho_{-n} \left|\Omega, \mu\right\rangle$ [17].

Let us remark that the derivation of the edge CFT presented in this section requires some modifications in the case of higher filled Landau levels: these are described in our original work [1] presented in the next Chapter.

1.3.1 Anomaly Inflow

In the previous sections the Hall conductivity was obtained as a bulk transport coefficient by using the Chern-Simons action. In the edge theory, the Hall current follows from another crucial property: the existence of a chiral anomaly [19]. In the fermionic theory discussed in the previous section, the coupling to an electromagnetic field leads, via the Heisenberg equation of motion to the following result:

$$
\left(\partial_t + v\partial_x\right)\rho_R = \frac{1}{2\pi}E_x,
\tag{1.46}
$$

where E_x is the electric field along the edge coordinate $x = R\theta$. This implies that the classical conservation law of the charge $Q = \int dx\, \rho_R$ is violated. Charge non-conservation however is not possible in the whole system, that is made of non-relativistic electrons. The solution to this puzzle is that the bulk transverse current, the Hall current, cancels the edge anomaly by transporting charges from a boundary to the other, as in Fig. 1.4. The mechanism by which an anomaly is cancelled by a classical effect in a higher-dimensional theory is called anomaly inflow [20].

We can integrate the anomaly equation (1.46) in time to obtain the adiabatic charge accumulation at the edge:

$$Q\left(t=\infty\right) - Q\left(t=-\infty\right) = \frac{1}{2\pi}\int d^2x\, E_x = \frac{1}{2\pi}\int_{\partial\mathcal{M}}\mathcal{F} = n, \qquad (1.47)$$

where $\mathcal{F}$ is the $(1+1)$-dimensional two-form field strength. The equation (1.47) relates the accumulated charge to the first Chern class, $1/2\pi\int\mathcal{F} = n$, that is an integer topological number. Namely it is independent of continuous deformations of the geometry of the sample and of the background fields. In $(1+1)$-dimensional relativistic theory, the result (1.47) is called the index theorem of the Dirac operator [21]. It is an exact result. The edge chiral anomaly therefore reproduces the robustness and the quantization of the Hall conductivity given by the ratio between the transported charge and the number of fluxes injected.

Let us note that, as previously said, the universality of the quantum Hall conductivity was originally obtained by the Kubo formula of the linear response theory in [22]. Thouless et al. showed that the Hall conductivity is related to the Berry phase. This is defined on the toroidal space of the first Brilluoin zone, and it does not depend on short range interactions, namely it is a topological invariant. However, in this Thesis, we use a quantum field theory approach to explain this robustness. The main motivation will be more clear when we extend the argument for fractional fillings where the Thouless argument based on free band theory, is not applicable.

Furthermore, the connection between the edge anomaly and the bulk Hall conductivity is the first ingredient needed to build a bulk-boundary correspondence for the electromagnetic response in the quantum Hall states. We are going to analyze such a correspondence in more details in the next section.

The anomaly inflow mechanism is actually equivalent to the Laughlin's flux insertion argument [23] used to explain the charge transport from the inner to the outer edge in the annulus geometry, as shown in Fig. 1.4. The adiabatic insertion of a quantum unit of magnetic flux $\Phi_0 = 2\pi$ in the system induces a Faraday electric field $d\Phi/dt$ going around the annulus, which in turn generates a radial Hall current $I = \sigma_H d\Phi/dt$. When $\Phi = \Phi_0$, the vector potential can be elimated by a gauge transformation, so the Hamiltonian has returned to its original form at $\Phi = 0$. Although the spectrum does not change, states drift one into the next, leading to the so called spectral flow and the quantization of the transferred charge.

In the Laughlin fractional Hall state $\nu = 1/k$ we expect to transport a particle of charge $-1/k$ from an edge to the other. This means that the resulting Hall conductivity is $\sigma_H = 1/2\pi k$, as experimentally observed. In the next section, this result will be easily found in the effective field theory approach thanks to the exact bi-dimensional bosonization.
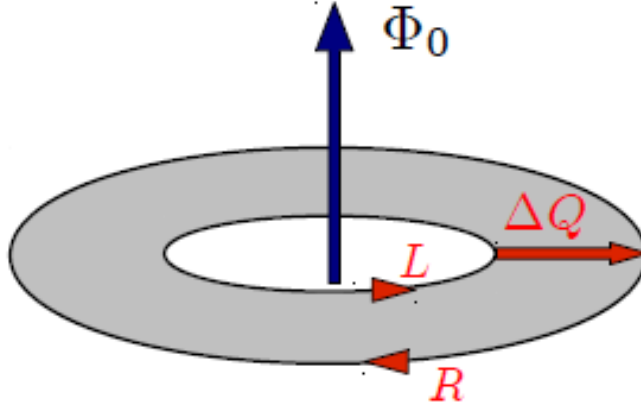
Figure 1.4: Laughlin's flux argument: the insertion of a quantum of flux Φ_0 inside the annulus moves a charge ΔQ from the inner to the outer edge.

1.4 Bulk-boundary correspondence

In the fractional case, the bulk theory is interacting, thus the edge Weyl fermions also acquire an interaction. In $(1+1)$ dimensions this problem can be solved by the bosonization tecnique, by which interacting fermions can be exactly mapped to a solvable yet non-trivial theory of bosons. The existence of the bosonic description can be explained by using the Chern-Simons effective field theory, and the connection between bulk and boundary [9, 24], as follows.

We consider the QH system in the geometry of a spatial disk of radius R as in the previous section. In such a geometry, the CS action (1.15) is no more gauge invariant: the gauge transformation $a \to a + d\Lambda$ gives the following term

$$S_{CS}[a] \to S_{CS}[a] - \frac{k}{4\pi} \int_{\partial\mathcal{M}} dt dx \, \Lambda \left(\partial_t a_x - \partial_x a_t \right), \tag{1.48}$$

where $x = R\theta$ is the coordinate along the boundary of the disk. If we want to preserve the gauge invariance, we need to restrict the gauge transformation Λ such that it vanishes at the boundary, $\Lambda\left(r = R\right) = 0$. However, this choice is not physically acceptable because we saw that there are propagating edge excitations which carry charge. We should then introduce an action for the edge dynamics whose gauge transformation cancels the term (1.48) [9, 19]. One method to obtain the edge theory is the following.

In the $a_0 = 0$ gauge, the CS equations of motion gives $a_i = \partial_i \varphi$. The action becomes a boundary symplectic term:

$$S_{edge} = -\frac{k}{4\pi} \int_{\partial\mathcal{M}} d^2x \, \partial_x \varphi \partial_t \varphi. \tag{1.49}$$

This action has vanishing Hamiltonian, being the reduction of a topological theory. The simplest Hamiltonian we can add is quadratic and of the form $H = +\frac{k}{4\pi} v \partial_x \varphi \partial_x \varphi$. We obtain the following action in $(1+1)$-dimensions

$$S_{edge} = -\frac{k}{4\pi} \int_C d^2x \, \partial_x \varphi \left(\partial_t \varphi - v \partial_x \varphi \right), \tag{1.50}$$

14

which is the chiral boson theory, first discussed by Floreanini-Jackiw [25]. The equation of motion,

$$(\partial_t + \partial_x)\,\partial_x\varphi = 0, \tag{1.51}$$

shows that the field is indeed chiral (we fix the velocity $v = 1$). The gauge invariance of the complete system, $\delta S_{CS} + \delta S_{edge} = 0$ is finally restored by transforming $\varphi \to \varphi + \Lambda$ and fixing the boundary gauge condition $a_0 = 0$.

We can summarize the argument by saying that gauge degrees of freedom become dynamical at the edge. This is the bulk-boundary correspondence: the universal physics of the bulk, including the electromagnetic response, is coded in the edge theory.

1.4.1 Conformal theory of compactified chiral boson

There is one important property of the scalar field φ that we haven't mentioned yet: it's periodic. Actually the $U(1)$ gauge field is compact,

$$g \in U(1)\,, \qquad g = e^{-i\varphi}\,, \qquad a_\mu \to a_\mu + ig^{-1}\partial_\mu g\,, \tag{1.52}$$

thus, the field φ is a periodic variable with period 2π. Let us first consider the more general periodicity

$$\varphi(\theta, t) \equiv \varphi(\theta, t) + 2\pi nr, \quad n \in \mathbb{Z}. \tag{1.53}$$

The field $\varphi(\theta)$ maps the edge circle into another circle with radius r, and is called compactified boson. Upon rescaling the time coordinate $t \to Rt$, the equation of motion for the edge action becomes,

$$(\partial_t + \partial_\theta)\,\partial_\theta\varphi = 0. \tag{1.54}$$

The field expansion

$$\varphi(\theta, t) = \varphi_0 - \alpha_0\,(\theta - t) + i\sum_{k \neq 0}\frac{\alpha_k}{k}\exp\left(ik\,(\theta - t)\right), \tag{1.55}$$

solves the equations of motion (1.54), with $\alpha_k^* = \alpha_{-k}$ and $\varphi_0 \equiv \varphi_0 + 2\pi r$ to satisfy (1.53). Note that the field expansion contains both solitonic modes (φ_0, α_0) and oscillating terms. Imposing canonical commutation relations on the field and its momentum $\Pi(\theta, t) = \delta\mathcal{L}/\delta\dot{\phi} = -p/4\pi\partial_\theta\varphi$, [25, 16] [4]

$$\left[\varphi(\theta, t), \Pi(\theta', t)\right] = \frac{i}{2}\delta(\theta - \theta'), \tag{1.56}$$

we infer the following commutation relations of the modes,

$$[\varphi_0, \alpha_0] = \frac{i}{k}, \quad [\alpha_n, \alpha_m] = \frac{n}{k}\delta_{n+m,0}. \tag{1.57}$$

Upon quantization, the coefficients φ_0, α_0 and α_n become operators acting on a bosonic Fock space, whose ground state $|\Omega\rangle$ is defined as

$$\alpha_n\,|\Omega\rangle = 0, \quad n > 0. \tag{1.58}$$

In the previous section, we saw that the Weyl fermion corresponds to a conformal theory with central charge $c = 1$. Now we will show that also the chiral boson possesses

---

[4]The factor of $1/2$ is explained in [16]

$c = 1$ and then, furthermore, it is able to describe the edge states at both integer and fractional values of ν. First of all, we define Virasoro operators as:

$$L_0 \equiv \frac{k}{2}\alpha_0^2 + k\sum_{l=1}^{\infty}\alpha_{-l}\alpha_l,$$

$$L_n \equiv \frac{k}{2}\sum_{l=-\infty}^{\infty}\alpha_{n-l}\alpha_l. \tag{1.59}$$

By using the commutation relations (1.57) paying attention to the necessary normal ordering, one obtains the current algebra [16]:

$$[\alpha_n, \alpha_m] = \frac{n}{k}\delta_{n+m,0}, \tag{1.60}$$

$$[L_n, \alpha_m] = -m\alpha_{n+m}, \tag{1.61}$$

$$[L_n, L_m] = (n-m)L_{n+m} + \frac{c}{12}n(n^2-1)\delta_{n+m,0}, \qquad c = 1. \tag{1.62}$$

The states of the conformal theory are described by representations of this algebra: the free fermionic theory (1.42) will be later obtained in the special case $k = 1$.

Since φ_0 is periodic $2\pi r$, and φ_0 and $k\alpha_0$ are canonically conjugate, we should require

$$k\alpha_0 = \frac{m}{r}, \qquad m \in \mathbb{Z}. \tag{1.63}$$

Altogether, we obtain two periodicities

$$\varphi(2\pi, t) = \varphi(0, t) + 2\pi r\left(n + \frac{m}{kr^2}\right), \qquad n, m \in \mathbb{Z}, \tag{1.64}$$

whose commensurability requires kr^2 to take rational values, $kr^2 = p/q$, with p and q coprime integers [16].

A further physical condition comes from the requirement that $S_{edge}[\varphi]$ should reproduce the bulk fractional charged excitations. The edge charge is the integral of the edge current $j_0 = -\frac{1}{2\pi}\partial_\theta\varphi$ that is obtained by the bulk expression using (1.13) as follows,

$$Q = \int_{D^2} d^2x\, j^0 = -\frac{1}{2\pi}\int_{S^1} d\theta\, a_\theta = -\frac{1}{2\pi}\left(\varphi(2\pi) - \varphi(0)\right) = \alpha_0. \tag{1.65}$$

The spectrum (1.63) reproduces the Laughlin quasiparticles charges for $r = 1$, as expected from (1.52). Fractional charge excitations $Q = m/k$ in the bulk correspond to edge states $|\alpha_0 = m/k\rangle$, such that

$$\alpha_0\,|\alpha_0 = m/k\rangle = \frac{m}{k}\,|\alpha_0 = m/k\rangle, \qquad m \in \mathbb{Z}. \tag{1.66}$$

This is another aspect of the bulk-boundary correspondence: an anyonic bulk charge corresponds to a solitonic mode α_0 in the chiral edge theory. The corresponding conformal dimensions are given by eigenvalues of L_0,

$$L_0\,|\alpha_0 = \frac{m}{k}\rangle = h_m\,|\alpha_0 = \frac{m}{k}\rangle, \qquad h_m = \frac{m^2}{2k}. \tag{1.67}$$

Note that more general quantizations with $r \neq 1$ would not be consistent with the derivation (1.48-1.50) from Chern-Simons theory.

In the conformal field theory, the eigenstate of α_0 is called highest weight state, i.e. the ground state in a solitonic sector, that satisfies $\alpha_n |\alpha_0\rangle = 0$, for $n > 0$. On the other hand, the oscillators α_{-n} with $n > 0$ create neutral excitations leading to the complete tower of conformal descendant states with conformal dimensions $h_n = m^2/k + n$.

Furthermore, the state $|\alpha_0\rangle$ is created by the so-called vertex operator,

$$V_m(z) =: \exp\left(i\frac{m}{k}\varphi(z)\right): \qquad z = \exp(v\tau + i\theta), \tag{1.68}$$

which satisfy the following commutation relations

$$[L_0, V_m(z)] = \left(z\frac{\partial}{\partial z} + \frac{m^2}{2k}\right) V_m(z), \tag{1.69}$$

$$[\alpha_0, V_m(z)] = \frac{m}{k} V_m(z). \tag{1.70}$$

This algebra shows that the vertex operators $V_m(z)$, $m > 0$, describe the insertion at point z on the boundary of a charged excitation with fractional charge $Q_m = m/k$ and conformal dimension $h_m = m^2/2k$. Moreover, the operator product expansion (OPE) of two vertex operators is [17, 18, 26]

$$\lim_{z_1 \to z_2} V_{m_1}(z_1)V_{m_2}(z_2) \simeq (z_1 - z_2)^{m_1 m_2/k} V_{m_1+m_2}(z_2). \tag{1.71}$$

One can easily see that this phase gives the right value of the fractional statistics θ/π that is identified with the conformal dimensions $2h_m$ [16].

These results are in agreement with those obtained from the bulk effective action, i.e. Eq.(1.22). Therefore the number of bulk anyonic charges, namely the degeneracy of the quantum ground state on the torus, coincides with the number of solitonic sectors in the edge theory. Because k is odd, the spectrum always allows the excitation V_k with the quantum numbers $Q = 1$ and $\theta_n = 2\pi k$, that is the electron. In the following, we shall also prove that the Hall current of the bosonic theory is $\sigma_H = 1/2\pi k$. Therefore this theory describes the long-range universal properties at the boundary of the Laughlin series.

We now compute the euclidean grand-canonical partition function of edge excitations: the space circle and the euclidean time period β realize the geometry of a torus (see Fig. 1.5). Owing to the knowledge of the spectrum of edge excitations, (1.66) and (1.67), the trace on the Hilbert space can be decomposed into orthogonal solitonic sectors $\mathcal{H}^{(\lambda)}$, corresponding to the basic anyons plus any number of electrons [27]. There are k sectors, for $\lambda = 1, \ldots, k$, which contains representations with charges $Q_n = \lambda/k + n$ of the $\hat{U}(1)$ current algebra of the $c = 1$ CFT. The partition function for each sector takes the following form [27]:

$$\begin{aligned}
K_\lambda(\tau, \zeta; k) &= \mathrm{Tr}_{\mathcal{H}^{(\lambda)}}[\exp\left(i2\pi\tau L_0 + i2\pi\zeta Q\right)] \\
&= \frac{F(\mathrm{Im}\tau, \mathrm{Im}\zeta)}{\eta(\tau)} \sum_{n\in\mathbb{Z}} \exp\left(i2\pi\left(\tau\frac{(nk+\lambda)^2}{2k} + \zeta\frac{nk+\lambda}{k}\right)\right),
\end{aligned} \tag{1.72}$$

where $\eta(\tau)$ is the Dedekind function

$$\eta(\tau) = q^{1/24} \prod_{n=1}^{\infty} (1 - q^n), \qquad \text{with} \quad q = \exp(2\pi i\tau), \tag{1.73}$$
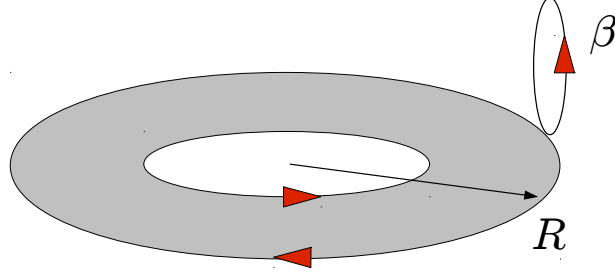
Figure 1.5: In the space annulus geometry, each edge is given by a torus once we compactified the imaginary time with period β. We consider the outer edge geometry given by a torus of periods $(2\pi R, \beta)$.

and $F(\text{Im}\,\tau, \text{Im}\,\zeta)$ is a pre-factor explained in [27]. The function K_λ is parameterized by the two complex numbers,

$$\tau = \frac{i\beta}{2\pi R} + l/R, \qquad \zeta = \frac{\beta}{2\pi}(iV_o + \mu), \tag{1.74}$$

that are the modular parameter τ and the 'coordinate' ζ. $\text{Im}\,\tau > 0$ is related to the euclidean time period β, while $\text{Re}\,\tau$ is the parameter conjugate to momentum P corresponding to a spatial twist added in the temporal boundary conditions; ζ contains V_o and μ, respectively the electric and chemical potentials. These functions K_λ have the periodicity $K_{\lambda+k} = K_\lambda$, corresponding to the k anyon sectors [27].

Let us mention that the same bosonic CFT theory can also be applied to describe bulk wave functions in two spatial dimensions [10]. Indeed, the Laughlin wave function (1.11) is basically the same expression as the $N-$point correlator of vertex operators $V_p(z)$ for electrons (1.68), now located at the points $z = x + iy$ of the plane [28]. The description of quasi-hole and quasiparticle wave functions requires some modifications of the conformal fields that are described in the works [29, 30]. This different use of CFT techniques will not be developed in this thesis.

1.4.2 The free fermion theory: bosonization in $(1+1)$ dimensions

Let us now recall the equivalence between the compactified boson with $k = 1$ and the Weyl fermion. This is the bosonization in $(1+1)$ dimensions, an exact map between two theories, that gives to two descriptions of the same Hilbert space of states [31]. The two theories have the same conformal charge $c = 1$ and satisfy the same chiral algebra (1.42). The bosonic vertex operators represent the fermion fields ψ and $\psi^\dagger$ as follows:

$$\psi(\theta, t) = V_{-1} =: \exp(-i\varphi(\theta, t)) :, \qquad \psi^\dagger(\theta, t) = V_1 =: \exp(i\varphi(\theta, t)) : . \tag{1.75}$$

18

Indeed, these fields satisfy the usual anti-commutation relations [31]:

$$\left\{\psi(\theta,t),\psi(\theta',t)\right\} = \left\{\psi^\dagger(\theta,t),\psi^\dagger(\theta',t)\right\} = 0, \tag{1.76}$$

$$\left\{\psi(\theta,t),\psi^\dagger(\theta',t)\right\} = 2\pi\delta(\theta-\theta'). \tag{1.77}$$

The fermionic charge density $\rho =: \psi^\dagger\psi :$ can be accordingly expressed in terms of the bosonic field as

$$\rho = -\frac{1}{2\pi R}\partial_\theta\varphi, \tag{1.78}$$

which implies the mapping $\rho_n = \alpha_n$ among the modes of the fields. In particular, the total charge ρ_0 is represented in the bosonic theory by α_0, in agreement with the previous results (1.66).

Thanks to this identification, one can couple the chiral boson to the electromagnetic field by adding the following term to the Floreanini-Jackiw action (1.50),

$$S_{int} = \frac{1}{2\pi}\int_{\partial\mathcal{M}} d^2x \left(A_t\partial_x\varphi - A_x\partial_t\varphi\right). \tag{1.79}$$

In such way the equations of motion become:

$$(\partial_t + \partial_x)\left(-\frac{1}{2\pi}\partial_x\varphi\right) = \frac{1}{2\pi k}E_x, \tag{1.80}$$

which generalizes to $k > 1$ the chiral anomaly equation (1.46). This proves that the Hall conductivity is $\sigma_H = 1/2\pi k$.

In conclusion, the chiral boson theory displays the chiral anomaly and generalizes the anomaly inflow mechanism to fractional fillings. It is rather remarkable that the robustness of the quantization of the Hall current and the universality of fractional charge and statistics can be proven in free and interacting systems by using the effective field theory approach and exact bosonization.

1.5   Other transport properties: geometric responses

The Hall states possess other interesting responses beyond the transport of electromagnetic charge as, for instance, heat transport or the response of the incompressible fluid under mechanical strain. Such phenomena can be effectively described through the coupling of the low energy degrees of freedom to a spatial background metric. Gravitational field in condensed matter systems can be understood either as a way to represent deformational strains in the material, or as a technical tool allowing to compute correlation functions of the stress tensor describing matter (heat) current.

In elasticty theory [32], deformations of a continuum system are parametrized by the displacement field $u_i(x) = x_i'(x) - x_i$, expressing the dislocation of each point of the sample. So we have a new line element

$$dl^2 = dx_i dx_j \left(\delta_{ij} + \partial_{(i}u_{j)} + \partial_i u_k \partial_j u_k\right). \tag{1.81}$$

By neglecting the quadratic term, the deformation has the same form of a diffeomorphism of the flat metric $g_{ij} = \delta_{ij}$. Therefore the response under mechanical strain can be described

by introducing a spatial external metric coupled to the physical degrees of freedom, in our case the hydrodynamic field a_μ. Naturally, we observe physical effects that are not invariant under diffeomorphisms because we are not dealing with general relativity.

The geometric response [33] of quantum Hall states has been extensively investigated in the recent literature [34, 35]. The low-energy effective action has been extended by coupling to a background metric, leading to the Wen-Zee terms [36, 37, 38]. Other methods have also been developed, such as explicit wave-function constructions [39, 40, 41], hydrodynamic theory [42, 43], the W_∞ symmetry [44], and bi-metric theories [45, 46].

1.5.1 Fröhlich-Wen-Zee action

The coupling of the Chern-Simons action to a gravitational background has been introduced by Fröhlich and collaborators [47] and by Wen and Zee [36]. In order to find its form, we exploit the canonical coupling between a spinor and gravity. In the relativistic $(2 + 1)$-dimensional Dirac equation, this is given by the term

$$\Delta\mathcal{L} = \omega_\mu^{ab}\bar{\psi}\gamma^\mu\frac{1}{4}\left[\gamma_a, \gamma_b\right]\psi, \qquad a, b = 0, 1, 2, \tag{1.82}$$

where ω_μ^{ab} is the spin connection that can be expressed in terms of the vielbein e_μ^{a}[5]. In the non-relativistic limit we consider just a spatial metric $g_{ij} = g_{ij}(\mathbf{x}, t)$. This reduces the local Lorentz symmetry to the rotation in the plane $O(2)$ with abelian connection $\omega_\mu = \varepsilon_{012}\omega_\mu^{12}$. Therefore the interaction (1.82) takes the form of another Abelian background, i.e. $\omega_\mu\bar{\psi}\gamma^\mu\psi$. This suggests to add the gravity background to the effective theory (1.15) as follows:

$$j^\mu A_\mu \to j^\mu\left(A_\mu + s\omega_\mu\right), \tag{1.83}$$

where the coupling constant s is interpreted as the 'intrinsic orbital spin' of the energy excitations.

In full generality, we will consider the multicomponent case (1.33), using the notation of forms, i.e. $a = a_\mu dx^\mu$, and summing over the m fluid components. We write the effective action with the geometric coupling as follows

$$S[a, A, \omega] = -\frac{1}{4\pi}\int K_{(i)(j)}a_{(i)}da_{(j)} + \frac{1}{2\pi}\int a_{(i)}\left(t_{(i)}dA + s_{(i)}d\omega\right), \tag{1.84}$$

where $s_{(i)}$ is the orbital spin value for the ith component. The integration over $a_{(i)}$ fields yields the induced action [37],

$$S_{\text{ind}}[A, g] = \frac{\nu}{4\pi}\int\left(AdA + 2\bar{s}\,\omega dA + \overline{s^2}\,\omega d\omega\right) + \frac{c}{96\pi}\int\text{Tr}\left(\Gamma d\Gamma + \frac{2}{3}\Gamma^3\right), \tag{1.85}$$

with the following expressions for the parameters [9]:

$$\nu = t_{(i)}K_{(i)(j)}^{-1}t_{(j)}, \qquad \nu\bar{s} = s_{(i)}K_{(i)(j)}^{-1}t_{(j)}, \qquad \nu\overline{s^2} = s_{(i)}K_{(i)(j)}^{-1}s_{(j)}, \qquad c = n, \tag{1.86}$$

---

[5]The relation actually involve the vielbein e_μ^a and its inverse E_a^μ. Upon imposing null torsion and a metric compatible connection, we find

$$\omega_\mu^{ab} = frac12\left(E^{\nu[a}\partial_{[\mu}e_{\nu]}^{b]} - E^{\nu[a}E^{b]\sigma}e_{c\mu}\partial_\nu e_\sigma^c\right),$$

corresponding to the filling fraction ν, the average orbital spin $\overline{s}$, the average square $\overline{s^2}$ and the central charge c, respectively. The conventional naming for these quantities refers to the case of integer filling, where $K_{(i)(j)}$ is the identity matrix.

In the expression of the induced action (1.85), the first term is the Chern-Simons theory (1.16) responsible for the Hall conductance, and the following terms are called respectively, the Wen-Zee term

$$S_{WZ}[A,g] = \frac{\nu \overline{s}}{2\pi} \int \omega dA, \tag{1.87}$$

and the gravitational Wen-Zee term

$$S_{gWZ} = \frac{\nu \overline{s^2}}{4\pi} \int \omega d\omega. \tag{1.88}$$

The last term in (1.85) is called gravitational Chern-Simons action and involves the full $(2+1)$-dimensional Christoffel connection $\Gamma^\mu_\nu = \Gamma^\mu_{\nu\lambda} dx^\lambda$. This contribution arises from the measure of integration for the $a_{(i)}$ path-integral, and it expresses the gravitational anomaly as we will see in the following.

The correctness of the action (1.85) has been verified by integrating the microscopic theory of electrons in Landau levels, for integer filling [48]. In this case, the $s_{(i)}$ values are

$$s_{(i)} = \frac{2i+1}{2}, \qquad i = 0, \dots, n-1. \tag{1.89}$$

The correcteness of this result can be verified by computing the total angular momentum $M_{(i)}$ of each level filled with N electrons, using the formula:

$$M_{(i)} = \frac{N^2}{2} - N s_{(i)}. \tag{1.90}$$

for each level.

In an actual system, the effective action (1.85) is accompanied by other non-geometrical terms that are local and gauge invariant and depend on details of the microscopic Hamiltonian [49, 48]. These non-universal parts will not be considered here, while the issue of universality of the Wen-Zee terms will be discussed later.

1.5.2 Hall viscosity

Let us consider small strain deformations around the flat metric. For small fluctuations, we can write $\delta g_{ij} = 2\delta e_{ij}$ to express the zweibeins $e_{ij} = \delta_{ia} e_j^a$ in terms of the metric. The spin connection components are then found to be:

$$\omega_0 = -\frac{1}{8}\varepsilon^{ik}\delta g_{ij}\delta \dot{g}_{jk}, \qquad \omega_j = \frac{1}{2}\varepsilon^{ki}\partial_i \delta g_{kj}. \tag{1.91}$$

Moreover, to linear order the spatial zweibein is proportional to the affine connection, $\omega_i = \frac{1}{2}\varepsilon^{jk}\Gamma_{j,ik} = \frac{1}{2}\Gamma_i$. Upon expanding the scalar curvature in g_{ij},

$$\mathcal{R} = \frac{2\partial_i \omega_j \varepsilon^{ij}}{\sqrt{g}} = \left(\partial_i \partial_j - \delta_{ij}\partial^2\right)\delta g_{ij}, \tag{1.92}$$

we rewrite the Wen-Zee action to the quadratic order in the fluctuations of both metric and electromagnetic background. It reads

$$S_{WZ} \simeq \frac{\nu \overline{s}}{4\pi} \int d^3x \left(A_0 \mathcal{R} + \varepsilon^{ij}\dot{A}_i \Gamma_j - \frac{B}{4}\varepsilon^{ij}\delta g_{ik}\delta \dot{g}_{jk} \right). \tag{1.93}$$
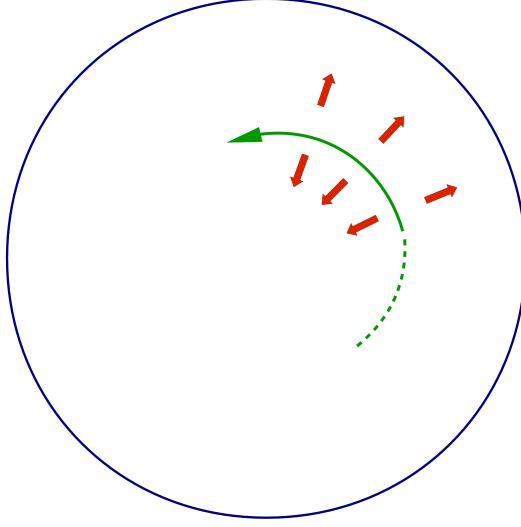
Figure 1.6: Illustration of the Hall viscosity: a counter-clockwise stirring of the fluid in the bulk of the droplet causes an orthogonal force (red arrows).

From this expression, we can compute the induced stress tensor to leading order for constant magnetic field $B = B_0$, obtaining the result [44]:

$$T_{ij} = 2\frac{\delta S_{WZ}}{\delta g^{ij}} \simeq -\frac{\eta_H}{2}\left(\varepsilon_{im}\dot{g}_{jm} + \varepsilon_{jm}\dot{g}_{mi}\right), \tag{1.94}$$

with

$$\eta_H = \frac{\nu \bar{s} B_0}{4\pi}. \tag{1.95}$$

The parameter η_H is called Hall viscosity: it parameterizes the response of the fluid to stirring, say at constant velocity. It corresponds to an orthogonal force (see Fig. 1.5.2) that is not dissipative [33, 50]. Avron, Seiler and Zograf were the first to discuss the Hall viscosity from the adiabatic response [33], followed by other authors [35, 51, 52, 39, 41]; in particular, the relation between the Hall viscosity and $\bar{s}$ (1.95) has been shown to hold for general Hall fluids [34]. Since $\bar{s}$ is a coupling constant of an action of Chern-Simons type, it is independent of local dynamics. Moreover it is associated to a topological quantity in compact geometries. On the other hand, it is not related to an anomaly of the edge theory, and its physical meaning at the edge has so far remained unclear. In the next chapter, we are going to present our work that clarifies this issue and explain to which extent the intrinsic spin is a universal quantity.

1.5.3 Thermal current and gravitational anomaly

The Wen-Zee action in Section 1.5 contains the gravitational Chern-Simons term,

$$S_{gCS} = \frac{c}{96\pi}\int_{\mathcal{M}}\mathrm{Tr}\left(\Gamma d\Gamma + \frac{2}{3}\Gamma^3\right). \tag{1.96}$$

In analogy with the Abelian Chern-Simons theory discussed in Section 1.2, the action is invariant under local coordinate transformations, i.e. diffeomorphisms, when it is defined

on compact manifolds $\mathcal{M}$. For geometries with a boundary, it is not invariant by a total derivative. As in the Abelian case, this term is compensated by the non-invariance of the edge theory under diffeomorphisms [53, 54, 55, 56], that is the gravitational anomaly [57].

In conformal field theory, this anomaly is parameterized by central charge c of the Virasoro algebra (1.62) [17]. More precisely, when the edge theory involves both chiral and antichiral modes, the effect is proportional to the difference of central charges $(c - \bar{c})$, i.e. it is chiral. Such cases occur for some Jain states.

The lack of diffeomorphism invariance corresponds to the non-conservation of the stress tensor, that takes the form

$$\nabla^{\mu} T_{\mu\nu} = -\frac{(c - \bar{c})}{24} \nabla_{\nu} \mathcal{R}. \tag{1.97}$$

in (1+1) dimensions, where $\mathcal{R}$ is the scalar curvature. This equation can be shown to imply a non-vanishing ground state value of the momentum density on the edge, i.e. a matter current [54]wh. Its space average gives the thermal current, $J_T \propto T^2$, that is proportional to the temperature squared. Such ground state value, in general, is not measurable by itself since its like a Casimir effect in the edge theory. However, in the physical geometry of the annulus, we can measure the difference of currents on the two edges, that is non vanishing in presence of a temperature gradient

$$\Delta J_T = \kappa_H \Delta T, \qquad \kappa_H = \frac{\pi}{6} (c - \bar{c}). \tag{1.98}$$

The coefficient κ_H is the thermal Hall conductivity, that is proportional to the gravitational anomaly and thus universal. We thus have another example of universal transport properties determined by anomalies. Note that the current is longitudinal to the edge and orthogonal to the tempertaure gradient.

In conclusion, the bulk-boundary correspondence is again realized: a classical non-conservation in the bulk action is compensated by a quantum effect in the edge theory, in agreement with the anomaly inflow mechanism. Note, however, that the correspondence does not imply a bulk current in this case, because the heat current flow on the edge only [56, 54].

Chapter 2

Bulk-Boundary Correspondence in Quantum Hall Effect

In this chapter, we analyze the geometric response involving the electron orbital spin s and describe its role in the edge theory [1]. In particular, we explain the universal features that can be associated to this quantity, thus providing a further instance of the bulk-boundary correspondence. In the first section, we build the theory of edge excitations for n filled Landau levels, by taking a straightforward limit of the microscopic states near the edge. This analysis was not done in the past beyond the lowest level $\nu = 1$, and is relevant for our problem, because the orbital spin takes different values in different levels (1.89). Next we discuss the edge spectrum and its dependence on s, describing some physical consequences of this fact in several settings.

In the second part, we show how to generalize these results to fractional fillings $\nu < 1$ by using another approach that employs the symmetry of Laughlin incompressible fluids under quantum area-preserving diffeomorphisms (W_∞ symmetry).

Then, we briefly discuss the possibility of measuring s by a tunneling experiment in the Coulomb blockade regime [25] and by quadrupole deformation of the confining potential.

In the last section, we present some recent progress in studying the W_∞ algebra for incompressible fluids.

2.1 Geometric response at the edge

As in any topological phase of matter, the responses have a dual manifestation in the bulk and at the edge of the system, and their interplay is called the bulk-boundary correspondence [9]. We have already seen how this correspondence works in the electromagnetic response: the bulk Hall current compensates the chiral anomaly at the edge [16]. Since the anomaly is an exact and universal feature of the conformal field theory of edge excitations [17, 18], and is related to topological invariant quantities, we can infer that the bulk Hall conductivity σ_H is also universal and exact [9].

Let us now to discuss the boundary terms needed to correct the Wen-Zee terms,

$$S_{WZ}[A, g] = \frac{\nu}{4\pi} \int_{\mathcal{M}} 2\bar{s}\omega dA, \qquad S_{gWZ}[A, g] = \frac{\nu}{4\pi} \int_{\mathcal{M}} \overline{s^2}\omega d\omega . \qquad (2.1)$$

In the recent work [58], the authors showed that in geometries with a boundary, the Wen-Zee actions are modified by the addition of two edge terms that restore the invariance under $SO(2)$ local frame rotations. These terms involve the one-form of the extrinsic curvature of the boundary [58], $K = K_\alpha dx^\alpha$[1]:

$$S_{WZ,b} = \frac{\nu\overline{s}}{2\pi} \int_{\partial\mathcal{M}} AK, \qquad S_{gWZ,b} = \frac{\nu\overline{s^2}}{4\pi} \int_{\partial\mathcal{M}} \omega K, \qquad (2.2)$$

while the spin connection ω and the electromagnetic field A are restricted on the boundary $\partial\mathcal{M}$. The expressions (2.2) are local in $(1+1)$ dimensions. In quantum field theory, local terms of the action are not universal in the sense that they depend on the detailed dynamics and can be modified, according to different (possible) definitions of the renormalized quantities. Furthermore, the local terms (2.2) can also be considered for an interface between two regions in the bulk where $\overline{s}$ and $\overline{s^2}$ take different values [58]. At this point the gap does not vanish and there are no edge excitations. This result should be contrasted with the non-invariance of the CS action under $U(1)$ gauge symmetry. In that case, the compensation by the anomaly of massless edge states cannot be written as a local expression in $(1+1)$ dimensions and in agreement with the fact that anomalies correspond to universal quantities. In conclusion, the results (2.2) for the Wen-Zee action raise dubts on the universality of the intrinsic orbital spin s, that, on the other side, parameterizes physical effects in the bulk such as the Hall viscosity.

In our work [1], we have investigated the meaning of s in the edge physics, by an in-dept analysis of the conformal field theory and found an answer to these questions. Anticipating the result, we showed that s parameterized a Casimir effect in the edge energy spectrum, namely a non zero ground state energy. As a consequence, its absolute value is not physical, but differences of values, $s_i - s_j$, that occur in the case of multiple edge modes, have an unambiguous universal meaning.

Let us first summarize the observable quantities that can be derived by the Wen-Zee action including the boundary terms. Its complete expression is given by [58]

$$S_{ind}[A, g] = S_{CS} + S_{WZ} + S_{WZ,b} + S_{gWZ} + S_{gWZ,b} + S_{gCS} + S_{CFT}. \qquad (2.3)$$

Currents and response coefficients are found by taking variations of this action. Let us mention two results that are useful for the following analysis:

- The relation between the total number of particles and the number of flux quanta is modified. In presence of a boundary, the total number of particles is given by the space integral over a spatial slice Σ of the density, $\sqrt{g}J^0 = \delta S_{\text{ind}}/\delta A_0$, and reads:

$$
\begin{aligned}
N &= \frac{\nu}{2\pi} \int_\Sigma \sqrt{g}dA \;+\; \frac{\nu\overline{s}}{4\pi} \int_\Sigma \sqrt{g}\mathcal{R} \;+\; \frac{\nu\overline{s}}{2\pi} \int_{\partial\Sigma} K + Q_{CFT} \\
&= \nu N_\phi + \nu\overline{s}\chi + Q_{CFT}.
\end{aligned}
\qquad (2.4)
$$

  In this expression, there appear the scalar curvature, $\mathcal{R}_{ij} = 2\partial_i\omega_j/\sqrt{g}$, the number N_ϕ of magnetic fluxes through the surface and the Euler characteristic χ. Note that

---

[1]The extrinsic curvature is defined as $K_\alpha = n_i D_\alpha t^i$, where t^i and n_i are the tangent and vector and the orthogonal vector w.r.t the boundary, respectively. The covariant derivative D_α is the covariant bulk derivative D_μ 'pull-backed' on $\partial\mathcal{M}$

the bulk and boundary terms S_{WZ} and $S_{WZ,b}$ in the action combine themselves to give the correct expression of the Gauss-Bonnet theorem for surfaces with a boundary, including the geodesic curvature K, that reads $\chi = 2 - 2h + b$, where h and b are the number of handles and boundaries, respectively.

- The spin density can be obtained by the variation of the action with respect to the spin connection at fixed metric, $\sqrt{g}s^0 = \delta S_{ind}/\delta\omega_0|_g$. We are interested in the boundary contribution that originates from the term $S_{gWZ,b}$ (2.2) for the geometry of the flat disk ($\chi = 1$). It reads:

$$\mathcal{S}_b = \int_{S_1} s^0 = \frac{\nu \overline{s^2}}{4\pi} \int_0^{2\pi R} dx\, K = \frac{\nu \overline{s^2}}{2}. \tag{2.5}$$

Summarizing, in the geometry of the disk, the Wen-Zee action supplemented by the boundary terms (2.2) predicts non-vanishing ground-state values for the spin $\mathcal{S}_b$ (2.5) and the charge Q_b,

$$Q_b = \nu \overline{s} + Q_{CFT}, \tag{2.6}$$

at the boundary [58]. In section 2.3, we shall recover and extend these results by studying the edge conformal theory and explain to which extent these quantities are universal.

2.2 Multicomponent edge theory

In this section, we construct the conformal theory of edge excitations by taking an explicit limit of the microscopic states for n filled Landau levels. This result will set the stage for the analysis in our work [1]. Although the limit to the edge was already considered in section 1.3, for the one-component case [16], there are some subtleties in the multicomponent case. We recall from the previous chapter, that the magnetic length $\ell_B = \sqrt{2\hbar c/eB}$, c, e, $\hbar$ and the electron mass M are set to one, and that the Hamiltonian and angular momentum take the form (1.3) in terms of two pairs of mutually commuting creation-annihilation operators,

$$a = \frac{z}{2} + \overline{\partial}, \qquad a^\dagger = \frac{\overline{z}}{2} - \partial, \qquad \left[a, a^\dagger\right] = 1,$$
$$b = \frac{\overline{z}}{2} + \partial, \qquad b^\dagger = \frac{z}{2} - \overline{\partial}, \qquad \left[b, b^\dagger\right] = 1, \tag{2.7}$$

involving the complex coordinate of the plane, $z = r\exp(i\theta)$. The single particle wave functions $\psi_{n,m}(z, \overline{z})$ in (1.4) are characterized by the values of the level index $n = 0, 1, \ldots$ and angular momentum $m = -n, -n + 1, \ldots$.

2.2.1 Edge limit of wave functions

We consider the Hall state made by filling up to N electrons per level, thus forming a droplet of fluid of radius $R \sim \sqrt{N}$. A confining radial potential breaks the degeneracy of Landau levels near the boundary and creates a Fermi surface around that point. The specific form of the potential will be discussed later and is not relevant momentarily.

According to the edge limit described for the lowest level in section 1.3, the edge theory is defined by particle-hole excitations around the Fermi surface in a finite range of energy,

i.e. of angular momentum m, in the limit $R \to \infty$. The states in the i-th Landau level, $i = 0, 1, \ldots$, filled with N electrons have momenta $-i \le m < N - i$. The edge theory is defined in the range [16]:

$$L - \sqrt{L} < m < L + \sqrt{L}, \qquad L \equiv R^2 \to \infty, \tag{2.8}$$

where $L \sim N$ is the value of momentum near the Fermi surface and the range of m is chosen to fit a linear spectrum of edge energies, $\varepsilon_m \sim v(m - L)/R$.

As is well known, the wave functions $|\psi_{n,m}(r)|$ are localized around the semiclassical orbits with $r^2 \sim m$. Thus, we can also expand the edge states for $r \sim R$ and consider the combined limit for the angular momentum (2.8) and the radial coordinate,

$$r = R + x, \qquad x = O(1), \qquad R \to \infty. \tag{2.9}$$

Let us take this limit of the functions of the first level $n = 0$: we redefine the momentum w.r.t. the Fermi surface $m = L + m'$ and use the Stirling approximation. We obtain:

$$\psi_{0,L+m'}(r, \theta) \simeq \mathcal{N} \frac{e^{i(L+m')\theta}}{\sqrt{2\pi R}} \, e^{-\left(x - \frac{m'}{2R}\right)^2} \left(1 + O\left(\frac{1}{R}, \frac{m'}{R^2}\right)\right),$$
$$|m'| \le R, \qquad R^2 = L \to \infty, \tag{2.10}$$

where the normalization constant is $\mathcal{N} = (2/\pi)^{1/4}$. These wave functions are plotted in Fig. 2.1(a).

In the expression (2.10), the first factor corresponds to the wave function $\psi_{m'}(\theta) = e^{im'\theta}/\sqrt{2\pi R}$ for the $(1+1)$-dimensional Weyl fermion of the edge theory, while the radial part is peaked at $r \sim R$ with spread $O(\ell_B = 1)$ for $R \to \infty$. In the earlier discussion, we eliminated the radial dependence by fixing $r = R$, i.e. $x = 0$; the remaining term $\exp(-(m'/2R)^2)$ becomes irrelevant for $R \to \infty$.

It turns out that neglecting the radius is not appropriate for higher Landau levels. In order to understand the problem, let us consider the form of the second Landau level wave functions:

$$\psi_{1,m} = \frac{z^m}{\sqrt{\pi (m+1)!}} \left(r^2 - m - 1\right) e^{-r^2/2}. \tag{2.11}$$

Upon taking the limit to the edge, we find:

$$\psi_{1,L+m'-1} \simeq \mathcal{N} \frac{e^{i(L+m'-1)\theta}}{\sqrt{2\pi R}} \, 2\left(x - \frac{m'}{2R}\right) e^{-\left(x - \frac{m'}{2R}\right)^2}. \tag{2.12}$$

The radial function now shows an oscillation of size $x = O(1)$ near the edge, as shown in Fig. 2.1(b).

The oscillating behaviour is also present in the higher levels, for the simple reason that the wave functions should be orthogonal among themselves at fixed angular momentum, i.e. in r space. Owing to the Gaussian factor, it is rather easy to guess that the radial functions should map into the harmonic oscillator basis involving the Hermite polynomials H_n. This is indeed the case: in Eq. (2.12), the polynomial is identified as $(x - m'/(2R)) \sim H_1(x - m'/(2R))$. The inspection of the next few cases leads to the following result:

$$\psi_{n,L+m}(R + x, \theta) \simeq \mathcal{M} \frac{e^{i(m+L)\theta}}{\sqrt{2\pi R}} H_n\left[\sqrt{2}\left(x - \frac{m+n}{2R}\right)\right] e^{-\left(x - \frac{m+n}{2R}\right)^2}, \tag{2.13}$$
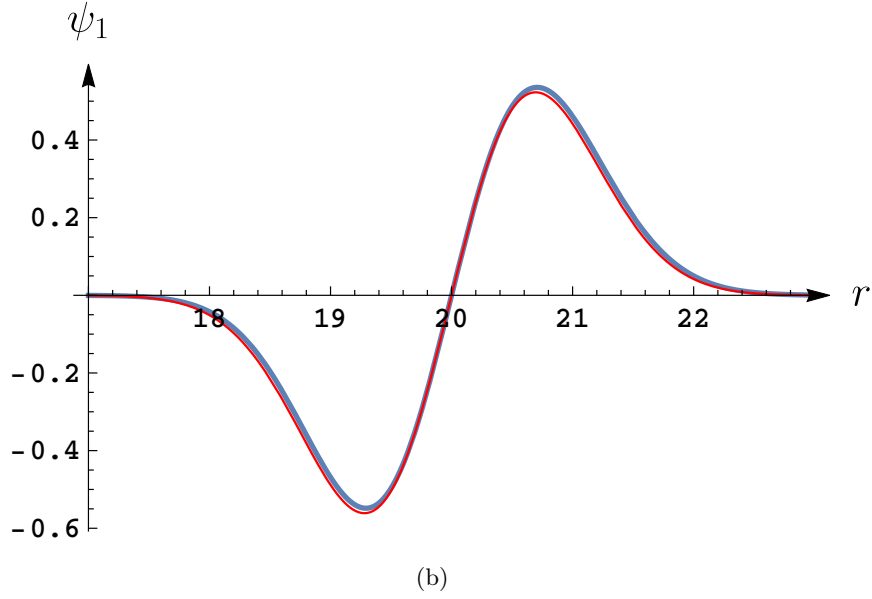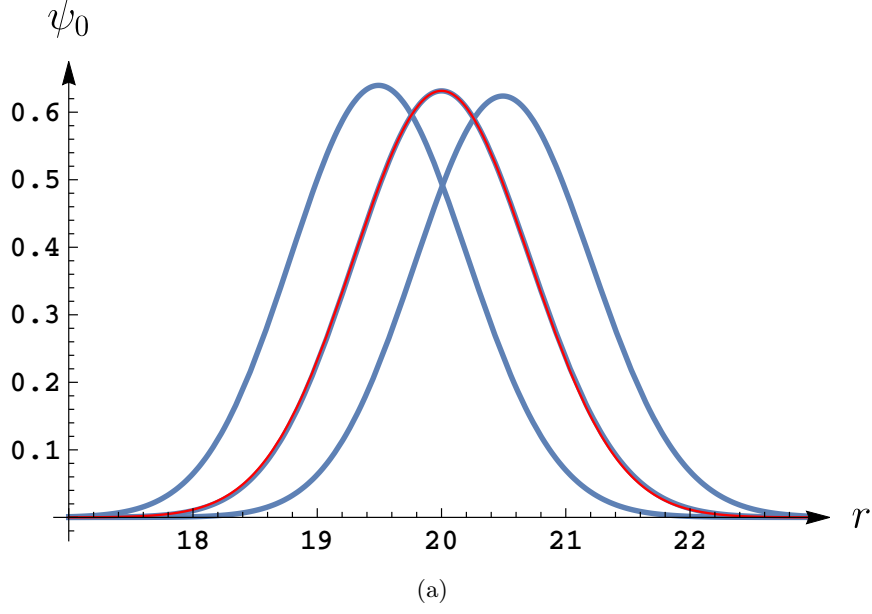
Figure 2.1: (a): radial dependence of $\psi_{0,L+m'}$, for $L = R^2 = 400$ and $m' = \{-20, 0, 20\}$ (blue), and its leading approximation (2.10) (red), for $m' = 0$. (b): radial dependence of $\psi_{1,L-1+m'}$ (blue) and its approximation (2.12) (red), for $L = R^2 = 400$ and $m' = 0$.

where $\mathcal{M}$ is another normalization factor.

The shift of the radial coordinate by $m/2R$ in (2.13) is also easily explained. In the limit $R \to \infty$, the disk geometry can be approximated by the half plane, defined by $x < 0$ in (x, y) coordinates. In this geometry, the Landau levels in the linear gauge $(A_x, A_y) = (0, Bx) = (0, 2x)$ have the form:

$$\widetilde{\psi}_{n,k_y}(x, y) \sim e^{ik_y y} H_n \left[\sqrt{2} \left(x - \frac{k_y}{2} \right) \right] e^{-\left(x - \frac{k_y}{2} \right)^2}. \tag{2.14}$$

Owing to the periodicity of the edge of the disk, the half plane is wrapped in the y direction to form a cylinder, such that the corresponding momentum is quantized by $k_y = m/R$. We thus recover the expression (2.13) up to an overall phase for the different gauge choice.

Note, however, that the functions (2.14) for the cylinder match those of the disk (2.13) with a level-dependent shift of momentum $m/R \to (m + n)/R$ that will be crucial in our discussion [1]. This difference is due to the extrinsic curvature of the boundary of the disc, that vanishes for the half-plane. This is a first sign of the presence of the orbital spin $s_n \propto n$ in the edge theory.

In conclusion, the wave functions of edge states are Gaussians localized in a spatial region $O(\ell_B = 1)$ around $r = R$ and a momentum range $O(\sqrt{L})$ around $L = R^2$. The spatial separation $\Delta x = 1/2R$ between neighbour states is in agreement with the degeneracy/flux relation, since $N_\phi \to N_\phi + 1$ amounts to $R^2 \to (R + 1/2R)^2 \sim R^2 + 1$. The states of higher Landau levels display an oscillating radial dependence that is required by orthogonality. A glimpse of this fact had already appeared in analysis of density shapes of Ref.[59].

2.2.2 Multicomponent conformal theory

We now construct the conformal theory of Weyl fermions that describes the edge excitations for $\nu = n$. The strategy is to consider bilinears of Fermi fields that are observable quantities, in particular the modes of the density $\hat{\rho}_k$ that are the building blocks of the Abelian conformal theory [17, 18].

Let us start from the second-quantized field operator for n Landau levels,

$$\hat{\Psi}(z, \bar{z}) = \sum_{m=0}^{\infty} \psi_{0,m} \hat{c}_m^{(0)} + \sum_{m=-1}^{\infty} \psi_{1,m} \hat{c}_m^{(1)} + \ldots + \sum_{m=-n+1}^{\infty} \psi_{n-1,m} \hat{c}_m^{(n-1)}, \tag{2.15}$$

where $\hat{c}_m^{(i)}$ are fermionic destruction operator for the i-th level. We consider the density, $\hat{\rho}(z, \bar{z}) = \hat{\Psi}^\dagger \hat{\Psi}$: we analyze the Fourier modes at the edge and integrate over the radial coordinate obtaining

$$\hat{\rho}_k \equiv \int_0^\infty dr\, r \int_0^{2\pi} d\theta\, \hat{\rho}(r, \theta) e^{-ik\theta}. \tag{2.16}$$

This expression evaluated in the edge limit of the previous section, namely $R \to \infty$ with $r = R + x$, $x = O(1)$, $R^2 = L$, $m = L + m'$, $|m'| < \sqrt{L}$. First we substitute the field expansion (2.15):

$$\hat{\rho}_k = \int_{-R}^\infty (R + x)\, dx \int_0^{2\pi} d\theta \sum_{m,n} \left(\psi_{0,L+m}(x, \theta) \hat{b}_m^{(0)} + \psi_{1,L+m}(x, \theta) \hat{b}_m^{(1)} + \ldots \right) \times$$
$$\left(\psi_{0,L+n}^*(x, \theta) \hat{b}_n^{(0)\dagger} + \psi_{1,L+n}^*(x, \theta) \hat{b}_n^{(1)\dagger} + \ldots \right) e^{-ik\theta}, \tag{2.17}$$

having redefined $\hat{b}_m^{(i)} \equiv \hat{c}_{L+m}^{(i)}$. We then take the edge limit on wave functions and use the orthogonality of Hermite polynomials; to leading order $O(1)$ in the $1/R$ expansion, we find:

$$\hat{\rho}_k = \sum_{m \in \mathbb{Z}} \left(\hat{b}_{m-k}^{(0)\dagger} \hat{b}_m^{(0)} + \hat{b}_{m-k}^{(1)\dagger} \hat{b}_m^{(1)} + \hat{b}_{m-k}^{(2)\dagger} \hat{b}_m^{(2)} + \ldots \right) + \mathcal{O}\left(\frac{1}{R}, \frac{k}{R} \right)$$

$$= \hat{\rho}_k^{CFT(0)} + \hat{\rho}_k^{CFT(1)} + \hat{\rho}_k^{CFT(2)} + \ldots + \mathcal{O}\left(\frac{1}{R}, \frac{k}{R} \right). \tag{2.18}$$

In this calculation we neglected the shifts in the coordinate, $x - \Delta m/R \sim x$, of order $O(1/R)$.

The result (2.18) shows that the edge Fourier modes of the two-dimensional charge decompose into n independent contributions $\hat{\rho}_k^{CFT(i)}$, $i = 0, \ldots, n-1$, that act on the Fock spaces of the respective Landau levels. Their expressions match the fermionic representation of the multicomponent Abelian conformal theory with $c = n$. This result also agrees with the multicomponent effective theory approach shown in section 1.2, where the edge fields $\varphi^{(i)}$ realize the bosonic representation of the same conformal theory, i.e. $\hat{\rho}^{CFT(i)}(\theta) = \partial_\theta \varphi^{(i)}(\theta)/2\pi$ [9].

In conclusion, the n edge densities are obtained by radial integration of the bulk density in the limit $R \to \infty$. More precisely, the edge states are found by averaging the radial dependence of microscopic states near the edge in a shell $R - \Delta < r < R + \Delta$, with $\Delta = O(1)$, i.e. of the size of the ultraviolet cutoff ℓ_B. Similar result were obtained in the work [60].

Other observables of the conformal theory are similarly obtained by radial integration of bulk quantities. For example, the edge correlator is defined by:

$$\langle \psi(\theta)\psi^\dagger(\theta') \rangle_{CFT} \simeq \int dr \, r \, \langle \Omega | \, \Psi(r,\theta)\Psi^\dagger(r,\theta') \, |\Omega\rangle. \tag{2.19}$$

This expression also decomposes in independent contributions for each branch of edge excitations. Finally note that no non-locality is introduced by this approach, that is simply a low-energy expansion.

Next, we observe that the contribution of one level can be singled out from the total current (2.16) by integrating in r with a suitable weight function $f_j(r)$, and using the orthogonality of Hermite polynomials. For example, let us suppose that we would like to remove the contribution of the lowest level $\hat{\rho}_0^{(0)}$ from the sum (2.18). We can use the weight,

$$f_{(0)}(x) = 1 - 4x^2, \tag{2.20}$$

and compute $\hat{\rho}_k' = \int d^2x f_{(0)} \hat{\rho}(r,\theta) e^{-ik\theta}$. We find that the lowest level does not contribute to leading order $O(1)$, because:

$$\int_{-\infty}^{\infty} dr\, r\, f_{(0)}\, \psi_{0,L+m}\, \psi_{0,L+m+k}^* = O\left(\frac{1}{R} \right). \tag{2.21}$$

We now recall some basic facts of the free chiral fermionic theory discussed in section 1.3 on the geometry of the spacetime cylinder. The Virasoro and current modes are written in terms of fermionic Fock space operators as in (1.39) and (1.40), by normal ordering with respect to the vacuum $|\Omega, \mu\rangle$ in (1.41).

The Hamiltonian of the conformal theory on the cylinder is expressed in terms of the Virasoro generator $\hat{L}_0$,

$$\hat{H} = \frac{v}{R}\left(\hat{L}_0 - \frac{c}{24}\right), \qquad c = 1, \qquad (2.22)$$

and it includes the Casimir energy proportional to c. Furthermore, the conformal dimension h, eigenvalue of $\hat{L}_0$, determines the fractional statistics $\theta/\pi = 2h$ of the excitation through the two point functions.

As shown in section 1.3, the chemical potential μ parameterizes ground-state expectation values for energy, (1.44), and charge (1.45). Let us remember that these two quantities are related among themselves by the current algebra (1.42). Conformal invariance of the ground-state requires that such values vanish and thus the chemical potential is dynamically tuned to $\mu = 1/2$, corresponding to standard antiperiodic boundary conditions for fermions. Other values of μ are possible, but they have specific physical meaning: for example, $\mu = 0$ for periodic fermions corresponds to another (Ramond) sectors of the theory, that is related to the (Neveu-Schwarz) antiperiodic sector by adding half magnetic flux to the system [61]. In the following, the values $\mu = 1/2 + \mathbb{Z}$ will also be considered for realizing features of the dynamics of edge states.

2.3 Orbital spin in the edge theory

In section 2.1, we saw that the Wen-Zee effective theory (2.3) predicts non-vanishing ground state values for charge and spin at the edge of the disc, proportional to the average orbital spin $\overline{s}$ and average square $\overline{s^2}$, Eqs.(2.5), (2.6), respectively. In this section, we are going to discuss how these are realized in the microscopic description of the edge for integer fillings. These values of charge and spin follow from a kind of Casimir effect in the relativistic conformal theory.

2.3.1 Qualitative boundary conditions

We already discussed that, in compactified spatial geometries, the linear relation between Landau level degeneracy and flux is corrected by a finite amount, the so-called shift, proportional to the orbital spin s_n, as shown by Eq. (2.4). For integer Hall effect on the sphere, the degeneracy is given by $N_D = N_\phi + 2s_n = N_\phi + 2n + 1$, where $n = 0, 1, \ldots$ is the level.

In the case of the disk, half of this correction can indeed be realized when the levels are filled up to a common value L of angular momentum, leading to $N_D = L + n$ (see Fig.2.2). This truncation of the spectrum, dubbed $L - max$, can ideally be obtained by cutting the sphere in two disks. The question we want to address in the following is whether this boundary condition can be realized in a physical boundary with dynamic edge excitations.

Let us start with some qualitative arguments that lead to two possible pictures. The analysis of wave functions with momenta m near L, $m = L + m'$, Eq. (2.13), has showed that they are Gaussian peaked at positions $x = (m' + n)/2R$, with $r = R + x$, $R^2 = L$. This implies that for a common value of momenta, e.g. $m' = 0$, the states of higher levels are slightly displaced outward by $\Delta x = n/R$. Therefore, in presence of boundary conditions due to a confining potential or a maximum spatial extension, dubbed $R - max$, such states acquire higher energies. Then, we may expect that the filling of levels up to a common
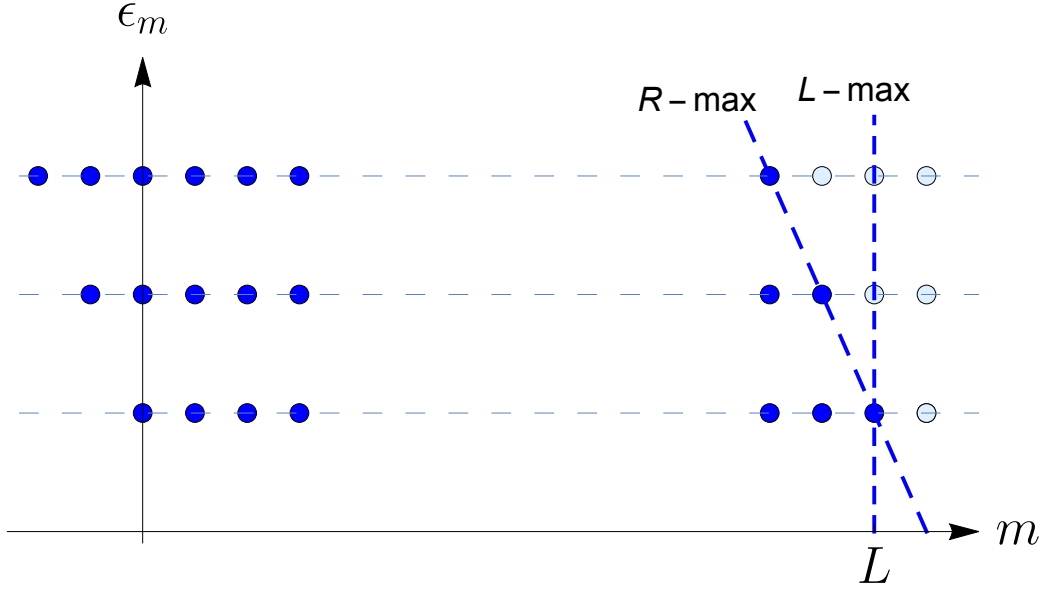
Figure 2.2: $L-max$ versus $R-max$ qualitative boundary conditions.

Fermi energy could imply $m \leq L - n$, leading to equal filling $N_D = L$ for each level (see Fig.2.2). In this case, the shift predicted by the effective action of section 2.1 would not be observed.

In conclusion, a 'geometric' boundary condition of the kind $L-max$ would realize the prediction of Eq. (2.4), while a 'dynamic' condition of the kind $R-max$ would give no effect. In the following, we describe the detailed realization of these two cases.

2.3.2 Edge spectrum and map to conformal field theory

As anticipated in the previous chapter, the edge conformal Weyl fermion possesses a linear spectrum of the form [16]:

$$\epsilon(k) = \frac{v}{R}(m' - \mu) \equiv v\left(k - k_F - \frac{\mu}{R}\right), \qquad |m'| < O(\sqrt{L}), \quad L = R^2, \qquad (2.23)$$

where $k = m'/R$ is the edge momentum, v and k_F are the Fermi velocity and momentum, μ is the chemical potential and m' the angular momentum with respect to the value L near the boundary. Indeed, by inserting this spectrum in the second-quantized fermion Hamiltonian, one reproduces the expected form $\hat{H} = v\hat{L}_0/R + \text{const.}$ (2.22) with the Virasoro generator given by (1.39).

We now discuss the confining potentials that can lead to a linear spectrum. We consider 'macroscopic' potentials of the form $V(r) \sim r^k/R^{k-1}$, with $k = 1, 2, \ldots$, that are smooth functions of the coordinate r and have a linear term in the expansion near the edge $r = R + x$, $x = O(1)$ for $R \to \infty$. Upon subtracting infinite terms, the expansion near the edge takes the form:

$$V(x, R) = a_1 x + a_2 \frac{x^2}{R} + a_3 \frac{x^3}{R^2} + \cdots, \qquad (2.24)$$

where the coefficients a_i are dimensionless numbers (the common dimensional scale $1/\ell_B^2$ is implicit). We could consider other forms of the potential polynomial in x, but they

would introduce dimensional constants that break scale invariance: such terms correspond to non-relativistic corrections to the conformal theory that are disregarded here.

The determination of the energy spectrum of the Landau levels with potential (2.24) can be done analytically in the limit $R \to \infty$ and the result is the following (see Appendix A). The terms $O(x^k/R^{k-1})$ with $k = 3, 4, \ldots$ in (2.24) yield subleading corrections with respect to $O(1/R)$. So one is left with a one-parameter family of potentials corresponding to the linear and quadratic terms whose corresponding spectrum is:

$$\epsilon_{n,m'} = 2n + 1 + \frac{v}{R}\left(m' + n(2+b)\right) + \text{const.}, \qquad |m'| < O(R), \qquad (2.25)$$

where $n = 0, 1, \ldots$ is the Landau level index, $(2n+1)$ is the bulk energy and the constants are $a_1 = 2v$ and $a_2 = v(1+b)$. In particular, $b = 0$ corresponds to the simpler quadratic potential $V = vr^2/R$.

The result (2.25) shows that in higher Landau levels the spectrum at fixed momentum m' is shifted upward by an amount $O(n/R)$ as anticipated by the qualitative argument at the beginning of this chapter. This is the effect of the orbital spin at the edge or, more precisely, of the differences $s_n - s_{n-1} = n$ between levels, because a constant term can be added at will.

In conclusion, the microscopic Hamiltonian of the $\nu = n$ Hall effect with boundary potential takes the form:

$$\begin{aligned} \hat{H} &= \hat{H}_0 + \frac{v}{R}\int dz^2 \hat{\Psi}^\dagger \, V(x,R) \, \hat{\Psi} + \text{const.} \\ &= \sum_{i=0}^{n}\sum_{m_i \in \mathbb{Z}}\left[2i + \frac{v}{R}\left(m_i + s_i(2+b) - \alpha\right)\right]\hat{b}_{m_i}^{(i)\dagger}\hat{b}_{m_i}^{(i)} + \text{const.} \, . \end{aligned} \qquad (2.26)$$

In this equation, $\hat{H}_0$ is the bulk Hamiltonian (1.2), the momenta m_i are measured w.r.t. $L = R^2$ and the constant term α is put explicitly. The correction to the linear edge dispersion relations (2.26) due to the shifts s_i is rather relevant for the following discussion.

We now identify the edge Hamiltonian (2.26) with the conformal theory form (1.39), i.e. compare the following two expressions level by level,

$$\hat{H}^{(i)} = \frac{v}{R}\sum_{m_i \in \mathbb{Z}}\left[2i + \frac{v}{R}\left(m_i + \frac{(2i+1)(2+b)}{2}\right)\right]\hat{b}_{m_i}^{(i)\dagger}\hat{b}_{m_i}^{(i)}, \qquad (2.27)$$

$$\frac{v}{R}\hat{L}_0^{(i)} = \frac{v}{R}\sum_{k_i \in \mathbb{Z}}(k_i - \mu_i) : \hat{b}_{k_i}^{(i)\dagger}\hat{b}_{k_i}^{(i)} :, \qquad i = 0, 1, \ldots . \qquad (2.28)$$

Note that the conformal Hamiltonian does not include the bulk energy, that is assumed to be constant for edge physics. The conformal description is robust to deformations that set independent Fermi velocities for each level, $v \to v_i$, being non-universal parameters; in the following, we keep a single velocity without loss of generality.

This matching of the two Hamiltonians (2.27),(2.28) involves two aspects:

- The $2s_i = 2i+1$ shift in the dispersion relation can be accounted for by assuming level-dependent values for the chemical potential μ_i in the conformal theory description of the i-th level. This setting leads to physically observable effects of the orbital spin.

- The conformal mode index k_i in (2.28) can also be shifted w.r.t. the edge momentum m_i, in order to match the actual filling of the i-th Landau level with the conformal vacuum (1.41), conventionally filled up to level $k_i = 0$.

Let us first identify the conformal theory for the lowest Landau level, $i = 0$[2]. For $N = L + 1$ electrons, the ground-state is filled up to level $m = L$, thus the conformal mode and edge momentum precisely match, $k_0 = m_0$. The conformal invariant value $\mu = 1/2$ for the chemical potential is fixed by adjusting the constant α of the confining potential (2.26), as follows:

$$\mu_0 = \frac{1}{2}, \qquad \alpha = \frac{3}{2}, \qquad (k_0 = m_0). \tag{2.29}$$

Next, we identify the conformal theories for the higher levels. As anticipated in Section 2.3.1, there are actually two possible cases, depending on the physical setting.

Smooth boundary

Let us consider the filling of the first two Landau levels up to a common Fermi energy, in presence of the boundary potential (2.24) (see Fig.2.3). The comparison of energies (2.25), $\varepsilon_{0,m_0} = \varepsilon_{1,m_1}$, gives:

$$m_0 = \frac{2R}{v} + m_1 + 2. \tag{2.30}$$

Being $m_0 = 0$ for the lowest-level ground-state, this equation shows that the second edge branch is located around momenta $m_1 \sim -2R/v$. Therefore, the corresponding conformal theory should be defined with respect to shifted momenta, as follows:

$$k_1 = m_1 + 2R/v + 2, \qquad \mu_1 = \frac{1}{2}. \tag{2.31}$$

Recalling that $R = \sqrt{L}$ is large, this can be adjusted by $O(1)$ corrections such that the difference $k_1 - m_1$ is an integer and independent of s_1, in particular. The chemical potential μ_1 is again fixed by requiring vanishing ground-state charge and conformal spin.

This is the realization of the $R - max$ boundary condition described at the beginning of this section: the effect of the shift is cancelled because the conformal field theories of the two edge branches are defined independently one of the other. Note that the corresponding wave functions are at distance $\Delta m \sim 2R$, see Fig. 2.3, i.e. $\Delta x = \Delta m/2R \sim 1$ and thus have exponentially small overlaps. There are no particle exchanges between the two edges in agreement with the independent conservation of the relative charges.

In conclusion, for isolated droplets with smooth confining potentials the edge excitations of different levels are orthogonal and the system realizes the $R - max$ qualitative boundary setting, leading to no orbital spin effects. Furthermore, for systems connected to a reservoir, the edge branches are let to interact, but their chemical potentials level off and there is no effect either.

---

[2]For simplicity, we consider momentarly the simpler quadratic confining potential, i.e. we set the parameter $b = 0$.
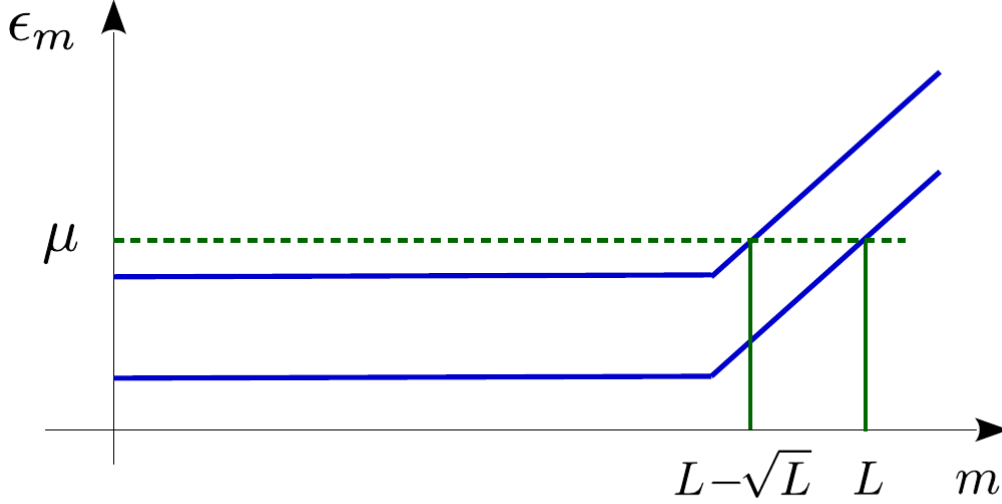
Figure 2.3: Filling of two Landau level according to the spectrum (2.25).

Sharp boundary

We now discuss the realization of the $L - max$ sharp boundary condition introduced at the beginning of this section. Let us assume that the bulk energy of Landau levels in (2.25) is absent [1]. The dispersion relations $\epsilon_{n,m}$ (2.25) show that the different branches of edges occur in the same $O(1/R)$ range of energies and for close momenta m_i values, such that the corresponding wave functions do overlap. The n branches are now parts of the same $c = n$ conformal theory and it is necessary to define a unique ground-state with a common definition of edge momentum. This is given by:

$$k_i = m_i = m_0, \qquad i = 1, 2, \ldots, \tag{2.32}$$

such that all levels are filled up to $m_i = 0$. This is the $L - max$ boundary condition discussed earlier, (Fig. (2.4(b))).

Note that the matching of microscopic and conformal Hamiltonians (2.27), (2.28) is achieved in this case by allowing a different chemical potential for each level:

$$\mu_i = \frac{1}{2} - 2i, \qquad i = 1, \ldots, n - 1. \tag{2.33}$$

These values of μ_i imply that the higher Landau levels possess non-vanishing ground-state values of charge and conformal spin (dimension), as described in section 1.3, Eqs. (1.44, 1.45):

$$\hat{\rho}_0^{(i)} |\Omega, \mu_i\rangle = 2i \, |\Omega, \mu_i\rangle, \tag{2.34}$$

$$\hat{L}_0^{(i)} |\Omega, \mu_i\rangle = 2i^2 \, |\Omega, \mu_i\rangle. \tag{2.35}$$

These states are actually charged excitations with respect of the standard vacuum with $\mu = 1/2$.

(a)   (b)
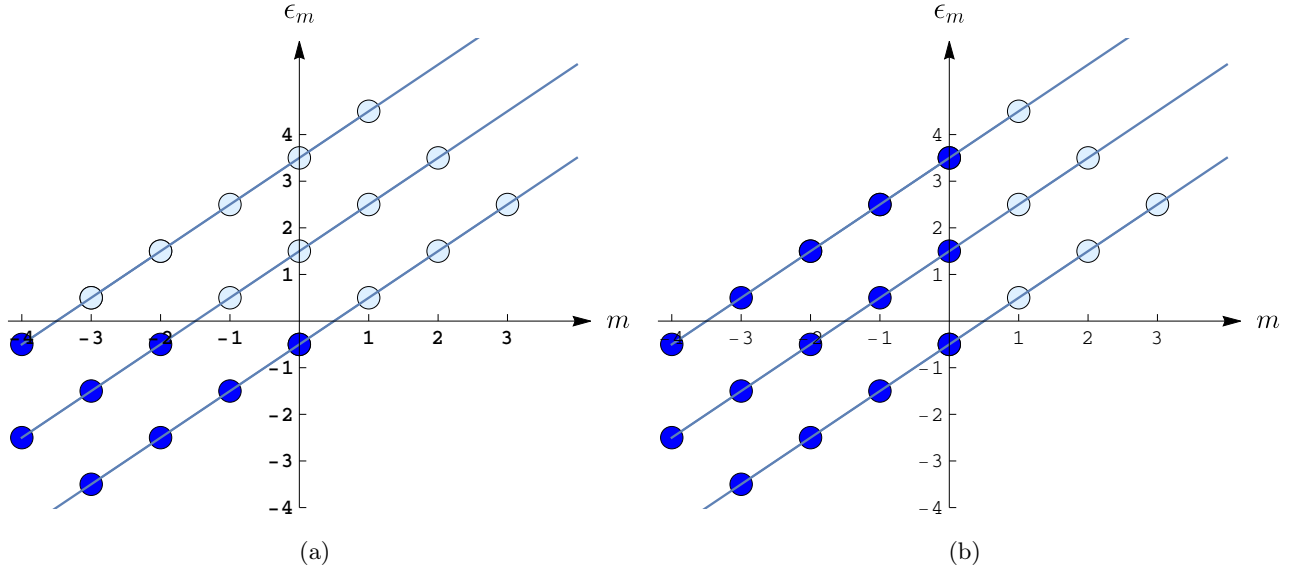
Figure 2.4: Fock space near the Fermi surface of the $\nu = 3$ droplet in two different setups: (a) all levels with same chemical potential, $\mu_i = 1/2$, corresponding to vanishing ground-state energy; (b) all levels filled up to the same momentum $m_i = 0$.

The total ground-state charge and conformal spin for $\nu = n$ are given by the sum of the contributions of all the levels:

$$
\begin{aligned}
Q_b &= \sum_{i=0}^{n-1} 2i = n(n-1), \\
\mathcal{S}_b &= \sum_{i=0}^{n-1} 2i^2 = \frac{n(n-1)(2n-1)}{3}.
\end{aligned}
\tag{2.36}
$$

These also imply the ground-state energy:

$$
E_b = \frac{v}{R} \left(\mathcal{S}_b - \frac{c}{24} \right), \qquad c = n.
\tag{2.37}
$$

We thus have shown that the orbital spin is associated to a ground state energy in the edge theory, as anticipated.

Let us add some remarks:

- The ground-state values (2.34), (2.35) acquire factors $(1+b/2)$ and $(1+b/2)^2$, respectively, for general the confining potential (2.24) with $b \neq 0$. However, the allowed values of the chemical potential are $\mu_i = 1/2 + \mathbb{Z}$, corresponding to antiperiodic boundary conditions for fermions; other real values of μ_i would cause unphysical non-analyticities in electron correlators. In other words, the charge accumulated in the ground-state Q_b should be an integer. This implies that b should only take integer values, that are compatible with conformal invariance at the edge. A mechanism for self-tuning of b is the quadrupole deformation of the droplet discussed later.

- The ground-state values (2.34), (2.35) agree with the effective field theory results (2.6), (2.5) for the special case $b = -1$.

In conclusion, we have found that the edge effects parameterized by the orbital spin, predicted by the Wen-Zee action (2.1), can indeed been found in the microscopic description in the case of sharp boundary, where a unique conformal theory encompasses all edges branches. In this case, only the difference $(s_i - s_j)$ have physical meaning. One may argue that sharp boundaries are rather non-generic in the case of the integer Hall effect, where separate non-interacting branches are possibles. Indeed, in this case, we can fix the edge momentum independently and fill each level at the same energy. However, it turns out that a unique conformal theory (sharp boundary) is necessary for interacting electrons, i.e. in case of fractional Hall effect, that will be discussed in the next section.

2.4 Area preserving diffeomorphisms and fractional fillings

In this section, the edge theory with integer fillings is rederived by using the symmetry of incompressible Hall fluids under area-preserving diffeomorphisms of the plane, the W_∞ symmetry [62] [63, 64] [65]. This reformulation allows us to extend our analysis to fractional fillings and in particular to hierarchical states, which also possess several branches of edge modes and corresponding s_i values.

2.4.1 Edge excitations as W_∞ transformations

We consider the filled lowest Landau level as a starting point of our discussion. A droplet of two-dimensional incompressible fluid is characterized at the classical level by a constant density ρ. For a circular geometry, the fluid has the shape of a disk and fluctuations amount only to shape deformations. Indeed, given the number of electrons $N = \rho \mathcal{A}$ fixed, the area $\mathcal{A}$ is constant. Therefore, the allowed fluctuations correspond to droplets of same area and different shapes. These configurations of the fluid can be generated by coordinate transformations of the plane that keep the density constant in the bulk, namely by area-preserving diffeomorphisms [62] [63, 64] [65].

At the classical level, these reparameterizations are expressed in terms of a scalar generating function $w(z, \bar{z})$ and Poisson brackets. Their action on the coordinate and the density ρ is given by the following expressions:

$$\delta_\omega z = \{z, w\} = \varepsilon^{z\bar{z}} \partial_z z \partial_{\bar{z}} w + (z \leftrightarrow \bar{z}), \qquad \delta_w \rho = \{\rho, w\}, \tag{2.38}$$

where $\varepsilon^{z\bar{z}} = -\varepsilon^{\bar{z}z} = -2i$. The Poisson brackets remind of the canonical transformations in a two-dimensional phase space.

In the geometry of the disk, the ground-state density is constant in the bulk and goes to zero at the boundary: the deformation by Poisson brackets (2.38) involves the derivative of the density that is non-vanishing at the boundary, as expected.

A basis of generators can be obtained by expanding the function $w(z, \bar{z})$ in power series,

$$\mathcal{L}_{n,m} = z^{n+1} \bar{z}^{m+1}, \qquad w(z, \bar{z}) = \sum_{n,m \geq -1} c_{nm} z^{n+1} \bar{z}^{m+1}. \tag{2.39}$$

The $\mathcal{L}_{n,m}$ generators obey the so called w_∞ algebra of area-preserving diffeomorphisms,

$$\{\mathcal{L}_{n,m}, \mathcal{L}_{k,l}\} = ((m+1)(k+1) - (n+1)(l+1)) \mathcal{L}_{n+k,m+l}. \tag{2.40}$$

At the quantum level, the quantities in (2.38) become one-body operators expressed in terms of bilinears of lowest Landau level field operators $\hat{\Psi}(z\bar{z})$[3]:

$$\hat{\rho} = \hat{\Psi}^\dagger \hat{\Psi}, \qquad \hat{w} = \int d^2 z \hat{\Psi}^\dagger(z,\bar{z}) w(z,\bar{z}) \hat{\Psi}(z,\bar{z}). \qquad (2.41)$$

The classical generators $\mathcal{L}_{n,m}$ become quantum operators $\hat{\mathcal{L}}_{n,m}$. Upon using the commutation relations of field operators, one can find the quantum algebra of the generators

$$\left[\hat{\mathcal{L}}_{n,m}, \hat{\mathcal{L}}_{k,l}\right] = \sum_{s=1}^{Min(m,k)} \frac{\ell_B^{2s} (m+1)! (k+1)!}{(m-s+1)!(k-s+1)!s!} \hat{\mathcal{L}}_{n+k-s+1,m+l-s+1} \qquad (2.42)$$
$$- (m \leftrightarrow l, n \leftrightarrow k).$$

This is called the W_∞ algebra of quantum area-preserving transformations. The terms on the right hand side form an expansion in powers of $\ell_B^2 = 2\hbar/B$: the first term corresponds to the quantization of the classical algebra (2.40), while the others are higher quantum corrections $O(\hbar^s)$.

The W_∞ symmetry acts as a dynamical symmetry among the excited state in the Hilbert space. Furthermore, it has been investigated in several works that studied its implementation in the conformal theory. In particular, the W_∞ generators are connected to Fourier modes of the higher spin conserved currents in the edge conformal theory. In particular, the quantum operators $\hat{\mathcal{L}}_{n,m}$ are related to higher spin operators of the edge conformal field theory as follows:

$$\hat{V}_{-n}^{(i+2)} = -\hat{\mathcal{L}}_{n+i,i}, \qquad (2.43)$$

where the index $i+2$ represents the spin of the conformal operators and n the conformal mode. For instance, $\hat{V}_n^{(2)}$ are the Virasoro operator $\hat{L}_n$. In particular, the commutation $\left[\hat{\mathcal{L}}_{0,0}, \hat{\mathcal{L}}_{n,m}\right] = (n-m)\hat{\mathcal{L}}_{n,m}$ reproduces the commutation between $\hat{L}_0$ and higher spins [17]. In the last section, we will show how to construct such operators via the Laplace transform of the density in the edge limit.

Coming back to the quantum algebra, Poisson brackets (2.38) are replaced by commutators, $\delta\hat{\rho} = i[\hat{\rho}, \hat{w}]$. The ground-state expectation value gives the transformation of the density function, that takes the following form [65] [44]:

$$\delta\rho(z,\bar{z}) = \langle\Omega| [\hat{\rho}(z,\bar{z}), \hat{w}] |\Omega\rangle = i\sum_{n=1}^\infty \frac{(2\hbar)^n}{B^n n!} (\partial_{\bar{z}}^n \rho \partial_z^n w - \partial_z^n \rho \partial_{\bar{z}}^n w) = \{\rho, w\}_M, \qquad (2.44)$$

where ρ and w are the expectation values in the ground state of the quantum operators $\hat{\rho}$ and $\hat{w}$. This formula defines the Moyal brackets $\{\rho, w\}_M$, that are non-local due to the non-commutativity of coordinates in the lowest Landau level. There appears an expansion in $\hbar/B$, whose first term reproduces the classical transformation law (2.38).

Equation (2.44) expresses the W_∞ transformations of the density at the quantum level. Another formulation of this symmetry involves the Girvin-MacDonald-Platzman sin-algebra [66], that corresponds to the commutator of two densities in Fourier space: similar to Eq.(2.44), this algebra is given by the Moyal brackets of the classical densities.

---

[3]We reintroduced the hat to indicate the second quantized operators.

In the following, we discuss the form of the leading $O(1/B)$ term in the Moyal brackets, while the higher orders $O(1/B^k)$ will be briefly discussed in Appendix B. The density $\rho^{(0)}$ of the filled lowest level in the disk geometry is a function of the radius only, $\rho^{(0)} = \rho^{(0)}(r)$. Thus, the leading W_∞ deformation of the ground-state can be written as follows:

$$\delta\rho^{(0)}(r,\theta) = \frac{2i}{B}\,\bar{\partial}\rho^{(0)}\,\partial w + h.c. = \frac{1}{rB}\left(\partial_r\rho^{(0)}(r)\right)\partial_\theta w(r,\theta). \tag{2.45}$$

We now define the Fourier modes of the edge density by integrating in space the bulk density, following the same steps of the analysis in section 1.3,

$$\delta\rho_k^{(0)} = \int d\theta\, e^{-ik\theta} \int dr\, r\, \delta\rho^{(0)}. \tag{2.46}$$

It is also convenient to expand the generating function in Fourier modes, leading to ($B = 2$ hereafter):

$$\delta\rho_k^{(0)} = \frac{ik}{2}\int dr\left(\partial_r\rho^{(0)}(r)\right)w_k(r), \qquad w(r,\theta) = \frac{1}{2\pi}\sum_{n\in\mathbb{Z}} w_n(r)\, e^{in\theta}. \tag{2.47}$$

The remaining integral over the radial dependence is non-vanishing in a shell $r = R \pm O(1)$. In order to compute the integral, we can use the exact expression for the derivative of the density of filled Landau levels derived in Ref.[59]. For the i-th level filled with N electrons, it reads:

$$\frac{d}{dr^2}\rho^{(i)}(r) = -i!\,\frac{e^{-r^2}r^{2N-2i-2}}{(N-1)!}L_i^{N-i-1}(r^2)\,L_i^{N-i}(r^2). \tag{2.48}$$

The expression for the lowest level is evaluated in the limit defined in section 2.3, giving the result,

$$\partial_r\rho^{(0)}(R+x) \simeq -2e^{-2x^2}, \qquad R \to \infty, \quad x = O(1). \tag{2.49}$$

It is again useful to use Hermite polynomials $H_{2n}(2x)$ for analyzing the radial dependence of edge excitations. We obtain:

$$\delta\rho_k^{(0)} = -ik\, w_{0k}, \qquad w(r,\theta) = \frac{1}{2\pi}\sum_{n\in\mathbb{Z}}\sum_{i=0}^{\infty} w_{ik}\, H_{2i}(\sqrt{2}x)\, e^{in\theta}. \tag{2.50}$$

This classical amplitude of fluctuations should be compared with the simplest excitation of the $c = 1$ conformal theory, that is given by the current-algebra mode applied to the ground state, $|ex\rangle \sim \hat{\rho}_{-m}^{CFT}|\Omega\rangle$. Therefore, the conformal theory analog of the W_∞ density fluctuation (2.50) reads,

$$\delta\rho_{k,m}^{CFT} = i\,\langle\Omega|\left[\hat{\rho}_k^{CFT},\hat{\rho}_{-m}^{CFT}\right]|\Omega\rangle = i\delta_{km}k. \tag{2.51}$$

The equivalence of the results (2.50) and (2.51) directly shows the relation between the bulk W_∞ symmetry and the edge conformal symmetry.

The W_∞ deformations in higher filled levels are described in similar fashion. The transformations act horizontally within each level [62], that can be analyzed independently; this matches the fact already discussed that the corresponding branches of edge excitations are orthogonal. The fluctuations of the second level are given by:

$$\delta\rho^{(1)} = i\,\langle\Omega^{(1)}|\left[\hat{\rho}^{(1)},\hat{w}^{(1)}\right]|\Omega^{(1)}\rangle, \tag{2.52}$$

where $\hat{\rho}^{(1)} = \hat{\Psi}^{(1)\dagger}\hat{\Psi}^{(1)}$ is the corresponding density operator, and the generator is expressed as:

$$\hat{w}^{(1)} = \int d^2z\, \hat{\Psi}^{(1)\dagger} w\,(z, \bar{z})\, \hat{\Psi}^{(1)}, \tag{2.53}$$

in terms of the field operator $\hat{\Psi}^{(1)}$ restricted to the second level. We now remark that expressions like (2.52, 2.53) can be mapped into lowest level formulas by using the relations among wave functions (1.4), such as $\psi_{1,m} = a^{\dagger}\psi_{0,m+1}$, where $a^{\dagger}$ appear in (2.7). This corresponds to a differential relation between the quantities in the two levels, leading to:

$$\rho^{(1)} = \left(1 + \partial\bar{\partial}\right)\rho^{(0)}, \qquad w^{(1)} = \left(1 + \partial\bar{\partial}\right)w. \tag{2.54}$$

It follows that the classical amplitude of fluctuations $\delta\rho_k^{(1)}$ is analogous to (2.50) with a different radial moment of $w(r, \theta)$. In the same way as the conformal field theory (operator) description of section 2.2, the edge excitations of higher levels are associated to higher radial moments of the bulk density evaluated in the region $r = R + x$, with $x = O(1)$.

The combination of the previous results finally yield the edge excitations for integer filling fraction obtained from the W_∞ transformations of incompressible ground-states. For example, in the $\nu = 2$ case, we find using (2.50):

$$\delta\rho_k^{(\nu=2)} = \delta\rho_k^{(0)} + \delta\rho_k^{(1)} = -ik\left(a_0 w_{0k} + a_1 w_{1k} + a_2 w_{2k}\right), \tag{2.55}$$

where (a_0, a_1, a_2) are numerical coefficients that parameterize the radial dependence at the edge.

In conclusion, in this section we have shown that the W_∞ transformations of the ground-state for integer fillings $\nu = n$ generate edge excitations that match the conformal field theory description of section 2.2: in particular, the n independent branches of excitations are associated to different radial moments of the density in a finite shell at the boundary, $r - R = O(1)$.

2.4.2 Edge excitations and orbital spin for fractional fillings

The W_∞ description of edge excitations is particularly useful because it holds for any incompressible fluid ground-state, including the fractional fillings of the Jain hierarchy [67, 68]. The Moyal brackets (2.44) correctly give the low-energy excitations that can be divided in several branches by studying the radial moments of the density. In summary, this approach provides the general kinematics of edge excitations: it extends directly to the fractional Hall effect and provides a unique derivation of the edge conformal field theory.

The difference between the integer and fractional filling lies in the energetics of excitations, i.e. in the form of the edge Hamiltonian. In the integer case, a direct microscopic derivation was possible as shown in Section 2.3.2. For fractional states, the edge dynamics is due to the many-body interactions and cannot be derived analytically. The standard approach, based on the effective action of section 1.2 and bosonization of the edge fermions predicts that the Hamiltonian takes the Luttinger current-current form [17],

$$\hat{H} = \sum_i \frac{v^{(i)}}{R}\left(\hat{L}_0^{(i)} - \frac{1}{24}\right), \qquad \hat{L}_0^{(i)} = \sum_{k\in\mathbb{Z}} :\hat{\rho}_{-k}^{(i)}\hat{\rho}_k^{(i)}: \,. \tag{2.56}$$

This conformal theory still possesses integer central charge and the spectra of charges and conformal spins are given by the weight lattice with Gram matrix $K^{-1}_{(i)(j)}$ in Eq.(1.33-1.35) as follows:

$$Q_b = \ell^T K^{-1} t, \qquad \mathcal{S}_b = \frac{1}{2} \ell^T K^{-1} \ell, \qquad \ell = (\ell_1, \dots, \ell_n), \quad \lambda_i \in \mathbb{Z}, \qquad (2.57)$$

where $t = (1, 1, \dots, 1)$ is the so-called charge vector and ℓ_i characterize the excitations.

Regarding the role of the orbital spins s_i, we cannot prove that the analysis of previous section extends to Jain states, having no direct derivation of their effect on the energy spectrum. Nonetheless, based on some reasonable assumptions, we present a self-consistent argument for the existence of ground-state values of charge and spin in the edge theory in agreement with the effective theory of section 2.1.

Since the hierarchical states are interacting, their conformal theory should be built around a unique ground-state, requiring the $L - max$ boundary conditions of Fig.2.4(b). As discussed before, the resulting ground-state is actually an excited state from the conformal theory point of view, corresponding to a number of electrons added to the standard conformal vacuum $|\Omega\rangle_{CFT}$, obeying:

$$\hat{\rho}_0 |\Omega\rangle_{CFT} = \hat{L}_0 |\Omega\rangle_{CFT} = 0. \qquad (2.58)$$

Such ground-state $|\Omega, k, h_k\rangle$ with charge $Q_b = k \in \mathbb{Z}$ and conformal spin $\mathcal{S}_b = h_k$ has the form:

$$\begin{aligned}
|\Omega, k, h_k\rangle &= \lim_{\tau_k \to -\infty, \tau_1 > \tau_2 > \cdots > \tau_k} : V_e(\eta_k) \cdots V_e(\eta_1) : |\Omega\rangle_{CFT} \\
&= \lim_{\eta \to 0} V_{ke}(\eta) |\Omega\rangle_{CFT} .
\end{aligned} \qquad (2.59)$$

In this expression, $\eta_j = \exp((\tau_j + iR\theta_j)/R)$, where $\tau_j + iR\theta_j$ are the coordinates of the edge spacetime cylinder and $V_e(\eta)$ is the vertex operator for the electron field on the edge; the normal-ordering $(::)$ should be evaluated by fusing k electrons in the conformal theory, leading to the $Q_b = k$ field V_{ke}.

Let us assume that the edge ground-state (2.59) is realized and run the consistency check. We first determine the orbital spins s_i for the hierarchical states. In the multi-component Wen-Zee action (1.86), the parameters ν, $\nu\bar{s}$ and $\nu\overline{s^2}$ are given by the general expressions (1.86):

$$\nu = t^T K^{-1} t, \qquad \nu\bar{s} = t^T K^{-1} s, \qquad \nu\overline{s^2} = s^T K^{-1} s, \qquad (2.60)$$

upon inserting the $s = (s_0, s_1, \dots, s_{n-1})$ vector and the matrix $K = I + 2qC$, where C is the $n \times n$ matrix with all entries equal to one. One finds:

$$\nu = \frac{n}{n2q+1}, \qquad \nu\bar{s} = \frac{1}{n2q+1} \sum_i s_i = \frac{n}{n2q+1} \frac{q+n}{2}, \qquad (2.61)$$

with $n = 1, 2, \dots$ and $q = 0, 1, 2, \dots$. Note that we considered here only the positive Jain sequence; however we can follow similar steps for negative Jain sequence $\nu = n/n2q - 1$. In the second equation, we also wrote the value $\bar{s} = (q + n)/2$ obtained from the angular momentum of the Jain wave functions [11] and Eq.(1.90). The relation (2.61) identifies the following values:

$$s_i = \left(\frac{q+1}{2}, \frac{q+3}{2}, \dots, \frac{q+2n-1}{2} \right). \qquad (2.62)$$

Namely, they take half-integer values and their differences are integer, as expected.

The comparison of these bulk data with the edge conformal theory involves two steps: i) The ground-state charge Q_b and spin $\mathcal{S}_b$ should correspond to electron excitations of the edge theory; ii) They should be parameterized by integers ℓ_i that are equal to the orbital spin values (2.62) up to a constant, $\ell_i = s_i + \Delta$.

Let us verify that these two conditions can be met. The electron excitations have the spectrum:

$$Q_b = \Lambda^T t, \qquad \mathcal{S}_b = \frac{1}{2}\Lambda^T K \Lambda, \qquad \Lambda = (\Lambda_1, \ldots, \Lambda_n), \quad \Lambda_i \in \mathbb{Z}, \qquad (2.63)$$

corresponding to the integer-charge subset of the general excitation spectrum (2.57), i.e. $\ell = K\Lambda$.

Note the similarity between the expressions (2.57) for (fractional) charged excitations and those involving the s_i (2.60) that we want to reproduce. Since the orbital spin values differ by integers, $s_{i+1} - s_i = 1$, we seek for solutions ℓ_i with the same property $\ell_{i+1} - \ell_i = 1$. Upon inspection, we find that they do exist and are given by:

$$\ell_i = \Lambda_i + 2q \sum_j \Lambda_j, \qquad \Lambda_i = (0, 1, 2, \ldots, n-1), \qquad (2.64)$$

correctly obeying $l_i = s_i + \Delta$. Actually, these electron excitations are possible due to the particular form of the matrix K of Jain states.

The ground-state values of charge and spin are finally given by:

$$
\begin{aligned}
Q_b &= \sum_i \Lambda_i = \frac{n(n-1)}{2}, & \nu &= \frac{n}{n2q+1}, \\
\mathcal{S}_b &= \frac{n(n-1)(2n-1)}{12} + q\left(\frac{n(n-1)}{2}\right)^2.
\end{aligned}
\qquad (2.65)
$$

Note that the value of the integer charge is the same as in the $\nu = n$ case (2.36) (for parameter $b = -1$).

In conclusion, we have found the expressions of the orbital spins s_i of Jain states (2.62) and shown that their values shifted by a common constant correctly parameterize ground-state charge and conformal spin in the edge theory. We can thus argue that the differences $s_i - s_j$ are universal quantities of the fractional Hall effect in the multicomponent case.

2.5 Signatures of the orbital spin at the edge

2.5.1 Coulomb blockade

In the experiment of Coulomb blockade, an electron tunnels into an isolated droplet at zero bias. As discussed in Ref. [69, 70], the energy of charged edge states can be continuously deformed by changing the capacity of the droplet, i.e. by squeezing its area. The energy of the k-electron excitation over the ground-state, as given by the eigenvalue of the Virasoro operator $\hat{L}_0$, is modified by the charging energy as follows:

$$E_k = \frac{v}{R}\frac{(k-\sigma)^2}{2}, \qquad \nu = 1, \qquad (2.66)$$

42
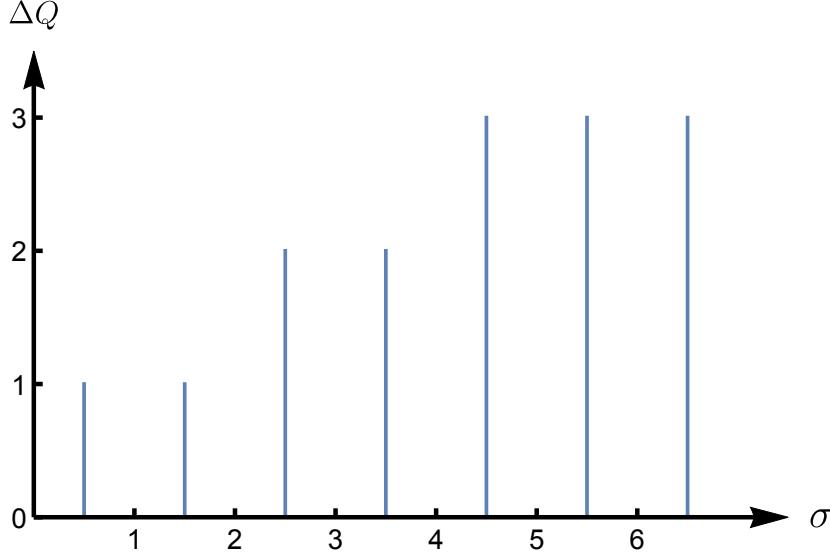
Figure 2.5: Peaks of tunneling electrons obtained by varying the number of flux quanta σ (area) of an isolated droplet with $\nu = 3$ (see Eq.(2.68)).

where σ is the change of flux quanta due to the squeezing of the area. When $\sigma = 1/2$, the energies of the ground and one-electron states become degenerate, $E_0 = E_1$, and an electron can tunnel inside the droplet at zero bias, causing a peak in the conductance, i.e. $\Delta Q = 1$. Successive peaks are found when σ passes the values $1/2 + j$, for $j = 1, 2, \ldots$.

In the case of the isolated droplet with sharp boundary discussed in section 2.3, the electrons of the i-th level possess higher activation energies for larger i values, owing to the different chemical potentials. The previous equation is modified into:

$$E_k^{(i)} = \frac{v}{R}\left[\frac{(k-\sigma)^2}{2} + 2i(k-\sigma)\right] = \frac{v}{2R}\left[(k-\sigma+2i)^2 - 4i^2\right], \qquad i = 0, \ldots, n-1.$$
(2.67)

This equation shows that for the i-th level, the first degeneracy point $E_0^{(i)} = E_1^{(i)}$ occurs at the value $\sigma = 1/2 + 2i$, while the following ones repeat at the same distance $\Delta\sigma = 1$. Namely, the different branches of edge states enter into play at different σ values, owing to the different activation energies.

In conclusion, a possible signature of the orbital spin could be seen at the beginning of the deformation, i.e. for small σ values. The sequence of electron tunnelings would be, for $\nu = 3$, for example,

$$\Delta Q = 1, 1, 2, 2, 3, 3, 3, 3, \ldots, \quad \text{for} \quad \sigma + \frac{1}{2} = 1, 2, 3, \ldots \qquad (\nu = 3), \qquad (2.68)$$

leading to a triangular comb plot for $\Delta Q(\sigma)$ (see Fig.2.5).

2.5.2   Quadrupole deformation

Another test of the orbital spin at the edge is made by deforming the shape of the droplet. This is suggested by the effective action, because the boundary terms (2.2) couple $\bar{s}$ and

43

$\overline{s^2}$ to the extrinsic curvature K, that measures shape deformations.

We considered a quadrupole deformation of the confining potential [71],

$$H \;\to\; H + V_\varepsilon = H + \frac{\varepsilon}{R}\left(z^2 + \bar{z}^2\right), \tag{2.69}$$

where $\varepsilon \ll 1$. We analyze this effect to first perturbative order in ε. Let us go back to the discussion of the confining potential before the limit to the edge, in Appendix A. The unperturbed states $|i, m\rangle$ have energy $E_m^{(i)} = (v/R)(m + 2i + 1)$, where i and m are level index and momentum. In the case of $\nu = n$, this unperturbed spectrum is n-times degenerate for given value of $k = m + 2i$. The expectation value of V_ε in this degenerate subspace form a $(n \times n)$ matrix whose eigenvalues give the the leading perturbative correction to the energy. The matrix is:

$$\begin{aligned}
(V_\varepsilon)_{ik,jk} &= \frac{\varepsilon}{R} \langle i, m | \, 2b^\dagger a + 2ba^\dagger \, | j, l \rangle \, |_{m+2i=l+2j=k} \\
&= \frac{2\varepsilon}{R}\left(\sqrt{(i+1)(k-i)}\,\delta_{i,j-1} + \sqrt{i(k-i+1)}\,\delta_{i,j+1}\right), \\
& \qquad i, j = 0, \dots, n-1.
\end{aligned} \tag{2.70}$$

The eigenvalues of this matrix are e.g. $(\pm 2\varepsilon\sqrt{k}/R)$ for two Landau levels and $(0, \pm 2\varepsilon\sqrt{3k-2}/R)$ for $\nu = 3$, et cetera.

Following the discussion of section 2.3, we should evaluate this correction in the edge limit, given by $R \to \infty$ with $r = R + x$ and $k = m + 2i = R^2 + m' + 2i$. We can thus approximate $k - i$ with R^2 in the matrix elements (2.70), simplifying the eigenvalue problem. We then find the following modification of the edge spectrum (2.25) (for $b = 0$):

$$v \, \langle j, L + m' | \, 2x + \varepsilon \cos 2\theta \, | j, L + m' \rangle = \frac{v}{R}\left(m' + 2j + 1 + 2\varepsilon\alpha_j\right). \tag{2.71}$$

In this equation, $j = 0, \dots, n-1$ is the index of the Landau levels (now mixed among themselves by the perturbation) and α_j are $O(1)$ constants, whose first few values are:

n	2	3	4	$\dots$
α_j	± 1	$0, \pm\sqrt{3}$	$\pm\sqrt{3 \pm \sqrt{6}}$	$\dots$

$$\tag{2.72}$$

In conclusion, the quadrupole perturbation amounts to rigid $O(1/R)$ translations of the branches of the edge spectrum among themselves. Upon tuning ε, one can exactly compensate the translation due to the shift, e.g. by setting $2j + 2\varepsilon\alpha_j = 0$ for a given value of j in (2.71). This result is consistent with the mentioned coupling of the orbital spin to the extrinsic curvature.

One physical application of the quadrupole perturbation of the Hall droplet could be the following. In the Coulomb blockade setting, a small non-integer shift among the levels could be useful to split the degeneracy of the peaks. For example, let us consider the value of σ at which two pairs of levels become degenerate, belonging to two branches of edge states, causing a $\Delta Q = 2$ peak (see Fig.2.5). In presence of the quadrupole deformation, this double peak splits in two $\Delta Q = 1$ peaks, occurring at slightly different values of σ. The same pattern repeats itself at distance $\Delta\sigma = 1$. This fact could help interpreting the experimental results.

In summary, in our work [1], we explicitly found the structure of edge excitations in the multicomponent case, and showed that the various branches are associated with edge radial moments of microscopic states. For integer fillings, we did a straightforward analysis of the large-system limit $R \to \infty$, while in fractional case we studied the W_∞ deformations of incompressible fluid states.

Using these results, we were able to identify Casimir-like ground-state values of charge and conformal spin in the edge theory that depend on the orbital spin, in agreement with the effective field theory approach. This Casimir effect, or chemical potential shift, is irrelevant for a single branch of edge excitations, or for several but independent edge branches (integer Hall effect).

On the contrary, in the case of several interacting branches, in the fractional case, these ground-state values of charge and spin are observable in isolated systems, and are parameterized by the integers $s_i - s_j$, $i, j = 0, 1, \ldots, n - 1$. This effect is a consistent deformation of the CFT for the Jain states.

2.6   Higher spin operators

In this last section, we present some recent progresses about the construction of the complete W_∞ dynamical symmetry. In particular, we analyze the relation between bulk radial moments of the density and higher spin operators of the edge conformal field theory (2.43). We define a clear way to obtain the complete W_∞ algebra (2.42) by taking the edge limit.

The basic idea is to generalize the definition (2.16) by introducing the Laplace transform of density

$$\hat{\rho}_k(\lambda) = \int_0^\infty dr \, r e^{-\lambda r^2} \int_0^{2\pi} d\theta \, e^{-ik\theta} \hat{\rho}(r, \theta). \tag{2.73}$$

Upon substituting the fermionic density operator in the first Landau level

$$\hat{\rho}(r, \theta) = \sum_{j,j'=0}^{\infty} \frac{\bar{z}^j z^{j'}}{\pi \sqrt{j! j'!}} e^{-z\bar{z}} \hat{c}_j^\dagger \hat{c}_{j'} \tag{2.74}$$

and taking the edge limit $R \to \infty$ discussed in section 2.2, we obtain

$$\hat{\rho}_k(\lambda) = \frac{1}{(1 + \lambda)^{R^2 + 1 + \mu_0}} \sum_{m=0}^{\infty} \frac{1}{(1 + \lambda)^{m+k/2-\mu_0}} \hat{b}_m^\dagger \hat{b}_{m+k}, \tag{2.75}$$

where we have rescaled the momentum $j = R^2 + m$. Once we remove the bulk factor $(1 + \lambda)^{R^2 + 1 + \mu_0}$ and expand in $\lambda \sim 0$ the operator in (2.75), one can easily read higher spin conformal operators. For instance, the linear term in λ is given by

$$\lambda \sum_{m=0}^{\infty} (m + k/2 - \mu_0) \, \hat{b}_m^\dagger \hat{b}_{m+k}, \tag{2.76}$$

which is previously the Virasoro operator $\hat{L}_k$ in (1.39).

Therefore, the Laplace transform of the density operator gives us all the conformal spin fields in the theory. In particular, once defining the normal ordering w.r.t. the ground

state (2.59), operators $\hat{\rho}_k(\lambda)$ satisfy the following closed algebra

$$[\hat{\rho}_k(\lambda), \hat{\rho}_n(\mu)] = \left(x^{-n/2}y^{k/2} - x^{n/2}y^{-k/2}\right)\hat{\rho}_{k+n}(\lambda\mu) + \sum_{l=1}^{k}(xy)^{l-\frac{k+1}{2}}\delta_{k+n,0}, \tag{2.77}$$

$$\text{with} \quad x = \frac{1}{1+\lambda} \quad \text{and} \quad y = \frac{1}{1+\mu}.$$

This algebra can be mapped to the complete W_∞ algebra discussed in previous sections and thus, operators $\hat{\rho}_k(\lambda)$ are able to describe all the possible excitations arising in quantum incompressible fluids. In particular, it is possible to obtain the radial dependence of neutral and charged edge excitations by computing expectation values of $\hat{\rho}_k(\lambda)$ and inverse Laplace transforming. The analysis extends to fractional filling due to the bosonization of all variables.

Furthermore, we have obtained the bosonic representation of the Haldane two-body interactions in terms of $\hat{\rho}_k(\lambda)$. This fact is important because it gives us the tools to analyze the bulk dynamics of Laughlin state. One of the issues is to obtain analytically spectrum at finite bulk momentum [66] and to check its universality [72].

Our anaysis shows that the algebra (2.77) can be generalized beyond the edge limit to energies and momenta that are finite for $R \to \infty$. In this limit, the Laplace variable λ can be replaced by the bulk momentum orthogonal to the edge. Therefore, our setting allows to address the bulk dynamics just mentioned. Our results show a rich spectrum of mixed bulk-edge excitations: we obtain the so called 'edge reconstruction', the tendency of the Hall droplet to detach an annulus at distance $O(\ell_B)$. Let us remark that this effect is obtained in a different limit of edge momenta and energies to the one defined in Section 2.3. In our analysis such limit corresponds to excitations which extend a bit in the bulk, beyond the conformal modes discussed previously. We also obtain the analytic spectrum corresponding to bulk oscillations in the droplet, that are exact in our limit.

Chapter 3

Effective Field Theories of $(3+1)$-dimensional Topological Insulators

In the previous chapters, we described the quantum Hall states, the best known topological phases of matter. They are characterized by massless edge excitations, ground state degeneracy and anyonic phases that are accounted for by topological gauge theories. In the last ten years, it became clear that there are other kinds of topological phases, in many condensed matter systems and in absence of magnetic fields. Our goal is to extend the effective field theory description to such states.

In this chapter, we will analyze the topological insulators in three spatial dimensions. These are *symmetry protected topological phases* (SPT phases) occuring in systems that are invariant under time-reversal (TR) symmetry. This protects the massless fermionic surface states in the sense that they cannot be gapped and trivial without breaking this symmetry explicitly. We divide this chapter in two parts.

In the first part, we will discuss the field theory description of time-reversal invariant topological phases following from the fermionic non-interacting representation of the bulk degrees of freedom. Using a dimensional reduction argument, we will show how massless degrees of freedom arise at the surface, and we will explain the anomaly cancellation occurring between bulk and boundary.

In the second part, we will present the bosonic effective field theory that can describe topological insulators in the interacting case, generalizing the Chern-Simons theory approach to $(3+1)$ dimensions. In analogy with the quantum Hall effect, we expect that the bulk is described by a topological gauge theory while the boundary excitations are massless bosons. Therefore, field theory methods are facing the problem of bosonization in $(2+1)$ dimensions, the map between fermionic and bosonic relativistic excitations. In this chapter, we will analyze a non-conformal massless boundary theory, while the study of a conformal dynamics will be discussed in the next chapter, based on our work [2].

class\d	$\mathcal{T}$	$\mathcal{C}$	$\mathcal{S}$	0	1	2	3	4	5	6	7
A	0	0	0	$\mathbb{Z}$	0	$\mathbb{Z}$	0	$\mathbb{Z}$	0	$\mathbb{Z}$	0
AIII	0	0	1	0	$\mathbb{Z}$	0	$\mathbb{Z}$	0	$\mathbb{Z}$	0	$\mathbb{Z}$
AI	$+$	0	0	$\mathbb{Z}$	0	0	0	$2\mathbb{Z}$	0	$\mathbb{Z}_2$	$\mathbb{Z}_2$
BDI	$+$	$+$	1	$\mathbb{Z}_2$	$\mathbb{Z}$	0	0	0	$2\mathbb{Z}$	0	$\mathbb{Z}_2$
D	0	$+$	0	$\mathbb{Z}_2$	$\mathbb{Z}_2$	$\mathbb{Z}$	0	0	0	$2\mathbb{Z}$	0
DIII	$-$	$+$	1	0	$\mathbb{Z}_2$	$\mathbb{Z}_2$	$\mathbb{Z}$	0	0	0	$2\mathbb{Z}$
AII	$-$	0	0	$2\mathbb{Z}$	0	$\mathbb{Z}_2$	$\mathbb{Z}_2$	$\mathbb{Z}$	0	0	0
CII	$-$	$-$	1	0	$2\mathbb{Z}$	0	$\mathbb{Z}_2$	$\mathbb{Z}_2$	$\mathbb{Z}$	0	0
C	0	$-$	0	0	0	$2\mathbb{Z}$	0	$\mathbb{Z}_2$	$\mathbb{Z}_2$	$\mathbb{Z}$	0
CI	$+$	$-$	1	0	0	0	$2\mathbb{Z}$	0	$\mathbb{Z}_2$	$\mathbb{Z}_2$	$\mathbb{Z}$

Figure 3.1: Periodic Table of non-interacting topological insulators and superconductors. The ten symmetry classes are labeled in the first column according to the notation by Atland and Zirnbauer [73]. The following columns specify the $\mathcal{T}$ symmetry, $\mathcal{C}$ symmetry and $\mathcal{S}$ symmetry, respectively, where (± 1) and (0) denote the presence and absence of the symmetry, respectively, with ($\pm$) specifying the values of $\mathcal{T}^2$ and $\mathcal{C}^2$ equal to ± 1. The topological invariant numbers characterizing the phase are listed according to the spatial dimensions d of the system, $0 \leq d \leq 7$.

3.1 Ten-Fold way classification

Non-interacting fermions in condensed matter are characterized by quadratic lattice Hamiltonians, whose spectrum forms band systems [10]. It turns out that the classification of topological phases depends on very general properties of these Hamiltonians and is analogous to the study of random matrices developed earlier by Atland and Zirnbauer [73]. It was found [74, 75, 76, 77] by Kitaev and Ludwig, Schnyder and Ryu, that there are corresponding ten classes of topological phase depending on the realization of the symmetries of time reversal $\mathcal{T}$, charge conjugation $\mathcal{C}$ and 'chiral symmetry' $\mathcal{S} = \mathcal{T}\mathcal{C}$. The result is shown in Fig.3.1. Each class depends on the presence (± 1) or absence (0) of $\mathcal{T}$ with $\mathcal{T}^2 = \pm 1$, and/or $\mathcal{C}$ with $\mathcal{C}^2 = \pm 1$, while $\mathcal{S} = \mathcal{T}\mathcal{C}$, can be present (1) or absent (0). The symbols in the table "$\mathbb{Z}$", "$\mathbb{Z}_2$", "$2\mathbb{Z}$" and "0" represent whether or not the phase exists for a given symmetry class in a given dimension. For example, "$2\mathbb{Z}$" means the topological phase is characterized by a topological invariant even integer, and "0" means the gapped phase is trivial. Remarkable features of this classification are the periodicty in the space-dimension d for $d \to d + 8$ and the ordering of phases as d changes.

In Fig.3.1, the quantum Hall state belongs to the class A in two spatial dimensions and is characterized by integer $\mathbb{Z}$, namely the first Chern class [22, 78]. TR invariant topological insulators belong to the class AII and are classified by a $\mathbb{Z}_2$ number in two and three spatial dimensions [79, 80].

Let us stress that the classification in Fig. (3.1) was obtained by the analysis of quadratic fermionic Hamiltonians. In the interacting case, the characterization of topological phases is an open problem, where the effective field theory approach can be useful [9, 10, 81, 82].

3.2 Effective field theory of free fermionic topological insulators

In this section, we will discuss non-interacting topological insulators in $(3+1)$ dimensions. About fifteen years ago, three groups independently found that these phases are possible in three spatial dimensions and are classified by a $\mathbb{Z}_2$ index [80, 83, 84]. This $\mathbb{Z}_2$ classification is connected to the parity of the number of massless Dirac fermion located at the surface. Actually, the theory of free massless fermions in $(2+1)$ dimensions is time-reversal invariant, but a mass term breaks the symmetry explicitly [85]. On the other hand, an even number of fermions can interact by a TR invariant mass and disappear from the low-energy theory. In the first case, the system realize the topological phase characterized by having a gap in the bulk and gapless surface states. In the second case, instead we have a trivial insulating phase in the bulk without surface states at low energy.

The robustness of the $\mathbb{Z}_2$ index can be understood by the presence of an anomaly in the field theory of fermions at the boundary which is the so-called parity anomaly in $(2+1)$ dimensions. Massless surface fermions interacting with the electromagnetic field generate a Chern-Simons effective action that is odd under TR and parity transformations [86, 87, 88]. This leads to an inconsistency: the quantum theory of a massless fermion cannot be coupled to the external field by preserving TR symmetry. However, as in the quantum Hall case, the $(2+1)$-dimensional theory is connected to the higher dimensional
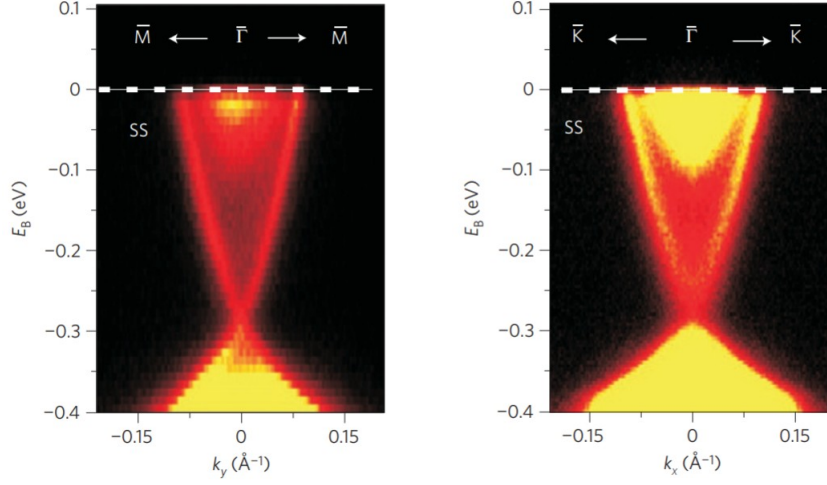
Figure 3.2: Dirac cone between the valence and conduction bands in Bi_2Se_3 found by using ARPES technology [91].

theory of the bulk that cancels the anomaly [89, 90, 61].

The experimental proof of the existence of massless surface states was obtained in [92, 91] by using the spin-ARPES (Angle-Resolved Photoemission Spectroscopy) method to reveal the Dirac cone between valence and conduction bands, see Fig. (3.2). In particular, the crystal Bi_2Se_3 was analyzed since it has a large band gap of ~ 0.3eV (3600 K), and can exhibit the topological behavior at room temperature, greatly increasing the potential for applications [93].

3.2.1 Jackiw-Rebbi dimensional reduction

The effective field theory of surface excitations can be obtained by Jackiw-Rebbi dimensional reduction [94] of the massive bulk theory.

We consider a $3D$ topological insulators with surface located at $z = 0$ separating the bulk of the material $z < 0$ from the empty space $z > 0$. We can model the non-interacting bulk dynamics by a $(3+1)$-dimensional fermion whose mass $M(z)$ varies in direction z. We take the kink profile with $\lim_{z\to-\infty} M(z) = M_0$ and $\lim_{z\to\infty} M(z) = -M_0$, see Fig. 3.3. The Dirac Hamiltonian takes the form:

$$H = -i\gamma^0\gamma^1\partial_x - i\gamma^0\gamma^2\partial_y - i\gamma^0\gamma^3\partial_z + \gamma^0 M(z) \equiv H_0 + H_z. \tag{3.1}$$

To show how the method works, we consider the following representation of the Dirac γ matrices in $(3+1)$ dimensions:

$$\gamma^0 = \begin{pmatrix} 0 & \sigma_3 \\ \sigma_3 & 0 \end{pmatrix}, \quad \gamma^1 = i\begin{pmatrix} 0 & \sigma_1 \\ \sigma_1 & 0 \end{pmatrix}, \quad \gamma^2 = i\begin{pmatrix} 0 & \sigma_2 \\ \sigma_2 & 0 \end{pmatrix}, \quad \gamma^3 = i\begin{pmatrix} 1 & 0 \\ 0 & -1 \end{pmatrix}, \tag{3.2}$$

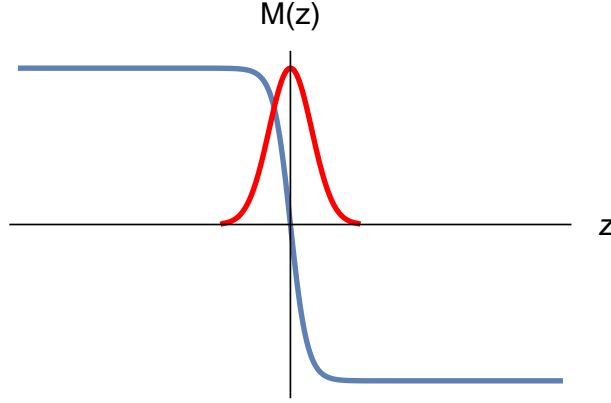where the σ's are the Pauli matrices.

Figure 3.3: (blue line): Mass profile $M = M(z)$; (red line): amplitude probability of the zero modes of the Hamiltonian H_z.

The surface fermion corresponds to low energy solutions localized near $z = 0$. These are the zero-energy eigenstates of H_z, obeying the equation

$$\left(i\partial_z + \gamma^3 M(z)\right)\psi = 0. \tag{3.3}$$

We look for a solution of the type

$$\psi(x, y, z) = f_\pm(z)u_\pm(x, y). \tag{3.4}$$

Consider the spinor function $u_\pm$ obeying $\gamma^3 u_\pm = \pm i u_\pm$; then, Eq. (3.3) becomes

$$\left(\partial_z \pm M(z)\right) f_\pm(z) = 0. \tag{3.5}$$

The normalizable solution to Eq.(3.3) and (3.5) corresponds to the $(-)$ negative eigenvalue of γ^3, i.e.

$$\psi(x, y, z) = \exp\left(-\int_0^z dz'\, M(z')\right) u_-(x, y). \tag{3.6}$$

This zero mode is indeed localized to the surface, as shown by the red curve in Fig. 3.3, thus realizing the dimensional reduction.

The surface dynamics is governed by the hamiltonian H_0 acting on spinors of the form $u_- = (0, \chi_-)$, with the lowest component χ_- a bicomponent spinor. Projecting H_0 in the subspace of χ_- through the operator

$$P_- = \frac{1 + i\gamma^3}{2} = \begin{pmatrix} 0 & 0 \\ 0 & 1 \end{pmatrix}, \tag{3.7}$$

we find the massless Dirac Hamiltonian in $(2 + 1)$ dimensions.

$$(k_y\sigma_1 - k_x\sigma_2)\chi_- = E\chi_-. \tag{3.8}$$

This is the Hamiltonian of a massless Dirac particle in $(2+1)$ dimensions, as expected. Of course, this results holds for low energies $E \ll M_0$.

In a physical setup, the system will have two boundaries along the z axis, at $z = 0$ and $z = -z_0$, with the second surface described by the inverted mass profile $M(z) \to -M(z + z_0)$. Performing the same steps as before, the normalizable zero mode is now given by the positive eigenvector in (3.6), i.e. $u_+ = (\chi_+, 0)$. It turns out that the bispinor χ_+ obeys the same Dirac equation (3.8).
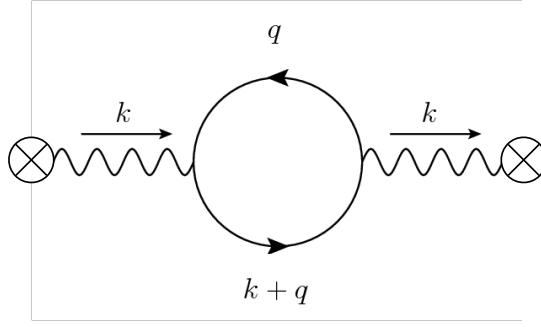
Figure 3.4: One loop vacuum polarization diagram

3.2.2 Parity anomaly and bulk θ-term

Now let us consider this surface massless fermion interacting with an external gauge potential A_μ and evaluate the induced action [86, 87]. In Minkowski signature, the Dirac Lagrangian of a two component spinor field ψ in $(2+1)$ dimensions $\mathcal{L} = \bar{\psi} \left(i\slashed{\partial} + e\slashed{A} \right) \psi$ is classically parity and TR invariant.

By performing the analytical continuation to the Euclidean time

$$x_0 \ \rightarrow \ ix_0, \quad A_0 \ \rightarrow \ -iA_0, \quad \gamma_k \ \rightarrow \ -i\gamma_k, \quad k = 1, 2, \tag{3.9}$$

and integrating out the fermion degrees of freedom, the induced action is given by the fermionic determinant

$$\mathrm{e}^{-S_{\mathrm{ind}}[A]} = \int \mathcal{D}\psi \mathcal{D}\overline{\psi} \, \exp\left(- \int d^3 x \overline{\psi} \left(\slashed{\partial} - ie\slashed{A} \right) \psi \right) = \frac{\det\left(\slashed{\partial} - ie\slashed{A} \right)}{\det\left(\slashed{\partial} \right)}. \tag{3.10}$$

For small fluctuations of the electromagnetic field, the induced action can be approximated by the two point Feynman diagram, i.e. the vacuum polarization in Fig. 3.4 [87]:

$$S_{ind}[A] = -\frac{e^2}{2} \int \frac{d^3 k}{(2\pi)^3} \, A_\mu(k) \Pi_{\mu\nu}(k) A_\nu(-k). \tag{3.11}$$

The vacuum polarization can be regularized by a Pauli-Villars subtraction:

$$\Pi_{\mu\nu}^{(2)REG}(k, \Lambda) = \Pi_{\mu\nu}^{(2)}(k^2) - \Pi_{\mu\nu}^{(2)}(k^2, |\Lambda| \to \infty), \tag{3.12}$$

where Λ is the mass of the Pauli-Villars regulator. The result for the induced action in Euclidean signature is given by [86, 87]:

$$S_{ind}[A] = S_{CS}[A] + S_{NL}[A] + O(A^3) , \tag{3.13}$$

$$S_{CS}[A] = \frac{ie^2}{4\pi} \left(\frac{1}{2} \mathrm{sign}(\Lambda) \right) \int d^3 x \, \epsilon^{\mu\nu\rho} A_\mu \partial_\nu A_\rho , \tag{3.14}$$

$$S_{NL}[A] = \frac{e^2}{64} \int d^3 x \, F_{\mu\nu} \frac{1}{\sqrt{\Box}} F^{\mu\nu} . \tag{3.15}$$

Let us note the ambiguity in the sign of the induced Chern-Simons term in (3.14) depending on the sign of the mass Λ of Pauli-Villars regulator. We can fix this sign by considering the

52

case of a massive fermion with mass m. In this case the regularized vacuum polarization is given by [61]:

$$\Pi_{\mu\nu}^{(2)REG}(k,m) = \frac{1}{4\pi}k_\alpha\epsilon^{\alpha\mu\nu}\left(\frac{m}{|m|}\frac{\arctan(x)}{x} - \frac{\Lambda}{|\Lambda|}\right)$$
$$- \left(k^2\delta_{\mu\nu} - k_\mu k_\nu\right)\frac{1}{8\pi|k|}\left(\frac{1}{x} - \frac{1-x^2}{x^2}\arctan(x)\right), \qquad x = \frac{|k|}{2|m|}. \quad (3.16)$$

For very large mass $|m| >> |k|$, once fixing

$$\text{sign}(\Lambda) = \text{sign}(m), \qquad (3.17)$$

the one loop induced action (3.11) reduces to the following subleading local term of order $O(1/|m|)$,

$$S_{ind}^{(2)}[A] = \frac{e^2}{48|m|}\int d^3x F_{\mu\nu}F_{\mu\nu}. \qquad (3.18)$$

This result is expected since a massive fermion disappears in the low energy limit. Within this choice of Λ, for $m \to 0$, the one loop induced action is given by the Chern-Simons term (3.14) with sign(Λ) =sign(m), and by the non-local term (3.15).

Let us analyze these two quadratic terms appearing in (3.13).

The first term is imaginary and amounts to the topological Chern-Simons action breaking both parity and TR symmetry. This term gives rise to the parity anomaly in $(2+1)$ dimensions.

The second term is real and non-local in the external potential: it contains the square root of D'Alambertian operator $\Box = -\partial_\mu\partial^\mu$ that is well defined in the Euclidean signature.

Our first problem is to solve the apparent contradiction between TR invariance in the bulk and the presence of the anomalous term at the boundary.

In [95], Hughes and Zhang suggested the presence of a bulk induced action, the so-called Abelian θ-term:

$$S_\theta[A] = i\frac{\theta e^2}{32\pi^2}\int d^4x\ \epsilon^{\mu\nu\lambda\rho}F_{\mu\nu}F_{\lambda\rho}. \qquad (3.19)$$

This Lagrangian is actually a total derivative and, for $\theta = \pi$ generates boundary Chern-Simons term

$$S_\theta[A] = \frac{e^2}{8\pi}\int_{\partial\mathcal{M}} d^3x\ \epsilon^{\mu\nu\rho}A_\mu\partial_\nu A_\rho, \qquad \theta = \pi. \qquad (3.20)$$

that can cancel the contribution of the surface (3.14). The bulk term restores the TR symmetry at the quantum level [61].

A few remarks are in order:

- In the case of N_f surface fermions, for $N_f > 1$, pairs of fermions can interact by a TR invariant mass term and disappear from the low-energy theory. The relevant cases are the trivial insulator $\theta = 0$ and the topological insulator $\theta = \pi$, leading to the expected $\mathbb{Z}_2$ index of the classification in Fig. 3.1.

- The anomaly cancellation between the $3D$ bulk and the $2D$ boundary is analogous to the anomaly inflow mechanism of the QHE of Section 1.3. However, the anomaly cancellation is not associated to a current in the bulk, because the θ-term is a topological quantity, $\delta S_\theta/\delta A_\mu = 0$.

- The cancellation by the bulk θ-term requires the matching with the sign of Chern-Simons coupling (3.14). The following argument can be made to show, that this sign does match. In the slab geometry with boundary planes located at $z = \pm z_0$; the anomalous CS actions are cancelled by the θ-term if they have opposite signs on the two planes. Let us consider the bulk fermion theory with an explicit TR breaking mass, $\Delta H = -i\gamma_0\gamma^5\widetilde{m}$. By repeating the Jackiw-Rebbi argument of the previous section, one can find that the dimensional reduced surface fermions possess opposite massess on the surface. Upon applying the reasoning presented before, we should fix the CS signs (3.14) in the limit $\widetilde{m} \to 0$, according to (3.17) with $m = \widetilde{m}$, see Ref. [61]. This condition leads to two CS terms of opposite signs and hence their cancellation with the bulk contribution.

- On compact manifold, the bulk θ-term (3.19) should be TR invariant by itself. This quantity is actually proportional to the second Chern class $\mathcal{C}_2$, that takes integer values, by $S_\theta = \theta\,\mathcal{C}_2$. Thus, θ and $\theta + 2\pi$ are equivalent in the path integral and $\mathcal{T}$ and $\mathcal{P}$ transformations change $\theta \to -\theta$. It follows that $\theta = 0$ and $\theta = \pm\pi$ lead to TR invariant effective actions on compact manifolds, with $\theta = \pm\pi$ indicating the non-trivial topological phase [90].

The θ-term causes interesting measurable effects. For instance, if TR symmetry is broken at the surface, the fermionic excitations become massive and disappear in the low energy limit. However, the surface term (3.20) remains and describes a quantum Hall effect with conductivity $\nu = 1/2$ [96]. Another consequence of the θ-term is the magneto-electric effect [95]: a contribution to the polarization (resp. the magnetization) that is proportional to the magnetic field (resp. electric field).

In conclusion, the effective field theory of the surface states of non-interacting topological insulators is made up by a bi-dimensional massless Dirac fermion. Such theory, once coupled to the electromagnetic field, generates an anomalous term that is cancelled by the bulk action. The effective induced action at the quadratic order in A is therefore given by the non-local term S_{NL} in (3.15).

3.3 Fractional topological insulator

In Section 1.2 we introduced gauge degrees of freedom for describing interacting electrons and the Chern-Simons theory (1.14). This effective theory accounts for universal long range features of the fractional quantum Hall effect, providing a complementary view to wave function approaches [9, 10]. Moreover, the associated scalar theory in $(1 + 1)$ dimensions of Section 1.4 gave us an exact description of edge dynamics [16]. In this section we will generalize the effective field theory approach to topological insulators [81] by reviewing the bulk BF theory proposed by Cho and Moore [97].

3.3.1 BF theory in $(3 + 1)$ dimensions

In a $(3 + 1)$ dimensional manifold $\mathcal{M}$, the low energy degrees of freedom can be modelled by conserved currents for quasiparticles J^μ and vortices $J^{\mu\nu}$,

$$J^\mu = \frac{1}{2\pi}\varepsilon^{\mu\nu\rho\sigma}\partial_\nu b_{\rho\sigma}, \qquad J^{\mu\nu} = \frac{1}{2\pi}\varepsilon^{\mu\nu\rho\sigma}\partial_\rho a_\sigma. \tag{3.21}$$

These expressions define two hydrodynamic gauge fields, the two-form $b = 1/2\, b_{\mu\nu}\, dx^\mu \wedge dx^\nu$ and the one-form $a = a_\mu dx^\mu$. Let us introduce the following action [97]

$$S_{BF}[a, b, A] = \int_\mathcal{M} \frac{k}{2\pi} b\, da + \frac{1}{2\pi} b\, dA + \frac{1}{8\pi}\, da\, dA - a_\mu \mathcal{J}^\mu - \frac{1}{2} b_{\mu\nu} \mathcal{J}^{\mu\nu}, \qquad (3.22)$$

where $A = A_\mu dx^\mu$ is the electromagnetic background, $\mathcal{J}^\mu$ and $\mathcal{J}^{\mu\nu}$ are, respectively, the particles and vortex sources. The first term in (3.22) is called BF theory.

Differently from the Chern-Simons theory, this action is TR invariant, as required, the transformation rules for fields being the following:

$$(a_0, \mathbf{a}) \to (a_0, -\mathbf{a}), \quad (A_0, \mathbf{A}) \to (A_0, -\mathbf{A}), \quad (b_{0i}, b_{ij}) \to (-b_{0i}, b_{ij}). \qquad (3.23)$$

The BF action is topological theory without local dynamics and it describes the gapped bulk at low energy.

Let us turn off the sources for now, $\mathcal{J}^\mu = \mathcal{J}^{\mu\nu} = 0$. Upon integrating the hydrodynamic fields a_μ and $b_{\mu\nu}$, we obtain the induced action

$$S_{ind}[A] = \frac{1}{32\pi k^2} \int_\mathcal{M} d^4x\, \epsilon^{\mu\nu\rho\sigma} F_{\mu\nu} F_{\rho\sigma}. \qquad (3.24)$$

which is exactly the fermionic non-interacting bulk term (3.19) for $k = 1$ and $\theta = \pi$. Different values of k can characterize interacting fermions, as in the case of the fractional QHE [98, 99, 100]. Finally note that this θ-term is consistent with Dirac quantization condition provided that the minimal electric charge of the system is [101]:

$$e_0 = \frac{1}{k}. \qquad (3.25)$$

This fractional value also occurs in the Aharonov-Bohm phases between bulk excitations, as we discuss in the following.

In absence of the background field A, the equations of motion are the following:

$$\mathcal{J}^\mu = -\frac{k}{4\pi} \varepsilon^{\mu\nu\rho\sigma} \partial_\nu b_{\rho\sigma}, \qquad (3.26)$$

$$\mathcal{J}^{\mu\nu} = -\frac{k}{2\pi} \varepsilon^{\mu\nu\rho\sigma} \partial_\rho a_\sigma. \qquad (3.27)$$

Introducing static sources of particles and vortex by the currents $\mathcal{J}_{\mu\nu}$ and $\mathcal{J}_\mu$, respectively, the equations of motion (3.26,3.27) imply the phase $\exp(i2\pi n_1 n_2 / k)$ for the monodromy of a particle of charge n_1 around a vortex of charge n_2. This is the $(3 + 1)$ dimensional extension of anyonic excitations described by the BF theory.

The coupling constant k is found to be integer for gauge invariance of the action, by extending arguments of CS theory discussed in Section 1.2. Moreover k is odd to comply with the existence of fermions [61].

3.3.2 Gauge invariance and surface theory

Now let us analyze the problem of the surface action corresponding to the BF theory. Under the following gauge transformations

$$a \to a + d\lambda, \qquad b \to b + d\xi, \qquad (3.28)$$

where λ and ξ are, respectively, a scalar function and a one-form the BF action is not invariant on a manifold $\mathcal{M}$ with boundary,

$$S_{BF} \to S_{BF} + \frac{k}{2\pi} \int_{\partial\mathcal{M}} d^3x \, \varepsilon^{\mu\nu\rho} \xi_\mu \partial_\nu a_\rho \qquad (A_\mu = 0). \qquad (3.29)$$

The symmetry can be recovered by introducing degrees of freedom living at the boundary $\partial\mathcal{M}$ that compensates this gauge non-invariance [61]. The following surface term

$$S_{surf}[\zeta, a, A] = -\frac{k}{2\pi} \int_{\partial\mathcal{M}} d^3x \varepsilon^{\mu\nu\rho} \zeta_\mu \partial_\nu a_\rho, \qquad (3.30)$$

defines the boundary gauge field ζ_μ. For the gauge transformation $\zeta_\mu \to \zeta_\mu + \xi_\mu$ we find that the action $S_{BF} + S_{surf}$ is invariant.

Now we consider the surface theory in the static gauge $\zeta_0 = a_0 = 0$,

$$S_{surf}[\zeta, a] = \frac{k}{2\pi} \int_{\partial\mathcal{M}} d^3x \, \epsilon^{ij} \zeta_i \partial_t a_j. \qquad (3.31)$$

The equation of motion of the field a in the bulk imposes the constraint $\epsilon^{0ij} \partial_j a_k = 0$ that can be solved by $a_i = \partial_i \varphi$, corresponding to a pure gauge configuration. The action becomes

$$S_{surf}[\zeta, \varphi] = \frac{k}{2\pi} \int_{\partial\mathcal{M}} d^3x \, \epsilon^{ij} \partial_i \zeta_j \partial_t \varphi. \qquad (3.32)$$

In analogy with the quantum Hall state, the surface theory is made up by the symplectic form only, i.e. the Hamiltonian vanishes. The canonical variables are the longitudinal part of a and the transverse one of ζ

$$\varphi, \qquad \Pi = \frac{k}{2\pi} \varepsilon^{ij} \partial_i \zeta_j = -\frac{k}{2\pi} \nabla^2 \chi. \qquad (3.33)$$

In conclusion, there are two scalar degrees of freedom located at the surface that are canonically conjugate.

In the work [61], the authors proposed to introduce a quadratic Hamiltonian for such fields,

$$\mathcal{H} = \frac{1}{2m} \Pi^2 - \frac{m}{2} (\partial_i \varphi)^2. \qquad (3.34)$$

The corresponding action $S_{surf} = \int (\Pi\dot\varphi - \mathcal{H})$ can be written in Lagrangian form as:

$$S_{surf} = \frac{m}{2} \int d^3x \, \partial_\mu \varphi \partial^\mu \varphi, \qquad (3.35)$$

by exploiting the Hamilton equations,

$$\Pi = m\dot\varphi, \qquad \dot\Pi = m\nabla^2\varphi. \qquad (3.36)$$

However, there is a problem: the dimensions of these fields, $[\varphi] = 0$ and $[\Pi] = 2$, are not the standard ones expected for a scalar boson in $(2+1)$ dimensions, which are $[\varphi] = 1/2$ and $[\Pi] = 3/2$. Therefore, the quadratic Hamiltonian (3.34) involves an external mass parameter m. The presence of an external length scale means that this surface theory cannot be conformal invariant.

The coupling of the surface theory with the electromagnetic field is inherited by the bulk (3.22):

$$\partial_\mu \varphi \to \partial_\mu \varphi + A_\mu/k\,. \tag{3.37}$$

Upon performing such substitution in (3.35) and integrating out the scalar field φ, we get the following induced action

$$S_{ind}[A] = \frac{m}{4k^2} \int d^3x\, F_{\mu\nu} \frac{1}{\Box} F^{\mu\nu}\,. \tag{3.38}$$

We remark that this action, for $k = 1$, differ qualitatively from the fermionic induced action S_{NL} in (3.15) in the low-energy limit.

Summarizing, the topological bulk theory based on the BF action (3.22) reproduces the non-interacting topological insulator for $k = 1$ and is able to describe fractionally charged excitations for $k > 1$.

Furthermore, it introduces bosonic degrees of freedom at the surface, the conjugate gauge fields a_μ and ζ_μ. Their dynamics, i.e. Hamiltonian, should be introduced on the basis of additional physical inputs/requirements. The quadratic dynamics just discussed cannot be used to describe bosonization of a free fermions, because the effective actions do not match for $k = 1$. A different dynamics will be introduced that is better suited to bosonize relativistic massless fermions. This original part of our thesis will be presented in Chapter 4.

In the rest of this chapter, we discuss other aspects of the present bosonic theory, that will be useful for comparing with the results of Chapter 4.

3.4 Quantization of the bosonic theory on a torus

3.4.1 Topological order of the BF theory and bulk-boundary correspondence

The quantization of the bulk BF theory (3.22) on the spatial three-torus $\mathcal{M} = \mathbb{T}^3 \times \mathbb{R}$, leads to the topological order of k^3 'anyon' sectors, for odd integer values of the coupling k. The proof of this results is analogous to the evaluation of Wilson loops in Section 1.2.1 [10, 102]. One considers the holonomies of the gauge fields a_μ and $b_{\mu\nu}$ defined by

$$\pi_{ij} = \int_{\Sigma_{ij}} b, \quad i \neq j, \qquad q_i = \int_{\gamma_i} a, \qquad i,j,k = 1,2,3\,, \tag{3.39}$$

where γ_i and Σ_{ij} are the non-trivial cycles and two-tori inside $\mathbb{T}^3$. This decomposition can be done in three different ways, corresponding to three pairs of conjugated variables. The canonical quantization of BF theory implies the commutators

$$[q_i, \pi_{ij}] = i\frac{2\pi}{k}\epsilon_{ijk}. \tag{3.40}$$

We can then construct three pairs of Wilson operators

$$W_k = e^{i\bar{a}_k}\,, \quad \tilde{W}_{ij} = e^{i\bar{b}_{ij}}\,, \quad i,j,k = 1,2,3\,, \quad i \neq j \neq k\,. \tag{3.41}$$
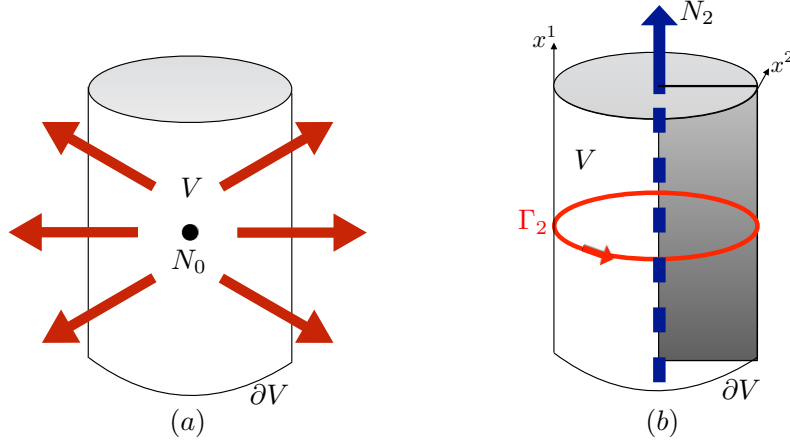
Figure 3.5: The thick two-torus $V = \mathbb{T}^2 \times I$ is represented as a filled cylinder with identified faces. (a): The bulk quasiparticle with charge N_0 creates a flux of the b field across the boundary surface ∂V. (b): In blue the bulk vortex of charge N_2 along the non-trivial cycle x^1, in red the closed line Γ_2 encircling on the surface the vortex excitation, in grey the branch cut surface from the vortex excitation to the boundary surface ∂V.

Each pair obeys the algebra (1.29), in analogy with the Chern-Simons case. Being k the dimension of the representation of each pair, the topological order, i.e. degeneracy of the ground state of BF theory, is k^3 on the torus $\mathbb{T}^3$.

In Chapter 1, we showed that the topological properties of bulk Chern-Simons theory are reproduced by the solitonic modes of boundary fields, as part of the bulk-boundary correspondence. In the three-dimensional case there are two types of bulk excitations: quasiparticles and vortices. We consider the spatial geometry of the solid torus $V = \mathbb{T}^2 \times I$, where I is a finite interval, whose boundary is $\mathbb{T}^2$. In Fig. 3.5 the solid torus is represented as a cylinder with the bases identified. If we put a static quasiparticle $\mathcal{J}^0 = N_0 \delta^{(3)} (\mathbf{x} - \mathbf{x}_0)$ at the point $\mathbf{x} = \mathbf{x}_0$, upon integrating the equation of motion (3.27) we get the following configuration for ζ_μ

$$\int_{\partial V} d^2 x \, \varepsilon^{ij} \partial_i \zeta_j = \frac{2\pi N_0}{k} \, . \tag{3.42}$$

The charge of the quasiparticle corresponds to a flux for ζ through the torus $\mathbb{T}^2$. On the other hand, a static vortex line along one of the two non-trivial cycles, say $\Gamma_i \, \mathcal{J}^{0i} = N_i \delta^{(2)} (\mathbf{x} - \mathbf{x}_0)$, gives a circuitation condition for $\partial_\mu \varphi$ along the other non-trivial cycle Γ_j,

$$\int_{\Gamma_j} dx^j \partial_j \varphi = \frac{2\pi N_i}{k} \qquad i \neq j = 1, 2 \, . \tag{3.43}$$

Therefore, the quantization of the boundary bosonic theory should contain the solitonic excitations (3.42) and (3.43).

3.4.2 Partition function of surface bosonic excitations

In this section, we briefly review the calculation of the partition function of the non-conformal scalar theory (3.35) on the space-time three torus $\mathbb{T}^3$ made by the spatial geometry previously considered and periodic time for temperature [61] [103, 104]. First of

all, we represent the three-torus $\mathbb{T}^3$ as $\mathbb{R}^3$ quotiented by the lattice defined by primitive vectors ω_μ, $\mu = 0, 1, 2$ with components $(\omega_\mu)_\nu$, $\nu = 0, 1, 2$. The definition of the partition function is

$$Z = \mathrm{Tr}\left[e^{-\beta H - i\omega_{01}P_1 - i\omega_{02}P_2}\right], \tag{3.44}$$

where P_1 and P_2 are the components of momentum along the directions ω_1 and ω_2, and β is the period of the compactified time.

Let us summarize the main steps of the canonical quantization of the theory with Hamiltonian (3.34). First of all, we have to solve the equations of motion involving the scalar field φ and its conjugated momentum $\Pi = (k/2\pi)\,\epsilon^{ij}\partial_i\zeta_j$, satisfying the boundary conditions (3.42) and (3.43) inherited from the bulk. The solutions are

$$
\begin{aligned}
\varphi(\mathbf{x}, t) =\,& \varphi_0 + 2\pi \sum_l \Lambda_l \mathbf{k}_l \cdot \mathbf{x} \\
& + \frac{1}{\sqrt{mV^{(2)}}} \sum_{\mathbf{n} \neq 0} \left(a_\mathbf{n} e^{-iE_\mathbf{n}t + 2\pi i \mathbf{k_n} \cdot \mathbf{x}} + h.c.\right),
\end{aligned} \tag{3.45}
$$

$$
\begin{aligned}
\zeta_i =\,& \frac{\varepsilon_{ij}}{V^2}\left(\omega_{2j}\gamma_1 - \omega_{1j}\gamma_2 + \pi\Lambda_0 x_i\right) \\
& + \sqrt{\frac{64\pi^4 m}{k^2 V^{(2)}}} \sum_\mathbf{n} \frac{\varepsilon_{ij}k_{\mathbf{n}l}}{\sqrt{(2E_\mathbf{n})^3}} \left(a_\mathbf{n} e^{-iE_\mathbf{n}t + 2\pi i\mathbf{k_n}\cdot\mathbf{x}} + h.c.\right).
\end{aligned} \tag{3.46}
$$

The quantities shown in these expressions are:

- $V^{(2)}$ is the spatial torus area, given by $V^{(2)} = |\omega_1 \times \omega_2|$

- $\Lambda_\mu = N_\mu/k$, with $\mu = 0, 1, 2$.

- $\mathbf{k}_\mu$ with $\mu = 0, 1, 2$ are the primitive vectors of the dual lattice, defined by $\omega_\mu \times \mathbf{k}_\nu = 2\pi \mathbb{I}_{\mu\nu}$ where $\mathbb{I}$ is the lattice identity matrix.

- The energies of excitations $E_\mathbf{n}$ and their momenta $\mathbf{k_n}$ are specified by two integer numbers $\mathbf{n} = (n_1, n_2)$ as follows:

$$E_\mathbf{n} = \frac{2\pi}{V^{(2)}}|n_1\omega_2 - n_2\omega_1|, \tag{3.47}$$

$$\mathbf{k_n} = (k_{\mathbf{n}1}, k_{\mathbf{n}2}) = \frac{1}{V^{(2)}}\left(n_1\omega_{22} - n_2\omega_{12}, n_2\omega_{11} - n_1\omega_{21}\right). \tag{3.48}$$

- Note the solitonic modes φ_0, and γ_1, γ_2.

Next we have to impose the canonical quantization conditions $[\varphi(\mathbf{x}, t), \Pi(\mathbf{y}, t)] = i\delta^{(2)}(\mathbf{x} - \mathbf{y})$, that imply the following algebra for the field modes, both solitonic and oscillator:

$$[a_\mathbf{n}, a_\mathbf{m}^\dagger] = \delta_{\mathbf{n}\mathbf{m}}, \quad [\varphi_0, \Lambda_0] = \frac{i}{k}, \quad [\gamma_1, \Lambda_2] = -\frac{i}{k}, \quad [\gamma_2, \Lambda_1] = \frac{i}{k}. \tag{3.49}$$

Thanks to the algebra of the solitonic modes and to the fact that $\Lambda_\mu \in \mathbb{Z}/k$, one can show that the field φ and ζ_i are compactified in analogy with the chiral boson theory discussed in Section 1.4.

Upon substituting the Hamiltonian and the momentum components evaluated on the solutions (3.45), the partition function is factorized in a solitonic and a oscillator contributions, $Z = Z_{sol} Z_{osc}$. For simplicity we consider the orthogonal torus geometry corresponding to $\omega_0 = (\beta, 0, 0)$, $\omega_1 = (0, 2\pi R_1, 0)$, $\omega_2 = (0, 0, 2\pi R_2)$. The solitonic part is given by [61]:

$$Z_{sol} = \sum_{N_\mu \in \mathbb{Z}^3} \exp\left\{ -\beta \left[\frac{N_0^2}{8\pi^2 R_1 R_2 m} + 2\pi^2 \frac{m}{k^2} \left(N_1^2 \frac{R_2}{R_1} + N_2^2 \frac{R_1}{R_2} \right) \right] \right\} . \tag{3.50}$$

The discussion of this result is postponed to the next chapter.

Let us observe that the trace on the solitonic modes corresponding to the sum on $\Lambda_\mu = N_\mu/k$, can be decomposed as follows:

$$\Lambda_\mu = M_\mu + \frac{m_\mu}{k}, \quad M_\mu \in \mathbb{Z}, \quad m_\mu = 0, 1, \cdots, k-1, \quad \mu = 0, 1, 2 . \tag{3.51}$$

The partition function is thus expressed in terms of a sum on the triplets (m_0, m_1, m_2):

$$Z_{sol} = \sum_{m_0, m_1, m_2 = 0}^{k-1} Z_{sol}^{(m_0, m_1, m_2)} . \tag{3.52}$$

This expression shows explicitly the presence of k^3 sectors in the surface theory, as expected from the topological order (cf. Section 3.3).

Chapter 4

$(2+1)$-dimensional Conformal Field Theory of Surface Excitations

In the previous chapter, we introduced a bosonic theory with a quadratic dynamics at the surface of topological insulators and showed that it cannot describe the bosonization of free fermions. In this chapter, we will consider a non-local dynamics, studied in our work [2], that is better appropriated to bosonize relativistic massless fermions. Indeed, this theory, known as *loop model* or non-local Abelian gauge theory, reproduces the fermionic action (3.15) in the electromagnetic background. It also describes massless excitations with fractional statistics, that exist at the surface of interacting topological insulators.

In literature, the loop model has appeared in a number of interesting recent research topics. First of all, it provides a neat example of a massless theory that is covariant under duality transformations in $(2+1)$ dimensions. In particular, the loop model is mapped to itself under particle-vortex duality. It also corresponds to the self-dual electrodynamics in mixed dimensions $QED_{4,3}$ [105, 106, 107], in the limit of large number N_f of fermion fields.

Furthermore, the phase diagram of this bosonic theory possesses a critical line [108]. These features remind of the compactified boson conformal theory in $(1+1)$ dimensions [17], corresponding to the massless phase of the XY statistical spin model [10]. The loop model similarly provides a non-trivial solvable conformal field theory in $(2+1)$ dimensions.

In the first section, we will introduce the loop model as the non-local surface dynamics of topological insulators suited to reproduce the induced action of free fermions.

Then, in sections 4.3 and 4.4 we will summarize the interesting features of the loop model. First, we will obtain its phase diagram using energy-entropy Peierls estimates. Then we will show that the loop model enjoys exact self-duality and matches the limit $N_f \to \infty$ of the $QED_{4,3}$.

In the last section, we will present our quantization procedure. Inspired by the relation with $QED_{4,3}$, we reformulate the loop model as a local theory in one extra dimension. This is electrodynamics in $(3+1)$ dimensions with the photons interacting with a BF action defined on a two-dimensional space slice. In this formulation, we can obtain the solitonic spectrum by the usual analysis of non-trivial solutions of the equations of motion. Finally we present the main result of our work [2], the evaluation of the partition function for two different geometries and the analysis of the spectrum of excitations.

We consider the local extension of the model on the toroidal geometry $\mathbb{T}_3 \times I$, where I is the interval in the extra dimension: an infrared cut-off is needed, that is actually a crucial aspect for the definition of the quantum theory. We obtain the partition function for two choices of the cut-off: a fixed scale $1/M$ and the finite size R of the torus. In the first case, the loop model reduces on-shell to the local theory analyzed in the previous chapter [61], providing a check. However, the mass M breaks scale invariance explicitly. The second choice of size-dependent cut-off instead leads to a conformal invariant quantum theory.

Next, we determine the solitonic spectrum and the partition function for the geometry $S^2 \times S^1$. This is related to flat space by a conformal transformation, where the Hamiltonian maps into the dilatation operator. Therefore, the solitonic energies determine the spectrum of conformal dimensions of the fields. This calculation give access to the spectrum of interacting fields that confirms the conformal invariance of the theory.

In the last section, we analyze our results and briefly describe the $(2+1)$-dimensional order-disorder fields of the loop model. In Appendix C, we give some details on the Peierls argument and in Appendix D we report details of the calculations for the partition function.

4.1 Non-local surface theory

In the previous chapter, we have seen that the topological BF gauge theory involves the following surface action in Euclidean signature, [1]

$$S_{surf}[\zeta, a] = \frac{i}{2\pi} \int_{\partial \mathcal{M}} \left(k\zeta da + \zeta dA \right), \qquad (4.1)$$

where we also restore the coupling with electromagnetic background A corresponding to the shift $a \to a + A/k$. Let us now consider the following interaction for the hydrodynamic field:

$$S_{int}[a] = \frac{g_0}{4\pi} \int d^3x \, d^3y \, a_\mu(x) \frac{1}{\sqrt{-\partial^2}}(x, y)(-\delta_{\mu\nu}\partial^2 + \partial_\mu\partial_\nu)a_\nu(y) , \qquad (4.2)$$

where g_0 is an dimensionless constant. For writing convenience, we introduce the following notation: $\partial \equiv \sqrt{-\partial^2}$. The surface action is thus given by:

$$S_{surf}[a, \zeta] = \frac{i}{2\pi} \int \left(k\zeta da + \zeta dA \right) + \frac{g_0}{4\pi} \int d^3x \, d^3y \, a_\mu \left(\frac{-\delta_{\mu\nu}\partial^2 + \partial_\mu\partial_\nu}{\partial} \right) a_\nu . \qquad (4.3)$$

The integration of the field ζ implies the constraint $a = A/k$ and leads to the induced action,

$$S_{ind}[A] = \frac{g_0}{4\pi k^2} \int d^3x d^3y \, A_\mu \left(\frac{-\delta_{\mu\nu}\partial^2 + \partial_\mu\partial_\nu}{\partial} \right) A_\nu. \qquad (4.4)$$

Note that this action reproduces the expected fermionic induced action (3.15) for $k = 1$ and $g_0 = e^2\pi/8$. This is a first indication that this dynamics is appropriate for bosonization.

Furthermore, remembering the expression of the Euclidean propagator in $(2+1)$ dimensions, we have:

$$\frac{1}{-\partial^2}(x, y) = \frac{1}{4\pi} \frac{1}{\sqrt{|x-y|}}, \quad \frac{1}{\sqrt{-\partial^2}}(x, y) = \frac{1}{2\pi^2} \frac{1}{|x-y|^2} . \qquad (4.5)$$

---

[1]The Euclidean formulation is better suited for the later evaluation of the partition function.

We can rewrite the expression (4.4) in the form

$$S_{ind}[A] = \frac{g_0}{16k\pi^3} \int d^3x \, d^3y \, F_{\mu\nu}(x) \frac{1}{|x-y|^2} F_{\mu\nu}(y) \,. \tag{4.6}$$

This action define the non-local QED in $(2+1)$ dimensions.

Let us return to the action (4.3) and now turn off the electromagnetic background A. The equation of motion for a is

$$i\frac{k}{2\pi}\varepsilon_{\mu\nu\rho}\partial_\nu\zeta_\rho = \frac{g_0}{2\pi}\sqrt{-\partial^2}a_\mu \,. \tag{4.7}$$

If a_μ were a pure gauge configuration, i.e. $a_\mu = \partial_\mu\varphi$, this relation would become the duality between the vector field ζ_μ and the 'dual photon' φ, i.e. the eletric-magnetic duality in $(2+1)$ dimensions [100, 109].

Furthermore, by integrating out the a field in (4.3), using the equations of motion (4.7), we obtain the action

$$S_{surf}[\zeta, A] = \frac{k^2}{4\pi g_0} \int \zeta_\mu \left(\frac{-\delta_{\mu\nu}\partial^2 + \partial_\mu\partial_\nu}{\partial} \right) \zeta_\nu + \frac{i}{2\pi} \int \zeta dA \,. \tag{4.8}$$

This corresponds to the non-local Abelian theory also called 'loop model' [110], that we will discuss in the next section.

Note that differently from the quadratic Hamiltonian (3.34), this non-local interaction does not involve dimensional parameters, as we expect for the bosonized version of the massless fermion. In conclusion, the physics of topological insulators provides a strong motivation for analyzing the theory (4.8), as it represents a viable theory for boson-fermion correspondence. The issue of bosonization will become more clear in the following sections.

4.2 Loop model

This model is defined by the following action [110, 111]:

$$S_{loop}[b_\mu] = \frac{g}{16\pi^3} \int d^3x \, d^3y \, f_{\mu\nu}(x) \frac{1}{(x-y)^2} f_{\mu\nu}(y) + i\frac{h}{4\pi} \int d^3x \, \varepsilon^{\mu\nu\rho} b_\mu \partial_\nu b_\rho, \tag{4.9}$$

where g and h are dimensionless couplings. In this expression, $f_{\mu\nu} = \partial_\mu b_\nu - \partial_\nu b_\mu$ and the gauge field is assumed to be compact, $b_\mu \sim b_\mu + 2\pi r n_\mu$, with r the compactification radius and $n_\mu \in \mathbb{Z}$. The theory is quadratic but non-trivial owing to its solitonic spectrum of electric and magnetic excitations. Note that for $h = 0$, the loop model (4.9) is the same as the surface theory, in the form (4.8), by using the expression of the kernel (4.5) and identifying the couplings by

$$g = \frac{k^2}{g_0} \qquad h = 0. \tag{4.10}$$

The action (4.9) can be written in terms of degrees of freedom that are conserved currents:

$$j^\mu = \frac{1}{2\pi}\varepsilon^{\mu\nu\rho}\partial_\nu b_\rho. \tag{4.11}$$

Once formulated on a Euclidean lattice, it defines a statistical model where currents describe random loops that interact by the potential $\int j_\mu (1/x^2) j^\mu$, giving rise to an interesting phase diagram. In this formulation, the theory is called 'loop model'. In the following we shall consider this theory in the case $h = 0$, to preserve time-reversal invariance.

4.2.1 Phase diagram

In this section, we determine the phase diagram of the model by using Peierls arguments [112]. These amounts to estimating the probability P for creating a 'disorder' excitation above the 'ordered' ground state:

$$P \propto \exp(-\beta \Delta F) = \exp(-\beta \Delta E + \Delta S). \tag{4.12}$$

If the energy cost ΔE of the excitation exceeds the entropy ΔS (logarithm of the multiplicity) in the thermodynamic limit, then the excitation is suppressed and the ordered phase is stable; otherwise the entropy wins and excitations proliferate, leading to a disordered (massive) phase.

A well-known examples is given by the estimate of free energy for one vortex in the massless phase of the XY spin model in two dimensions [112]. In this case, both energy and entropy grow logarithmically with the system size L, leading to $\beta \Delta F \sim (\beta - \beta_c) \log(L/a)$ (a is the lattice size, the UV cut-off). One finds that the massless phase is stable for $\beta > \beta_c$, i.e. $P \to 0$ for $L \to \infty$, while the disordered phase takes place for $\beta < \beta_c$. The massless phase corresponds to the critical line of the compactified boson conformal theory with central charge $c = 1$. Thanks to exact bosonization in $(1 + 1)$ dimensions, the bosonic theory describes both free and interacting massless fermions at different points of the critical line.

The loop model presents a similar behavior in one dimension higher, with a massless phase corresponding to the critical line $g > g_c$. In order to prove this fact, let us consider the action (4.9), with $h = 0$, but adding a local Yang-Mills term:

$$S[a_\mu] = \frac{g}{16\pi^3} \int d^3x \, d^3y \, f_{\mu\nu}(x) \frac{1}{(x - y)^2} f_{\mu\nu}(y) + \frac{t}{M} \int d^3x \, f_{\mu\nu} f_{\mu\nu} . \tag{4.13}$$

In this expression, g and t are dimensionless couplings and M is a mass scale. Note that in absence of matter fields, the Yang-Mills term is actually irrelevant in the renormalization-group sense.

Compact gauge fields, say on a lattice, possesses isolated monopole configurations, that obey the quantization condition:

$$\int_{S^2} f = 2\pi \frac{M_0}{q_0}, \quad M_0 \in \mathbb{Z}, \tag{4.14}$$

where f is the gauge field two-form and q_0 is the minimal charge in the theory, trade-off for the compactification radius.

The evaluation of the loop model action (4.13) for one monopole configuration of minimal magnetic charge ($M_0 = 1$) is carried out in Appendix C, leading to the following free energy:

$$\beta \Delta F = \frac{1}{2q_0^2} \left(\frac{g}{\pi} \log \left(\frac{L}{a} \right) + \frac{t}{Ma} \right) - 3 \log \left(\frac{L}{a} \right) . \tag{4.15}$$

We see that the non-local term yields a logarithmic energy, while the local Yang-Mills action gives a constant. The entropy is also logarithmic, counting the number of lattice cubes which can host monopoles. Therefore, in ordinary Yang-Mills theory ($g = 0$), the entropy always dominates and monopoles proliferate: the system is disordered for any

coupling and the ground state is gapped. We recover here Polyakov's result that compact Abelian Yang-Mills theory in $(2 + 1)$ dimensions is massive and confines charges [113].

The non-local term provides a completely different dynamics, allowing for a stable massless phase without monopoles for $g > g_c \sim 6\pi q_0^2$, which corresponds to the critical line of the loop model. The analogy with the XY model in one lower dimension is apparent.

In the massless phase $g > g_c$, we can consider other excitations corresponding to closed loops of flux lines. Let us now estimate whether large loops of length R are allowed or suppressed as a function of the couplings g and t. The number of possible configurations is given by the number of closed paths of length R one can draw on the lattice. In the thermodynamic limit, this quantity amounts to $5^{(R/a)}$ for a cubic lattice, leading to the entropy

$$\Delta S = k_B \frac{R}{a} \ln(5) \,. \tag{4.16}$$

The energy contribution is obtained by considering a line of flux ϕ directed along the z-axes. The configuration of the field $f_{12} = \Phi \, \delta(x)\delta(y)$, for $0 < z < R$ determines a linear energy contribution in the size of the loop R,

$$\beta \Delta E = \left(\frac{g\Phi^2}{16\pi^3} + \frac{t}{Ma} \right) \frac{R}{a} \,. \tag{4.17}$$

In conlusion, in the 'ordered' phase $g > g_c$, the free energy of a loop of length R turns out to be:

$$\beta \Delta F = \left(\frac{g\Phi^2}{16\pi^3} + \frac{t}{Ma} \right) \frac{R}{a} - k_B \ln(5) \left(\frac{R}{a} \right) \,, \quad (g > g_c) \,. \tag{4.18}$$

We see that both the local and nonlocal terms contribute to the energy of closed loops and that energy and entropy can balance. The condition $\beta \Delta F = 0$ defines the critical line $t_c(g) = a - bg$, with a, b positive constants, in the plane (g, t): this line separates the (massive) phase $t < t_c(g)$, in which large loops proliferate, from the phase $t > t_c(g)$ in which loops are tiny. Another interesting line is given by the condition of vanishing energy (Euclidean action) $g + ct = 0$, with c positive constant, below which the theory is not defined.

The loop model with action (4.13) has been simulated on a lattice in Ref.[108]: Fig.4.1 shows the numerical results for the phase diagram in the (g, t) plane, that are in qualitative agreement with the Peierls estimate (4.18). We remark that the simulation enforces the closed loop condition and cannot see the $g < g_c$ phase of free monopoles. We also note that the coupling t is irrelevant and thus disappears in the IR limit: therefore, in the low-energy effective action there remains the non-local term and the phase diagram reduces to the critical line parameterized by $g > g_c$.

4.3 Loop model and dualities

A duality of field theories is the possibility to represent the same physical system with two or more theories with different degrees of freedom, for instance fermions or bosons. The best known example is the Kramers-Wannier duality of the bidimensional Ising model [10]. This corresponds to a change of variables in the partition function which maps the system with temperature $1/\beta$ into the same system with temperature $\propto \beta$. This provides
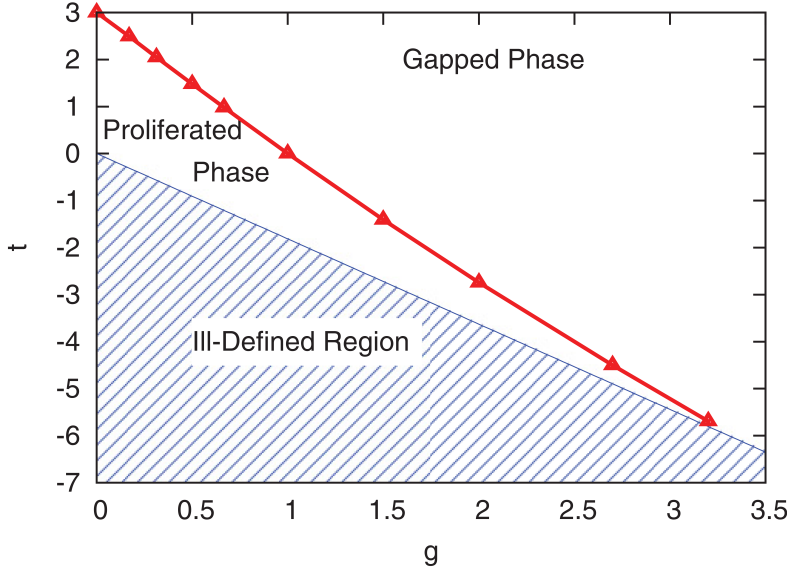
Figure 4.1: Phase diagram of the loop model found by numerical simulation [108]. The two phases with proliferating and small closed loops are separated by the critical line $t_c(g)$ drawn in red. Let us note the presence of the ill-defined region where the Euclidean action is negative.

a relation between low-temperature and high-temperature phases and maps order into disorder variables.

In this thesis we have already discuss an example of duality: in Chapter 1 we saw that bosonic massive particles can acquire fermion statistic once coupled to a Chern-Simons field. Recently it was supposed that this correspondence hold in the low-energy limit even for relativistic massless particles. For instance, the Abelian Higgs model at the critical point is believed to be dual to a massless Dirac fermion [114, 115]. Many other dualities were found which form the so called 'duality web' in $(2 + 1)$ dimensions [116, 117, 118, 119]. In order to verify these dualities, one would need to solve the interacting theories: in practice, we can consider computable limits like for instance large number of fields N. In this context, the loop model is relevant: it turns out that the dualities transformations are exact in this theory and are represented by $SL(2, \mathbb{Z})$ maps of the complex coupling constant $\tau = h + ig$, as we now describe.

4.3.1 Bosonic particle-vortex duality

The bosonic particle-vortex duality is schematically written as follows [120, 117]:

$$\mathcal{L}_B[\phi] + j_\mu^{(\phi)} A_\mu \sim \widetilde{\mathcal{L}}_B[\varphi] + j_\mu^{(\varphi)} a_\mu + \frac{i}{2\pi} a dA . \tag{4.19}$$

In this expression, on the l.h.s. the charge density $j_0^{(\phi)}$ of the ϕ field couples to the electric potential A_0: on the r.h.s., the a_0 equation of motion imply $j_0^{(\varphi)} \propto \varepsilon^{ij} \partial_i A_j$, meaning that the dual bosonic field φ is magnetically charged. This fact explains the name particle-vortex, or electric-magnetic transformation. In equation (4.19), all fields but the

background A_μ are supposed to be integrated over. Let us observe that the Lagrangians $\mathcal{L}_B$ and $\widetilde{\mathcal{L}}_B$, in general, contain self-interactions parameterized by some couplings. These are mapped from one side of (4.19) to the other by the duality map.

The partition functions of the two theories (4.19) in the external background, $Z[A]$ and $\widetilde{Z}[A]$, are related by the following map:

$$Z[A] = \int \mathcal{D}a_\mu \, \widetilde{Z}[a] \exp\left(\frac{i}{2\pi}\int adA\right). \tag{4.20}$$

Let us verify this relation for the loop model. Consider the action (4.9), including the term $h \neq 0$ for generality, and couple it to the background A as in (4.8). It can be rewritten as

$$S[b, A] = \frac{1}{4\pi}\int d^3x d^3y \, b_\mu(x) D_{\mu\nu}(g, h)(x, y) b_\nu(y) + \frac{i}{2\pi}\int bdA \tag{4.21}$$

in terms of the kernel

$$D_{\mu\nu}(g, h) = g\frac{1}{\partial}\left(-\delta_{\mu\nu}\partial^2 + \partial_\mu\partial_\nu\right) + ih\varepsilon_{\mu\nu\rho}\partial_\rho. \tag{4.22}$$

Next, use the action (4.21) to express $\widetilde{Z}[a]$ in (4.20). Integrating over the a and b fields, we obtain the induced action

$$Z[A] = \exp\left(-\frac{1}{4\pi}\int A_\mu D_{\mu\nu}(g, h)A_\nu\right). \tag{4.23}$$

Let us now check that $\widetilde{Z}[A]$ takes the same form as $Z[A]$, thus proving the duality map. We integrate the b field in (4.21) by using the algebraic identity

$$\int d^3x \, d^3y \, j_\mu D^{-1}(g, h)_{\mu\nu} j_\nu = \int d^3x \, d^3y \, a_\mu D_{\mu\nu}(\widehat{g}, \widehat{h}) a_\nu, \tag{4.24}$$

$$\widehat{g} = \frac{g}{g^2 + h^2}, \qquad \widehat{h} = \frac{-h}{g^2 + h^2}, \qquad j_\mu = \varepsilon_{\mu\nu\rho}\partial_\nu a_\rho, \tag{4.25}$$

$$\text{i.e.} \qquad \widehat{\tau} = \widehat{h} + i\widehat{g} = -1/\tau, \qquad \tau = h + ig. \tag{4.26}$$

It follows that $\widetilde{Z}[A]$ takes the same form (4.23) with coupling constants:

$$\widetilde{\tau} = -\frac{1}{\tau}. \tag{4.27}$$

Note that this map of the complex coupling constant τ defines the S generator of the $SL(2, \mathbb{Z})$ group.

Therefore, the loop model is explicitly self-dual [110, 111]. The physical meaning of this result will be more clear in the following, where we shall see that this theory corresponds to electrodynamics in the limit of large number $N_f \to \infty$ of matter fields.

A nice aspect of the duality transformation (4.20) is that it amounts to a Legendre transformation. Let us rewrite it,

$$\widetilde{S}[\mathcal{J}] = S[A] - \int \mathcal{J}^\mu A_\mu, \qquad \mathcal{J} = \frac{1}{2\pi} *(da). \tag{4.28}$$

This can be seen as a change of variable from the background A to the 'effective field' $\mathcal{J}$, where the new 'effective potential' $\widetilde{S}[\mathcal{J}] \equiv \widetilde{S}[a]$ is equal to the dual action. As is

well known, the second derivatives of Legendre transformed potentials S and $\widetilde{S}$ w.r.t. the respective variables are the inverse of each other, $\delta^2 S/\delta A_1 \delta A_2 \sim \left(\delta^2 \widetilde{S}/\delta \mathcal{J}_1 \delta \mathcal{J}_2\right)^{-1}$. The first variation w.r.t. to the background defines the induced current, while the second derivative is related to the conductivity. As a consequence, duality implies a reciprocal relation between the conductivity tensors, $\sigma_{ij}(\tau)$ and $\widetilde{\sigma}_{kn}(\widetilde{\tau})$, $i, j, k, n = 1, 2$, in the two theories, [106]:

$$\varepsilon^{ij}\, \sigma_{jk}(\tau)\, \varepsilon^{kn}\, \widetilde{\sigma}_{nm}(\widetilde{\tau}) = \frac{1}{4\pi^2}\delta^i_m \,. \tag{4.29}$$

4.3.2 Fermionic particle-vortex duality

The electric-magnetic duality for fermionic theories is conjectured to be [120, 117]:

$$\mathcal{L}_F[\psi] + j^{(\psi)}_\mu A_\mu \sim \widetilde{\mathcal{L}}_F[\chi] + j^{(\chi)}_\mu a_\mu + \frac{i}{4\pi}adA \,, \tag{4.30}$$

with the fermion field ψ and χ are dual. The map is the same as for bosonic fields (4.19) up to a normalization of the statistical field a.

As will be clear in the following, the loop model describes both (the large N limit of) bosonic and fermionic theories; thus, we can apply the map (4.30) to the effective action (4.23) again and obtain the relation (4.27) between the couplings up to a factor of four. Upon defining the 'fermionic' version of the loop model with shifted coupling $\tau_F = 2\tau$, we can write the fermionic duality (4.30) as:

$$\widetilde{\tau}_F = -\frac{1}{\tau_F}, \qquad \tau_F = 2\tau \equiv 2\tau_B. \tag{4.31}$$

4.3.3 Boson-fermion duality

Let us now consider the boson-fermion transformation:

$$\mathcal{L}_B[\varphi] + J_{B\mu}a_\mu + \frac{i}{4\pi}ada + \frac{i}{2\pi}adA \sim \mathcal{L}_F[\psi] + J_{F\mu}A_\mu - \frac{i}{8\pi}AdA \,. \tag{4.32}$$

On the bosonic side, first a Chern-Simons term ada is added that changes the statistics of particles; then the particle-vortex transformation (4.19) is applied. On the right side, note that the parity anomaly of the fermion is subtracted, as expected by the fact that the boson theory in $(2+1)$ dimensions does not suffer of this anomaly. The transformations on the bosonic left-hand side can be carried out in the loop model, where they correspond to the following maps:

$$T : \tau_B \ \to \ \tau_B + 1, \qquad S : \tau_B + 1 \ \to \ -\frac{1}{\tau_B + 1} \,. \tag{4.33}$$

On the fermionic side, the subtraction of the anomaly term corresponds to $T^{-1} : \tau_F \to \tau_F - 1$, taking into account the different normalization of the fermionic model (4.31) just discussed. The combined map is therefore:

$$-\frac{1}{\tau_B + 1} = \frac{\tau_F - 1}{2} \qquad \longrightarrow \qquad \tau_F = \frac{\tau_B - 1}{\tau_B + 1} \,. \tag{4.34}$$

Therefore, the loop model explicitly realizes the boson-fermion duality.

In the literature, the dualities of Abelian theories in $(2+1)$ dimensions have been related to those of Yang-Mills theory in $(3+1)$ dimensions [121] [116, 118, 109]. This fact can be explained within the bulk-boundary correspondence discussed in previous chapter: the topological bulk action (3.22) possesses the theta-term $\theta/8\pi^2 \int da\,da$, that under periodicity, $\theta \to \theta + 2\pi$, produces a Chern-Simons action at the boundary corresponding to the T transformation $\tau_B \to \tau_B + 1$ discussed above. Moreover the S transformations in $(3+1)$ and $(2+1)$ dimensions can be shown to correspond to each other.

Let us remark that the boson-fermion map (4.34) can be written group theoretically as follows:

$$\tau_F = T\Lambda ST(\tau_B)\,, \tag{4.35}$$

where appears another transformation $\Lambda : \tau_B \to \tau_F = 2\tau_B$ that does not belong to the $SL(2,\mathbb{Z})$ group. In matrix notation, it is diagonal, $\Lambda = \mathrm{diag}(2,1)$, with determinant 2. However, this transformation cannot be iterated, i.e. Λ^n does not make sense for $n \in \mathbb{Z}$, beside $n = 0, \pm 1$. Thus, it is not an ordinary group element and does not enlarge the duality group.

In conclusion, dualities including both bosonic and fermionic theories belong to the group $SL(2,\mathbb{Z})$, keeping in mind the coupling normalization just discussed. In the following, we do not discuss these issues any further because we are mostly concerned in the analysis of the bosonic loop model with vanishing Chern-Simons term ($h = 0$), for which the inversion $g \to 1/g$ suffices.

4.4 Electrodynamics in the large-N limit and loop model

The loop model is an unusual field theory because it does not contain a standard kinetic term. In this section, we will discuss the theories of $(2+1)$-dimensional particles interacting with $(2+1)$-dimensional photons, i.e. electrodynamics (QED_3), or with $(3+1)$-dimensional photons, corresponding to a mixed-dimensional modification called $QED_{4,3}$ [106] [107]. We will show that they both reduce to the loop model in the limit of large number of matter fields.

4.4.1 Loop model and QED_3

The action of QED_3 with N_F massless fermionic fields is,

$$S_{QED_3}[\psi, A] = \int d^3x \sum_{n=1}^{N_F} \bar{\psi}_n(i\slashed{\partial} - \slashed{A})\psi_n + \frac{1}{4e^2} \int d^3x\, F_{\mu\nu}F_{\mu\nu}\,. \tag{4.36}$$

Integration of the fermions produces the determinant of the Dirac operator raised to the N_F power. A simplification occurs in the large N_F-limit: by keeping the coupling $\lambda = e^2 N_F$ finite, the expansion of the determinant in powers of A_μ is dominated by the quadratic term and the higher orders are subdominant by powers of $N_F^{-1/2}$. Thus, the large-N_F limit gives us

$$Z = \int \mathcal{D}A \exp\left\{\mathrm{tr}\left(-\frac{\lambda}{2}\frac{1}{i\slashed{\partial}}\slashed{A}\frac{1}{i\slashed{\partial}}\slashed{A}\right) - \frac{1}{4}\int d^3x\, F_{\mu\nu}F_{\mu\nu}\right\}, \quad (N_F \to \infty)\,. \tag{4.37}$$

The first term is exactly the action in electromagnetic field induced by the dynamics of the free fermion (3.13). The effective action for large N_f is therefore given by

$$S_{QED_3}[A] = \frac{1}{2} \int A_\mu \left(\frac{1}{16} \frac{1}{\partial} + \frac{1}{\lambda} \right) \left(-\delta_{\mu\nu} \partial^2 + \partial_\mu \partial_\nu \right) A_\nu + i \frac{\eta}{8\pi\lambda} \int AdA, \qquad (4.38)$$

where we have rescaled the field $A_\mu \to A_\mu / \sqrt{\lambda}$. The parity anomaly term has a $\pm$ sign ambiguity for each fermion component, that can be resolved, as we have previously seen, by considering the limit $m \to 0^\pm$ of massive fields [86]. Without knowing this information or other physical input on the theory, we can only say that the parameter η in (4.38) is an integer taking one value in the interval $-N_F \le \eta \le N_F$.

Since the action is quadratic in electromagnetic field, we can directly read the propagator of the theory that assumes the form:

$$G_{\mu\nu}(k) = (\delta_{\mu\nu} k^2 - k_\mu k_\nu) \frac{16\lambda}{\lambda k + 16k^2}, \qquad (4.39)$$

where, for simplicity, we set the anomalous term to zero.

In the IR ($k \ll \lambda$) and UV ($k \gg \lambda$) regimes, the propagator becomes:

$$G_{\mu\nu}(k) = -(\delta_{\mu\nu} k^2 - k_\mu k_\nu) \begin{cases} \dfrac{\lambda}{k^2} & k \gg \lambda, \\[2mm] \dfrac{16}{k} & k \ll \lambda. \end{cases} \qquad (4.40)$$

Therefore the Maxwell term is irrelevant in the IR for any value of λ leading to the action:

$$S_{QED_3}[A] \sim \frac{1}{32} \int d^3x \, d^3y \, A_\mu \left(\frac{-\delta_{\mu\nu} \partial^2 + \partial_\mu \partial_\nu}{\partial} \right) A_\nu . \qquad (4.41)$$

We conclude that the large-N_F/low-energy effective theory for QED_3 is described by the loop model for values of the couplings $(g, h) = (\pi/4, \eta/\lambda)$ (using the fermion normalization (4.31)).

4.4.2 Loop model and $QED_{4,3}$

We now study the electrodynamics in $(3+1)$ dimensions, in which photons live in the whole space-time $\mathcal{M}_4$, while fermions are confined in the hyperplane $\mathcal{M}_3$. The Euclidean action is [105, 106],

$$S_{QED_{4,3}}[\psi, A] = \int_{\mathcal{M}_3} d^3x \sum_{n=1}^{N_F} \bar{\psi}(i\slashed{\partial} - \slashed{A})\psi + \frac{1}{4e^2} \int_{\mathcal{M}_4} d^4x \, F_{\mu\nu} F_{\mu\nu} . \qquad (4.42)$$

This theory is very interesting because it maps into itself under the fermionic particle-vortex duality (4.30) [106]. Let us review this result for $N_F = 1$.

We denote the coordinates as $X^\mu = (x^\alpha, x^3)$, and identify the hyperplane by $x^3 = 0$. The integration of the A_μ field in (4.42) leads to the term

$$S[j] \sim \int j_\alpha(x) \left(\frac{1}{-\partial_{(4)}^2}(x,y) \right) \Bigg|_{x_3 = y_3 = 0} j_\alpha(y), \qquad \alpha = 0, 1, 2, \qquad (4.43)$$

where three-dimensional currents interact with the four-dimensional propagator restricted to the hyperplane. The Green function of the four-dimensional Laplacian $\partial^2_{(4)}$ on the hyperplane can be written as:

$$\left.\frac{1}{-\partial^2_{(4)}}(X,Y)\right|_{x^3=y^3=0} = \int \frac{d^3p}{(2\pi)^3} e^{ip\cdot(x-y)} \int_{-\infty}^{\infty} \frac{dp_3}{2\pi} \frac{1}{p^2+p_3^2} = \frac{1}{2}\frac{1}{\partial}(x,y) \,, \qquad (4.44)$$

i.e. it corresponds to the kernel of the loop model. Therefore, we obtain the following three-dimensional action with long-range current-current interaction:

$$S_{QED_{4,3}}[\psi] = \int_{\mathcal{M}_3} \bar{\psi} i \slashed{\partial} \psi + \frac{e^2}{4} j_\alpha^{(\psi)} \frac{1}{\partial} j_\alpha^{(\psi)} \,, \qquad (4.45)$$

with $j_\alpha^{(\psi)} = \bar{\psi}\gamma_\alpha\psi$.

The dual theory with coupling constant $\widetilde{e}$ is obtained by applying the particle-vortex transformation (4.30) to (4.42):

$$\widetilde{S}_{QED_{4,3}}[\chi,a,A] = \int_{\mathcal{M}_3} d^3x \left[\bar{\chi}(i\slashed{\partial} - \slashed{a})\chi - \frac{i}{4\pi}\varepsilon_{\mu\nu\rho}a_\mu\partial_\nu A_\rho \right]$$
$$+ \frac{1}{4\widetilde{e}^2}\int_{\mathcal{M}_4} d^4x\, F_{\mu\nu}F_{\mu\nu} \,, \qquad (4.46)$$

where a_μ is the statistical field. Integration over the A_μ field following the same steps as before leads to the three-dimensional action:

$$\widetilde{S}_{QED_{4,3}}[\chi,a] = \int_{\mathcal{M}_3} \bar{\chi}(i\slashed{\partial} - \slashed{a})\chi + \frac{\widetilde{e}^2}{64\pi^2}\, a_\mu\left(\frac{-\delta_{\mu\nu}\partial^2 + \partial_\mu\partial_\nu}{\partial}\right)a_\nu \,. \qquad (4.47)$$

Finally, integrating out a with the help of the loop-model identity (4.26) gives,

$$\widetilde{S}_{QED_{4,3}}[\chi] = \int_{\mathcal{M}_3} \bar{\chi} i\slashed{\partial} \chi + \frac{16\pi^2}{\widetilde{e}^2}\, j_\mu^{(\chi)} \frac{1}{\partial} j_\mu^{(\chi)} \,, \qquad (4.48)$$

where $j_\mu^{(\chi)} = \bar{\chi}\gamma_\mu\chi$.

The comparison of the actions (4.45) and (4.48) establishes the self-duality of $QED_{4,3}$ with coupling constant relation:

$$\widetilde{e} = \frac{8\pi}{e} \,. \qquad (4.49)$$

The duality implies a inverse relation between the conductivities of the two theories, as discussed before [106]. Analogue results are obtained in the case of electrodynamics of scalar particles [107]; there is a difference of a factor of two in the relation (4.49), i.e. $\pi \to \pi/2$, stemming from the duality transformations (4.19) and (4.30).

Let us now discuss the large N_F-limit of $QED_{4,3}$. It is convenient to start from the dual action (4.47): the integration over the fermions yields as in the QED_3 the N_F power of the determinant. Its quadratic approximation holds for $N_F \to \infty$, leading to the following action

$$S_{QED_{4,3}}[a] = \left(\frac{1}{32} + \frac{\widetilde{e}^2}{64\pi^2 N_F}\right) \int d^3x, d^3y\, a_\mu\left(\frac{-\delta_{\mu\nu}\partial^2 + \partial_\mu\partial_\nu}{\partial}\right)a_\nu \,, \qquad (4.50)$$

where we have rescaled a_μ as $a_\mu \to a_\mu/\sqrt{N_F}$. The duality relation (4.49) imply that $\tilde{e}^2/N_F = 32\pi^2/\lambda$ and thus the action becomes[2]:

$$S_{QED_{4,3}}[a] = \left(\frac{1}{32} + \frac{1}{\lambda}\right) \int a_\mu \left(\frac{-\delta_{\mu\nu}\partial^2 + \partial_\mu\partial_\nu}{\partial}\right) a_\nu. \tag{4.51}$$

We conclude that $QED_{4,3}$ in the large N_F-limit is equivalent to the fermionic loop model (4.9) with coupling constant:

$$g = \pi \left(\frac{1}{4} + \frac{8}{\lambda}\right). \tag{4.52}$$

This result is very important because it establishes that the loop model is the limit of a viable theory of interacting electrons. One can think that the higher-dimensional photons on the surface of three-dimensional topological insulators could be physical and not merely a technical advantage. However, Hansson suggested us that if the photon was physical, the velocity of the conformal surface modes would equal the speed of light and that is not true as we are going to show in the next sections.

We conclude this section by adding some remarks:

- Eq. (4.52) shows that the dimensionless coupling constant $\lambda > 0$ of $QED_{4,3}$ remap the critical line $g > 1$ of the loop model. Note that QED_3 is found at the point $\lambda = \infty$ on this line.

- It is believed that $QED_{4,3}$ possesses a critical line also for finite N_F [122], that then spans $e^2 < 8\pi$ owing to the self-duality (4.49). Note, however, that the finite-N_F self-duality does not survive the large N_F limit and is replaced by the loop model duality at $N_F = \infty$.

- Finally, the analysis of scalar $QED_{4,3}$ in the large N_B limit reproduces again the loop model up to numerical factors in the coupling constant relation (4.52). Indeed, the quadratic expansion of the bosonic determinant has the same expression of the fermionic theory, but without the anomalous Chern-Simons term.

4.5   Quantization of the loop model on $\mathbb{T}^3$

We analyze the surface excitations of topological insulators with loop-model dynamics, as discussed in Section 4.1, for a toroidal geometry. We recall the expression of the action (4.3):

$$S_{surf}[a, \zeta, A = 0] = \frac{ik}{2\pi} \int \zeta da + \frac{g_0}{4\pi} \int a_\mu \left(\frac{-\delta_{\mu\nu}\partial^2 + \partial_\mu\partial_\nu}{\partial}\right) a_\nu, \tag{4.53}$$

where the A background has been switched off. This is the loop model without the anomalous Chern-Simons term, that, in TR topological insulators, is cancelled by the bulk. We consider a solid spatial torus $\mathbb{T}^2 \times I$ as the bulk of the system. The Euclidean surface theory is thus defined on the manifold $\mathcal{M}_3 = \mathbb{T}^2 \times S^1_\beta = \mathbb{T}^3$, with β being the period of the imaginary time. The non-trivial part of the surface dynamics is given by the solitonic excitations as in the case of the local bosonic theory analyzed in Section 3.4.1.

---

[2]We disregard the parity anomaly term

In addition, the compactness of the a field allows for magnetic solitons. The corresponding condition reads:

$$\int_{\mathbb{T}^2} \varepsilon^{ij} \partial_i a_j = \frac{2\pi}{q_0} M_0, \qquad M_0 \in \mathbb{Z}, \tag{4.54}$$

where q_0 is the minimal charge for the a field.

The usual method of quantization is based on expanding the fields in solitonic and oscillator parts and evaluate the partition function in terms of classical action and fluctuations around it. This analysis is not possible for the non-local theory (4.53) that does not have a Hamiltonian formulation and is not well defined on-shell.

This problem can be solved by a trick: we reformulate the loop model as a local theory in $(3+1)$ dimensions, as we now explain. We get inspired by the mixed-dimension $QED_{4,3}$: as seen in the previous section, integration of the $(3+1)$-dimensional photons yields the non-local loop model interaction on the $(2+1)$-dimensional surface.

We introduce an extra dimension and define the following action:

$$S_4[\hat{a}, \zeta] = \frac{1}{4e^2} \int_{\mathcal{M}_4} d^4x \, (\partial_\mu \hat{a}_\nu - \partial_\nu \hat{a}_\mu)^2 + i\frac{k}{2\pi} \int_{\mathcal{M}_3} a d\zeta. \tag{4.55}$$

The geometry $\mathcal{M}_3$ is the torus $\mathbb{T}^3$ with the following euclidean period vectors ω_i with $i = 0, 1, 2$,

$$\omega_1 = (0, 2\pi R_1, 0), \quad \omega_2 = (0, 0, 2\pi R_1), \quad \omega_0 = (2\pi T = \beta, 0, 0), \tag{4.56}$$

where R_1 and R_2 are the radii of the two non-trivial cycles Γ_1 and Γ_2 of the spatial torus. The four dimensional extension $\mathcal{M}_4$ is obtained by adding a straight direction with coordinate $x_3 \in \mathbb{R}$, such that the three torus is located at $x_3 = 0$. This geometry is represented in Fig.4.2.

In the expression (4.55), the field $\hat{a}_\mu$ is the four-dimensional extension of a_μ and e is a dimensionaless coupling to be determined later. The three-dimensional part of the action (4.55) can be written as the source term,

$$i \int_{\mathcal{M}_4} J^\mu \hat{a}_\mu, \qquad J_\alpha = \delta(\mathcal{M}_3) \frac{k}{2\pi} \varepsilon_{\alpha\beta\gamma} \partial_\beta \zeta_\gamma, \qquad J_3 = 0, \tag{4.57}$$

where $\delta(\mathcal{M}_3) = \delta(x_3)$ is the delta function on the hyperplane.

The $(3+1)$-dimensional action (4.55) corresponds to ordinary electrodynamics that is well defined on-shell. We can compute its partition function by decomposing the fields $\hat{a}$ and ζ into solitonic and oscillator parts:

$$Z = \sum_{sol\ config} e^{-S_4[\hat{a}_{sol}, \zeta_{sol}]} \int \mathcal{D}\hat{a}_{osc} \mathcal{D}\zeta_{osc} e^{-S_4[\hat{a}_{osc}, \zeta_{osc}]}, \tag{4.58}$$

where $\hat{a}_{sol}$ and ζ_{sol} are classical solutions of the $(3+1)$-dimensional equations of motion obeying the $(2+1)$-dimensional boundary conditions (3.42-3.43) and (4.54).

The integration of oscillator modes of the field $\hat{a}$ in $S_4[\hat{a}_{osc}, \zeta_{osc}]$, following usual steps, leads to the $(2+1)$-dimensional action for (the wave modes of) ζ_μ:

$$S[\zeta] = \frac{k^2 e^2}{16\pi^2} \int \zeta_\mu \left(\frac{-\delta_{\mu\nu}\partial^2 + \partial_\mu\partial_\nu}{\partial} \right) \zeta_\mu. \tag{4.59}$$
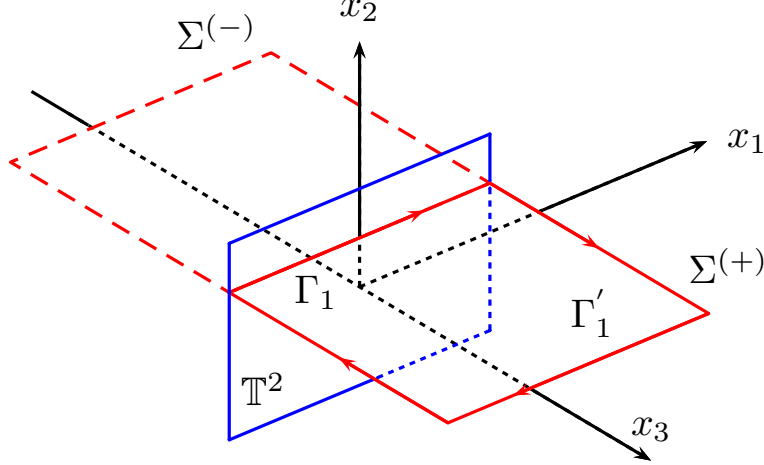
73

Figure 4.2: Three-dimensional extension of the spatial torus $\mathbb{T}^2$. The torus is drawn in blue, while the surfaces $\Sigma^{(+)}$ and $\Sigma^{(-)}$ are in red.

This expression matches the loop model action (4.8), leading to the coupling identification:

$$e^2 = \frac{4\pi}{g_0}. \tag{4.60}$$

In conclusion, the loop model (4.8) has been transformed into the local theory in $(3+1)$ dimensions (4.55). This allows for a proper definition and calculation of solitonic modes.

4.5.1 Evaluation of solitonic modes

The $(3+1)$-dimensional Minkowskian action for static solitonic configuration $S_4[\hat{a}_{sol}, \zeta_{sol}]$ corresponds to the Hamiltonian,

$$S_4[\hat{a}_{sol}, \zeta_{sol}] = -\beta\, H, \qquad H = \frac{1}{2e^2}\int d^3x\left(\mathbf{B}^2 + \mathbf{E}^2\right), \tag{4.61}$$

involving the electric and magnetic fields $\mathbf{E}$ and $\mathbf{B}$ of $\hat{a}_\mu$. The integration is done on the spatial part of $\mathcal{M}_4$ (cf. Fig.4.2), but requires the definition of a finite interval for the extra coordinate x_3

$$x_3 \in [-1/(2M), 1/(2M)] \tag{4.62}$$

where $1/M$ is the infrared cut-off to be discussed later.

Let us now solve the $\hat{a}_\mu(x)$ equations of motion with source term (4.57). The magnetic flux configuration for ζ_μ on $\mathbb{T}^2$ (3.42) determines a constant current J_0 on the $x_3 = 0$ plane, which is coupled to $\hat{a}_0$ by the Poisson equation:

$$\nabla^2 \hat{a}_0 = -e^2 J_0, \qquad J_0 = \delta(x_3)\frac{N_0}{V^{(2)}}, \qquad V^{(2)} = 4\pi^2 R_1 R_2. \tag{4.63}$$

The solution $\hat{a}_0 = \hat{a}_0(x_3)$ is easily found and it determines the electric field component along x_3:

$$E_3 = -\frac{d}{dx_3}\hat{a}_0 = \frac{e^2 N_0}{2V^{(2)}}\mathrm{sign}(x_3). \tag{4.64}$$

The contribution of the electric field to the Hamiltonian (4.61) is obtained by integrating over three-space, with the result:

$$H_{el} = \frac{e^2 N_0^2}{32\pi^2 R_1 R_2 M} . \tag{4.65}$$

Note the presence of the infrared cut-off.

Next we consider the configurations of electric flux for a on the $x^3 = 0$ plane (3.43), given by the line integral on Γ_1. This can be extended to a close circuit on the edge of the surface $\Sigma^{(+)}$ (cf. Fig.4.2); two sides of this contour cancel each other and the contribution Γ_1' at large x_3 vanishes by assumption. Thus, the a line integral can be rewritten as the flux of the magnetic field B_2 through $\Sigma^{(+)}$, leading to:

$$B_2 = \frac{2M}{k} \frac{N_1}{R_1} \mathrm{sign}(x_3) . \tag{4.66}$$

In this expression, the sign function appears for the possible exchange of $\Sigma^{(+)}$ with $\Sigma^{(-)}$. In analogous fashion, the other flux condition (3.43) on Γ_2 determines a magnetic field along x_1:

$$B_1 = \frac{2M}{k} \frac{N_2}{R_2} \mathrm{sign}(x_3) . \tag{4.67}$$

Finally, the magnetic flux configuration for a (4.54) on the $x^3 = 0$ plane is reproduced by the following x_3-independent field component:

$$B_3 = \frac{M_0}{q_0 2\pi R_1 R_2} . \tag{4.68}$$

The total magnetic contribution to the energy is then found to be:

$$H_{mag} = \frac{M_0^2}{4\pi e^2 q_0^2 M R_1 R_2} + \frac{8\pi^2 M}{e^2 k^2} \left(N_1^2 \frac{R_2}{R_1} + N_2^2 \frac{R_1}{R_2} \right) . \tag{4.69}$$

Before writing the solitonic partition function, let us stress that in these results, we chosse the solitonic solutions $\hat{a}_\mu(x)$ to be symmetric under $x_3 \to -x_3$. Indeed we also set a symmetric infrared cut-off (4.62) for simplicity. Asymmetric solutions might be relevant in other physical settings, but we did not consider them.

From the evaluation of the classical solutions we thus obtain the following expression of the solitonic part of the partition function of the loop model on $\mathbb{T}^3$:

$$Z_{sol} = \sum_{N_\mu, M_0 \in \mathbb{Z}} \exp \left\{ -\beta \left[\frac{2\pi g_0 M}{k^2} \left(N_1^2 \frac{R_2}{R_1} + N_2^2 \frac{R_1}{R_2} \right) + \frac{1}{R_1 R_2 M} \left(\frac{N_0^2}{8\pi g_0} + \frac{M_0^2 g_0}{16\pi^2 q_0^2} \right) \right] \right\}, \tag{4.70}$$

where we substituted the coupling g_0 using (4.60). Let us complete the calculation of the partition function before discussing this result.

4.5.2 Oscillator modes

The partition function of the oscillator modes can be obtained from the nonlocal $(2 + 1)$-dimensional Lagrangian (4.59) by computing the determinant of the positive definite Euclidean Laplacian. Choosing the Lorentz gauge, the spectral decomposition reads:

$$S = \frac{k^2}{4\pi g_0} \sum_{n_\alpha \in \mathbb{Z}^3 \neq (0,0,0)} \zeta_\mu(n) \sqrt{(k_n)^2} \zeta_\mu(n) , \tag{4.71}$$

where k_n^μ are the discretized momenta on $\mathbb{T}^3$. The field ζ possesses two physical polarizations, instead of one for local Yang-Mills theory. Thus, the oscillator part of the partition function is given by the determinant,

$$Z_{osc} = \left[\det' \left(\sqrt{-\partial^2} \right) \right]^{-1} = \left[\det' \left(-\partial^2 \right) \right]^{-1/2} , \qquad (4.72)$$

where the prime indicate the elimination of the zero modes. As a matter of fact, this oscillator partition function is equal to that of the local bosonic massless theory in (3.50), discussed in previous Chapter. Let us remark that Z_{osc} is independent of the coupling constant.

In conclusion, the partition function of the loop model on $\mathbb{T}^3$ is given by $Z = Z_{sol} Z_{osc}$, where the expressions of Z_{sol} and Z_{osc} are given in (4.70) and (3.50), respectively.

4.5.3 Interpolating theory and the choice of infrared cut-off

The torus partition function found in the previous section possesses striking similarities with the corresponding quantity in the local scalar theory of surface excitations discussed in Section 3.4. The oscillator part takes the same form; regarding the solitonic sum, let us compare the expression (4.70) with the analogous one of the scalar theory (3.50), reported in Section 3.4.2. We see that the terms parameterized by N_0, N_1, N_2 remarkably match in the two formulas, upon identifying the respective mass parameters by $m = Mg_0/\pi$. On the other hand, the M_0 term for a_μ magnetic solitons is absent in the scalar theory, because the latter corresponds to the longitudinal part of the gauge field, $a_\mu = \partial_\mu \varphi$ (c.f. Section 3.3.2).

This remarkable equivalence can be explained as follows: the two theories are different, but can be matched on-shell. For example, the off-shell induced actions $S_{ind}[A]$ (3.38) and (4.4) are unequal, and this fact originally motivated the study of the non-local theory.

In order to understand these results, we reformulate the loop model by introducing the infrared cut-off as an explicit photon mass $\widetilde{M}$. The modification of the action (4.53) reads:

$$S_{\widetilde{M}} = i \frac{k}{2\pi} \int \zeta da + \frac{g_0}{4\pi} \int a_\mu \left(\frac{\delta_{\mu\nu}(-\partial^2 + \widetilde{M}^2) + \partial_\mu \partial_\nu}{\sqrt{-\partial^2 + \widetilde{M}^2}} \right) a_\mu . \qquad (4.73)$$

In the Lorentz gauge, this becomes:

$$S_{\widetilde{M}}[a, \zeta] = \frac{ik}{2\pi} \int \zeta da + \frac{g_0}{4\pi} \int d^3x \, d^3y \, a_\mu \sqrt{-\partial^2 + \widetilde{M}^2} \, a_\mu . \qquad (4.74)$$

Upon integrating on a, this action describes conserved currents with cut-offed long-range interaction: $\int J_\mu (1/\partial) J_\mu \to \int J_\mu (1/\sqrt{-\partial^2 + \widetilde{M}^2}) J_\mu$. Therefore, $S_{\widetilde{M}}$ can be considered as an equivalent formulation of the loop model, where the cut-off is explicit and not added a-posteriori in the classical field solutions.

Let us now analyze the theory on-shell: the equations of motion for a,

$$- i \frac{k}{2\pi} \varepsilon_{\mu\nu\rho} \partial_\nu \zeta_\rho = \frac{g_0}{2\pi} \sqrt{-\partial^2 + \widetilde{M}^2} a_\mu \to \begin{cases} \dfrac{g_0}{2\pi} \partial a_\mu , & \text{UV} , \\[2ex] \dfrac{g_0}{2\pi} \widetilde{M} a_\mu , & \text{IR} , \end{cases} \qquad (4.75)$$

interpolate between those of the non-local and local theories, Eqs. (3.36) and (4.7). The equation of motion for ζ_μ imposes $a_\mu = \partial_\mu \varphi$: substituting in S_m, we find the reduced action,

$$S_{\widetilde{M}} = \frac{\widetilde{M} g_0}{4\pi} \int d^3 x \, \partial_\mu \varphi \partial_\mu \varphi \, , \qquad \text{(on-shell)} \, . \qquad (4.76)$$

Therefore, the massive non-local action (4.73) is equal to the local action (3.35) on-shell (up to a numerical factor). This implies that the two theories have same solitonic spectra and partition functions. On the other hand, the spectrum of $S_{\widetilde{M}}$ is also equal to that of the loop model in Section 3.1, because they correspond to different choices of cut-off in the same theory. These facts explain the matching of Z_{sol} for the local and nonlocal theories, Eqs. (3.50) and (4.70) (for $M_0 = 0$).

Two conclusions can be drawn from this analysis:

- This on-shell correspondence provides a check for the calculation of soliton configurations in Section 4.5 through the $(3 + 1)$-dimensional extension of the the loop model.

- The IR regularization of the loop model with a fixed mass parameter M violates scale invariance at the quantum level, in disagreement with the fermionic dynamics. Therefore, another choice of cut-off is needed.

Let us consider the cut-off given by the spatial dimension of the system, namely replace $M \to 1/\sqrt{R_1 R_2}$ in the expressions (4.70).

Within this choice, the solitonic partition function Z_{sol} (4.70) of the loop model becomes:

$$Z_{sol} = \sum_{N_0, N_1, N_2, M_0 \in \mathbb{Z}} \exp\left\{ -\beta \frac{1}{\sqrt{R_1 R_2}} \left[\frac{2\pi g_0}{k^2} \left(N_1^2 \frac{R_2}{R_1} + N_2^2 \frac{R_1}{R_2} \right) + \frac{N_0^2}{8\pi g_0} + \frac{M_0^2 g_0}{16\pi^2 q_0^2} \right] \right\} . \qquad (4.77)$$

This expression is manifestly scale invariant and also invariant under $R_1 \Leftrightarrow R_2$.

Let us remark that the choices of 'geometric cut-off' in (4.77) and 'fixed cut-off' in (4.70) and (4.73) actually amount to two different definitions of the non-local theory at the quantum level. In the following we adopt the second choice realizing a scale invariant theory. Further justifications will arise in the study of the partition function on the $S^2 \times \mathbb{R}$ geometry.

4.6 Quantization on the cylinder $S^2 \times \mathbb{R}$

In this section, we present another result of our work [2], the evaluation of the partition function for the manifold $S^2 \times \mathbb{R}$. The choice of this geometry is motivated by the following. As is well-known, the cylinder $S^2 \times \mathbb{R}$ can be mapped to flat space by the conformal transformation $r = R \exp(u/R)$, where r is the radius of $\mathbb{R}^3$ and u is Euclidean time on the cylinder. Time evolution on the cylinder corresponds to dilatations in $\mathbb{R}^3$, thus the energy spectrum gives access to conformal dimensions of the fields in the theory [17, 18] [123, 124]. The partition function is schematically:

$$Z = \sum_\Delta \exp\left(-\beta \frac{v \Delta}{R} \right) , \qquad (4.78)$$

77

where Δ are the conformal dimensions and v is the velocity of massless modes. In topological insulators, these modes live on the surface and their velocity v corresponds to the Fermi velocity of the system, in analogy with the quantum Hall state in $2+1$ dimensions.

The computation of the partition function will follow the same steps as in the previous section using the four-dimensional formulation. We consider the manifold $\mathcal{M}_4 = S^3 \times \mathbb{R}$ and embed the three-dimensional space $\mathcal{M}_3 = S^2 \times \mathbb{R}$ by identifying S^2 with the equator of S^3.

The four-dimensional Minkowskian action (4.55) on $\mathcal{M}_4 = S^3 \times \mathbb{R}$ takes the form:

$$S_4[\hat{a}, \zeta] = -\frac{1}{4e^2} \int_{\mathcal{M}_4} dx \sqrt{-g} g^{\mu\alpha} g^{\nu\beta} \hat{f}_{\mu\nu} \hat{f}_{\alpha\beta} + \frac{k}{2\pi} \int_{\mathcal{M}_3} a\, d\zeta \,, \tag{4.79}$$

where $g_{\mu\nu}$ is the metric tensor on $S^3 \times \mathbb{R}$.

This action is conformal invariant at the classical level: four-dimensional transformations may induce a nontrivial metric on $\mathcal{M}_3$, but this is ineffective on the Chern-Simons action.

4.6.1 Solitonic modes on S^2

The four-dimensional manifold $S^3 \times \mathbb{R}$ is described by the metric $ds^2 = dt^2 - R^2 d\Omega_3^2$, in terms of S^3 polar coordinates, $d\Omega_3^2 = \sin^2 \psi (d\theta^2 + \sin^2 \theta d\varphi^2)$, with $\psi, \theta \in [0, \pi]$ and $\varphi \in [0, 2\pi]$. The S^2 sphere at the equator is identified by $\psi = \pi/2$.

On the geometry of the sphere, there exist global magnetic fluxes for the a and ζ fields. These obey, as in (3.42) and (4.54),

$$\int_{S^2} da = \frac{2\pi}{q_0} M_0 \,, \qquad M_0 \in \mathbb{Z}, \tag{4.80}$$

$$\int_{S^2} d\zeta = \frac{2\pi}{k} N_0 \,, \qquad N_0 \in \mathbb{Z}. \tag{4.81}$$

The electric fluxes for the a field are instead absent because cycles on S^2 are topologically trivial.

Following the same steps as in the previous section, we solve the equations of motion for the action (4.79), with source term localized on $\mathcal{M}_3$. This can be rewritten:

$$\frac{k}{2\pi} \int_{\mathcal{M}_4} \delta(\mathcal{M}_3)\, a\, d\zeta, \qquad \delta(\mathcal{M}_3) = \frac{\delta(\psi - \pi/2)}{R \sin^2(\psi)} \,. \tag{4.82}$$

Note that the form of the delta function is covariant under translations along the ψ coordinate, i.e. displacements of S^2 from the equator of S^3.

The ζ magnetic flux (4.81) amounts to a 'charge density' located at $\psi = \pi/2$ coupled to $\hat{a}_0$ by the Poisson equation,

$$\nabla_\mu \nabla^\mu \hat{a}_0 = -\frac{e^2 N_0}{4\pi R^2} \frac{\delta(\psi - \pi/2)}{R \sin^2(\psi)} \,. \tag{4.83}$$

In this equation, it is natural to assume that $\hat{a}_0$ depends only on ψ, and thus the covariant Laplacian reduces to an ordinary differential equation. The solution is easily found to be:

$$\hat{a}_0(\alpha) = \frac{e^2 N_0}{8\pi R} |\tan(\alpha)| \,, \qquad \alpha = \psi - \frac{\pi}{2} \,. \tag{4.84}$$

The other solitonic solution (4.80) is a magnetic flux for the a field that is orthogonal to S^2 and can be chosen to be a constant for all ψ values, i.e. all embeddings $S^2 \subset S^3$:

$$B_\psi(\psi) = \hat{f}_{\theta\varphi}(\psi) = \frac{M_0}{2q_0} \frac{1}{R^2 \sin^2(\psi)} . \tag{4.85}$$

We now compute the energies associated to the two solitonic solutions (4.84), (4.85). The Hamiltonian is given by

$$H = \frac{1}{2e^2} \int_{S^3} d^3x \sqrt{g} \left[\hat{f}_{i0} \hat{f}_{j0} g^{ij} + \frac{1}{2} \hat{f}_{ij} \hat{f}_{lk} g^{il} g^{jk} \right] , \tag{4.86}$$

where we recognize the electric and magnetic parts. The electric contribution is obtained by inserting the solution (4.84) for $\hat{f}_{\psi 0} = \partial_\psi \hat{a}_0$:

$$H_{el} = \frac{1}{2e^2} \int_{S^3} d^3x \sqrt{g} \, g^{\psi\psi} (\partial_\psi \hat{a}_0)^2 = \frac{N_0 e^2}{32\pi R} \int_{-\pi/2}^{\pi/2} d\alpha \frac{1}{\cos^2(\alpha)} . \tag{4.87}$$

This integral is divergent at the two poles of S^3, $\alpha = \pm\pi/2$: an infrared cut-off is again needed. Let us first introduce a fixed scale, by setting a maximal 'length' $|R\tan(\alpha)| < 1/(2M)$: we obtain the result,

$$H_{el} = \frac{N_0^2}{8g_0 R} \left(\frac{1}{MR} \right) , \tag{4.88}$$

in terms of the loop model coupling g_0 given by (4.60).

The magnetic energy is similarly computed from the solution (4.85):

$$H_{mag} = \frac{1}{2e^2} \int_{S^3} d^3x \sqrt{g} \left(\hat{f}_{\theta\varphi} g^{\theta\varphi} \right)^2 = \frac{M_0^2 g_0}{8q_0^2 R} \int_{-\pi/2+\delta}^{\pi/2-\delta} d\alpha \frac{1}{\cos^2(\alpha)} . \tag{4.89}$$

This is the same divergent integral of the electric contribution: once regularized, it yields:

$$H_{mag} = \frac{M_0^2 g_0}{8q_0^2 R} \left(\frac{1}{MR} \right) . \tag{4.90}$$

Let us stress again that both the field solutions and the infrared cut-off are symmetric under the sign change of the extra coordinate, namely $\alpha \to -\alpha$.

The values of the classical energies (4.87), (4.90) determine the solitonic part of the partition function on the geometry $S^1 \times S^2$:

$$Z_{sol} = \sum_{N_0, M_0 \in \mathbb{Z}} \exp\left\{ -\frac{\beta}{R} \left(\frac{1}{8MR} \right) \left[\frac{N_0^2}{g_0} + \frac{g_0 M_0^2}{q_0^2} \right] \right\} . \tag{4.91}$$

We note again that the fixed cut-off M is incompatible with scale invariance. In analogy with the torus case, we replace this scale with the system dimension, $M = 1/(8\lambda R)$ with λ a numerical constant. We thus obtain:

$$Z_{sol} = \sum_{N_0, M_0 \in \mathbb{Z}} \exp\left\{ -\frac{\beta\lambda}{R} \left[\frac{N_0^2}{g_0} + g_0 \frac{M_0^2}{q_0^2} \right] \right\} . \tag{4.92}$$

The form of Z_{sol} is now in agreement with conformal invariance, Eq. (4.78): the free parameter λ enters in the definition of units of length and time and so in the non-universal Fermi velocity. The expression (4.92) is an important result of our work: we shall analyze it after completing the derivation of partition function.

4.6.2 Oscillator spectrum

The oscillator part Z_{osc} is obtained from the Euclidean $(2+1)$-dimensional action (4.59), by evaluating the determinant of the nonlocal kernel. The action can be rewritten in the form (for $\partial_\mu \zeta^\mu = 0$):

$$S[\zeta] = \frac{k^2}{2\pi g_0} \int_{\mathbb{R}_3} \zeta_\mu(x_1) \frac{\delta^{\mu\nu}}{(x_1 - x_2)^4} \zeta_\nu(x_2). \tag{4.93}$$

Under the conformal map $r = R\exp(u/R)$ from $\mathbb{R}^3$ to $\mathcal{M}_3 = \mathbb{R} \times S^2$, with respective coordinates $x^\mu = (r, \theta, \varphi)$ and $\widetilde{x}^\alpha = (u, \theta, \varphi)$, the action is covariant,

$$S[\zeta] = \frac{k^2}{2\pi g_0} \int_{\mathcal{M}_3} d^3\widetilde{x}_1 d^3\widetilde{x}_2 \sqrt{g(\widetilde{x}_1)g(\widetilde{x}_2)}\, \widetilde{\xi}_\alpha(\widetilde{x}_1) \left(\frac{e^{2(u_1+u_2)/R}}{(x_1-x_2)^4} \right) g^{\alpha\beta}\, \widetilde{\xi}_\beta(\widetilde{x}_2), \tag{4.94}$$

where the transformations are [123, 124], $b_\mu dx^\mu = \widetilde{b}_\alpha d\widetilde{x}^\alpha$, $g^{\alpha\beta} = \delta^{\alpha\beta} e^{(u_1+u_2)/R}$, and the expression in parenthesis is the correlator of scalar conformal fields with dimension $\Delta = 2$ on the cylinder.

The first step in the calculation of the determinant is that of finding the eigenvalues: these are obtained by the spectral decomposition of the $1/x^4$ correlator in the covariant basis of the cylinder, i.e. Fourier modes $\exp(i\omega u)$ and spherical harmonics $Y_\ell^m(\theta, \varphi)$. Next, the determinant is obtained by zeta-function regularization of the product of eigenvalues [123, 124]. This rather long calculation is done in Appendix D: here we report the main steps.

The spectral decomposition reads:

$$\frac{e^{2(u_1+u_2)/R}}{(x_1-x_2)^4} = \frac{8}{R^4} \sum_{\ell=0}^{\infty} \sum_{m=-\ell}^{m=\ell} \int_{\infty}^{\infty} d\omega\, e^{i\omega(u_1-u_2)}\, Y_\ell^m(\theta_1, \varphi_1)\, \lambda_{\omega,\ell}\, Y_\ell^{m*}(\theta_2, \varphi_2), \tag{4.95}$$

where the eigenvalues are,

$$\lambda_{\omega,\ell} = \sum_{k=0}^{\infty} \frac{2k+\ell+2}{(\omega R)^2 + (2k+\ell+2)^2} \frac{\Gamma(k+3/2)\Gamma(k+\ell+2)}{\Gamma(k+\ell+3/2)\Gamma(k+1)}. \tag{4.96}$$

The sum in this expression is ultraviolet divergent because $1/x^4$ is not a proper distribution. Rather surprisingly, it can be evaluated, with result:

$$\lambda_{\omega,\ell} = \left(\sum_{k=0}^{\infty} \frac{1}{2} \right) + \frac{\ell+1}{4} - \frac{\pi}{4} \left| \frac{\Gamma\left((\ell+2+i\omega R)/2\right)}{\Gamma\left((\ell+1+i\omega R)/2\right)} \right|^2. \tag{4.97}$$

The first two terms in this expression, respectively divergent and finite, correspond to functions with support for $x_1 = x_2$ only, that are subtracted for defining the renormalized $1/x^4$ kernel.

Next, the product of eigenvalues can be simplified by using an infinite-product representation of the Gamma function; dropping inessential factors, one finds:

$$\prod_{n\in\mathbb{Z},\, \ell\geq 0} \lambda_{n,\ell} \propto \prod_{n\in\mathbb{Z},\, \ell\geq 0} \widehat{\lambda}_{n,\ell}\,, \qquad \widehat{\lambda}_{n,\ell} = \left(\frac{2\pi n R}{\beta} \right)^2 + \Lambda_\ell, \tag{4.98}$$

where $\lambda_{n,\ell} = \lambda_{\omega,\ell}$ for discretized momentum $\omega = 2\pi n/\beta$ on S^1 and Λ_ℓ refer to angular momentum. The eigenvalues $\widehat{\lambda}_{n,\ell}$ have now the standard form of Laplace-type operators on the geometry $S^1 \times S^2$.

The regularization of the determinant is obtained by introducing the zeta-function:

$$\zeta_{S^1 \times S^2}(s) = \sum_{\ell=\ell_{min}}^{\infty} \sum_{n \in \mathbb{Z}} \frac{\delta(\ell)}{(\widehat{\lambda}_{n,\ell})^s}, \tag{4.99}$$

where $\delta(\ell)$ is the multiplicity of eigenvalues. The analytic continuation from large positive values of $\mathrm{Re}(s)$ to $s \sim 0$ leads to the following expression of the partition function [123, 124],

$$Z_{osc} = \exp\left\{\frac{1}{2}\frac{d}{ds}\zeta_{S^1 \times S^2}(s)\bigg|_{s=0}\right\} = e^{-\beta \mathcal{C}/R} \prod_{\ell=\ell_{min}}^{\infty} \left[1 - \exp\left(-\frac{\beta\sqrt{\Lambda_\ell}}{R}\right)\right]^{-\delta(\ell)}, \tag{4.100}$$

where the Casimir energy $\mathcal{C}/2R$ is obtained by evaluating the further zeta-function,

$$\mathcal{C} = \zeta_{S^2}(-1/2), \qquad \zeta_{S^2}(s) = \sum_{\ell=\ell_{min}}^{\infty} \frac{\delta(\ell)}{\Lambda_\ell^s}. \tag{4.101}$$

The resulting partition function for the loop model takes the form (4.100) with parameters $(\mathcal{C}, \sqrt{\Lambda_l}, \delta(\ell), \ell_{min})$ given in the first line of Table 4.1. The results of other quadratic theories are also reported in this Table for the following discussion.

4.7 Conformal invariance and spectrum of the loop model

In this section, we discuss some interesting information on the spectrum that can be drawn from the expression of $Z = Z_{sol}Z_{osc}$ on $S^1 \times S^2$, Eqs. (4.92) and (4.100).

4.7.1 Particle-vortex duality

The solitonic spectrum in Z_{sol} given by (4.92) involves 'electric' and 'magnetic' quantum numbers N_0 and M_0, respectively. In the fermionic case, corresponding to $k = 1$ and minimal charge $q_0 = 1$, the spectrum is manifestly invariant for $g_0 \to 1/g_0$. This self-duality is expected, because the conformal fields characterize many observables of the theory and should occur in self-dual pairs.

On the other hand, the solitonic spectrum on the torus $\mathbb{T}^3$, given by (4.70) is not self-dual, even for vanishing electric fluxes $N_1 = N_2 = 0$. Actually, the $(2+1)$-dimensional duality is not a symmetry of the partition function, but a Legendre transformation, as explained in Section 4.3.1.

4.7.2 Conformal invariance

The conformal invariance of the loop model is rather natural in the $(3+1)$-dimensional formulation (4.55), but is not obvious in the nonlocal form in $(2+1)$ dimensions (4.53). The quantization procedure has actually shown that scale invariance of the solitonic spectrum is only realized by using a proper IR cut-off. The oscillator part Z_{osc} (4.100) provides further evidences of conformal invariance at the quantum level, as follows:

Theory	dimension	$\mathcal{C}$	$\sqrt{\Lambda_\ell}$	$\delta(\ell)$	ℓ_{min}
loop model	$(2+1)$	0	ℓ	2ℓ	1
conformal scalar	$(2+1)$	0	$\ell + \frac{1}{2}$	$2\ell + 1$	0
vector	$(2+1)$	$\neq 0$	$\sqrt{\ell(\ell+1)}$	$2\ell + 1$	1
conformal scalar	$(3+1)$	$\frac{1}{120}$	ℓ	ℓ^2	1
vector	$(3+1)$	$\frac{3}{20}$	ℓ	$2(\ell^2 - 1)$	2

Table 4.1: Parameters entering in the partition function (4.100) of some quadratic theories [123, 124]: Casimir energy $\mathcal{C}$; energy level $\sqrt{\Lambda_\ell}$; eigenvalue degeneracy $\delta(\ell)$; minimal value ℓ_{min}

.

- In a conformal theory, the Casimir energy on $S^2 \times \mathbb{R}$ is related to the trace anomaly, that vanishes in $(2+1)$ dimensions [123, 124]. The result $\mathcal{C} = 0$ (cf. Table 4.1) matches this expectation.

- In a conformal theory, the descendant (derivative) fields have integer-spaced dimensions. These fields appear in the partition function in the oscillator part (4.100) that indeed shows integer spectrum $\sqrt{\Lambda_\ell} \in \mathbb{Z}$ (cf. first line of Table 4.1). This property is also apparent in the conformal scalar, the second line of Table 4.1. On the contrary, the spectrum of non-conformal Yang-Mills theory $(2+1)$ dimensions (cf. third line) does not have this property: actually, energies do not correspond to scale dimensions, because the theory is not covariant under the conformal map between the sphere and the plane.

4.7.3 Comparison with other theories

The loop model corresponds to the large N limit of mixed-dimension $QED_{4,3}$: it has a quadratic action but is not a free theory. The inclusion of solitonic modes makes it an interesting conformal theory, possessing fields with non-trivial dimensions and correlators. Let us compare it with other conformal theories in Table 4.1.

Besides the integer spaced spectrum already discussed the multiplicities $\delta(\ell)$ are linear in ℓ, a characteristic of $(2+1)$ dimensions, while that of $(3+1)$-dimensional theories are quadratic due to angular momentum on S^3.

Going back to the $(3+1)$-dimensional action (4.55) and integrating over the ζ field, one find that the loop model can be seen as a constrained Yang-Mills theory, enjoying a subspace of its Hilbert space. The comparison between the first and last lines of Table 4.1 shows this fact. In conclusion, the loop model is a conformal theory with mixed-dimension properties.

4.7.4 Anyon excitations

Let us analyze the results of Section 4 for $k > 1$, that are relevant for the dynamics at the surface of interacting topological insulators (cf. Section 2.3). In this case, the partition function (4.91) should describe excitations with fractional charge and statistics in $(2+1)$

dimensions. The subject is well understood for non-relativistic dynamics, as e.g. in the fractional quantum Hall effect. The loop model provides a description in the relativistic scale-invariant domain.

The form of the surface action (4.3) in Section 2.3.4,

$$S_{surf}[a, \zeta, A] = \frac{i}{2\pi} \int (k\zeta da + \zeta dA) + S_{loop}[a] \qquad (4.102)$$

tells us that:

- The ζ field is dual to the background A with minimal charge $e_0 = 1/k$, Eq. (3.25); thus, magnetic excitations of ζ possess minimal charge $\widetilde{e}_0 = 2\pi/k$ in agreement with the quantization condition (3.42).

- The a field is dual to ζ, i.e. it is electric, and possesses minimal charge $q_0 = 1$, as confirmed by the constraint $A \sim ka$ implemented by ζ. Therefore, its monopoles have minimal charge 2π in Eq.(4.54), i.e. $q_0 = 1 \; \forall k$.

- The map between the actions (4.9) and (4.8), i.e. by integrating the a field in (4.3), is a generalization of the particle-vortex duality transformation for theories with fractional charges (cf. Section 4.3.1). In this transformation, the loop-model coupling is mapped into:

$$\widetilde{g}_0 \equiv g = \frac{k^2}{g_0}. \qquad (4.103)$$

These results lead us to consider the solitonic spectrum (4.92) at the electric-magnetic self-dual point $g_0 = k$:

$$E_{sol} = \frac{v}{R} \Delta_{N_0, M_0}, \qquad \Delta_{N_0, M_0} = \frac{1}{2} \left[\frac{N_0^2}{k} + k M_0^2 \right], \qquad (g_0 = k). \qquad (4.104)$$

Upon writing $N_0 = kn + m$, with $m = 0, 1, \ldots, k - 1$ and $n \in \mathbb{Z}$, this spectrum contains states with fractional dimensions $\Delta = m^2/(2k) + \mathbb{Z}$. Thus, there are k independent anyonic sectors in agreement with the value k of the topological order on the $S^2 \times S^1$ geometry (this can be computed from the bulk BF theory, as done for the torus geometry in Section 4.5).

Furthermore, the behaviour of conformal correlators on the surface of topological insulators should match the known Aharonov-Bohm phases between excitations predicted by the BF theory (3.22),

$$\theta = \frac{2\pi n_1 n_2}{k}, \qquad n_1, n_2 \in \mathbb{Z} \qquad (4.105)$$

Let us explain this point in some detail.

As discussed in Ref.[125], order-disorder fields in $(2+1)$ dimensions require: i) Abelian gauge fields and ii) a symplectic structure. Given the equal-time commutation relations,

$$\left[a_i(x, t), \pi^j(y, t) \right] = i\delta_i^j \delta^{(2)}(x - y), \qquad i, j = 1, 2, \qquad (4.106)$$

between the gauge field a and its conjugate momentum π, the order and disorder operators take the form, respectively,

$$\begin{aligned} \sigma(x, t) &= \exp\left(-i\alpha \int_{-\infty}^{x} d\xi^i a_i(\xi, t) \right), \\ \mu(x, t) &= \exp\left(i\beta \int_{-\infty}^{x} d\xi^i \varepsilon_{ij} \pi^j(\xi, t) \right), \end{aligned} \qquad (4.107)$$

83

where the line integrals go to $-\infty$ along a given common direction, e.g. the negative real axis. Using the identity $\varepsilon^{ij}\partial_i\partial_j \mathrm{Arg}(x-y) = \pi\delta^{(2)}(x-y)$, one finds the following (equal-time) monodromy:

$$\mu\left(e^{i2\pi}z, t\right)\sigma(0,t) = e^{i2\alpha\beta}\,\mu(z,t)\sigma(0,t), \qquad\qquad z = x_1 + ix_2\,. \qquad (4.108)$$

In our setting, the term $\int k\,\zeta\,da$ of the action (4.102) gives the symplectic structure with canonical momentum $\pi^i = k/(2\pi)\varepsilon^{ij}\zeta_j$. The exponentials of line integrals (4.107) of the a and ζ fields realize the expected monodromies (4.105) at the surface of the topological insulators, by suitably choosing the α, β parameters.

The dynamics introduced by S_{loop} in (4.102) yields two-point functions of conformal fields, $\langle\phi(x)\phi(0)\rangle = (x^2)^\Delta$. Evaluated at equal time, $x_\mu = (0, x_1, x_2)$, the power-law behavior $|z|^{2\Delta}$ should match the monodromy phase (4.105) for reconstructing the analytic dependence $z^{2\Delta}$ of conformal invariance in the two-dimensional plane. The values of Δ in the spectrum (4.104) do verify this requirement.

In conclusion, the loop model with coupling constant at the self-dual point $g_0 = k$ describes surface excitations with the correct anyonic phases for reproducing the bulk monodromies (4.105). Therefore, the bosonic surface action (4.3) is specified by the single parameter k that span integer points of the critical line of the loop model. Let us remark again the similarity with the quantization of chiral boson in one less dimension. The theory has a critical line, but only discrete points parameterized by odd k value fit the bulk-boundary correspondence.

Chapter 5

Conclusions and Perspectives

In this thesis we have analyzed the boundary theories of quantum Hall states and time-reversal invariant topological insulators. In the first case, we have discussed the geometric responses at the edge of the incompressible Hall fluid. In the second case, we quantized the conformal invariant surface theory for interacting topological insulators.

The first part of this thesis contains our analysis of quantum Hall states where we clarified the bulk-boundary correspondence involving the intrinsic orbital spin s of electrons. Studying the spectrum of multiple branches of CFT at the edge, we were able to identify Casimir-like ground-state values of charge and conformal spin in the edge theory that depend on the orbital spin. This is in agreement with the bulk effective field theory [58] and can be interpreted as due to the extrinsic curvature of the edge. We also discussed the measure of these edge effects by a Coulomb blockade experiment.

Further results in the bulk-boundary correspondence in the quantum Hall effect were briefly discussed in the last section of Chapter 2. We developed an in-depth analysis of the fluctuations of quantum incompressible fluids, by using their dynamical W_∞ symmetry [3]. The construction of generators of these transformations and the bosonization of the two-body interaction led us to go beyond the conformal field theory setting. We can describe excitations that extend from the edge to the bulk interior. This approach provides an interesting scheme for understanding universal bulk physics in the Hall effect beyond the extreme low-energy limit of the topological theory.

In the second part of this thesis, we considered the $(3 + 1)$-dimensional topological insulators and the associated topological BF gauge theory. We analyzed the surface effective field theory and introduced non-local dynamics via the loop model. The formulation of this model as a local theory in $(3 + 1)$ dimensions allowed us to calculate partition functions in two geometries. We showed that this model can be defined to be a conformal invariant theory in $(2 + 1)$ dimensions that bears some similarities with the compactified boson in $(1 + 1)$ dimensions [17]. Its coupling constant spans a critical line along which the spectrum displays fermionic and anyonic excitations, thus providing the bosonization of free and interacting fermions.

Let us mention possible extensions of this line of research:

- The loop model can be generalized by including $1/N_F$ corrections stemming from the relation with the mixed-dimensional electrodynamics $QED_{4,3}$. In this respect, it provides a viable platform for quantitative analysis of duality maps and other

interesting aspects of $(2+1)$-dimensional physics.

- The analysis of order-disorder fields in the loop model can be extended beyond the simple observations of Section 4.7.4. The calculation of correlation functions may reveal the bosonization of fermionic fields in massless theories.

We conclude this thesis by stressing that effective field theory approach has many interesting direction to explore in the study of topological states: in particular, the role of the boundary conformal field theories. The effective theories for other topological phases appearing in the ten-fold classification are largely unknown. In some cases, this approach may explain the modification in the classification due to the interactions between electrons. It is also believed that the topological index should be related to other kinds of anomalies.

Recently, new phases have been introduced that possess stable edge states even if they are massless in the bulk. These are called gapless topological phases. In these cases, the conformal field theory at the boundary is protected by a symmetry in analogy to the symmetry protected topological phases and again allows to understand properties of the bulk.

Acknowledgments

Appendix A

Confining potentials

The simplest model is obtained by adding a quadratic confining potential $V = v|z|^2/R$ to the Landau level Hamiltonian in (1.3), as follows:

$$H^{(2)} = H + V = 2a^\dagger a + 1 + \frac{v}{R}\left(a^\dagger a + b^\dagger b + 1 + a^\dagger b^\dagger + ab\right), \qquad (A.1)$$

where z and $\bar{z}$ are expressed in terms of the a and b oscillators (2.7). The exact spectrum of H (A.1) can be obtained by a Bogoliubov transformation in the two-dimensional space of the oscillator pair (a, b), leading to the new pair (A, B) defined by:

$$\begin{cases} A = \cosh\left(\phi_b\right)a + \sinh\left(\phi_b\right)b^\dagger, & (A.2) \\ B = \cosh\left(\phi_b\right)b + \sinh\left(\phi_b\right)a^\dagger, & (A.3) \end{cases}$$

with $\tanh(2\phi_b) = \frac{v}{v+R}$. The result is:

$$H^{(2)} = \left(1 + \sqrt{1 + \frac{2v}{R}}\right)A^\dagger A + \left(\sqrt{1 + \frac{2v}{R}} - 1\right)B^\dagger B + \text{const.} . \qquad (A.4)$$

After the transformation, the angular momentum is $J = B^\dagger B - A^\dagger A$, with eigenvalue m, and the $A^\dagger A$ eigenvalue n gives the dressed Landau levels energies.

We now obtain the energy spectrum of the edge excitations by evaluating the spectrum of (A.4) in the limit to the edge defined in section three, namely $|z| = r = R + x$, $R \to \infty$ with $m = L + m'$, $L = R^2$, $|m'| < \sqrt{L}$. The result is:

$$\epsilon_{n,m'}^{(2)} = 2n + vR + v\frac{m' + 2n + 1}{R} + O\left(\frac{m'^2}{R^2}\right) + \text{const.}, \qquad (A.5)$$

where the divergent term must be subtracted from the potential, $V \to V - vR = 2x + x^2/R$, to obtain a finite linear term.

The spectrum with other potentials $V \sim r^k/R^{k-1}$ is necessary to disentangle the contribution of the linear and quadratic terms in the spectrum $\epsilon_{n,m}^{(2)}$ and to evaluate the higher terms x^3/R^2, etc. . . . The Bogoliubov transformation does not apply to generic potentials, and we use another method that works in the relevant limit $R \to \infty$. Note that the angular momentum $J = b^\dagger b - a^\dagger a$ is a good quantum number for any potential and it takes very large values in this limit; this means that the expectation values of $b^\dagger b$ is of order

R^2. Remembering the case of Bose-Einstein condensation, we can treat the b operator as a classical variable, and write:

$$b \sim b^\dagger \sim \sqrt{b^\dagger b} = \sqrt{R^2 + m' + a^\dagger a} \simeq R\left(1 + \frac{m' + a^\dagger a}{2R^2}\right) \sim R + O\left(\frac{1}{R}\right). \qquad (A.6)$$

We use this approximation in the original Hamiltonian (A.1) and find the expression:

$$H^{(2)} = 2\left(1 + \frac{v}{R}\right)a^\dagger a + v\frac{m'}{R} + v\left(a^\dagger + a\right) + \text{const..} \qquad (A.7)$$

This result can be checked with the $R \to \infty$ limit of the Bogoliubov transformation (A.2, A.3). Note that the rotation angle ϕ_b is small:

$$\begin{cases} A \simeq a + \dfrac{v}{2R}b^\dagger, & (A.8) \\[2mm] B \simeq b + \dfrac{v}{2R}a^\dagger. & (A.9) \end{cases}$$

Substituting these expressions and the approximation (A.6) into the exact result (A.4), we reobtain the expression (A.7). Furthermore, the result (A.7) also agrees with the $R \to \infty$ limit of the exact matrix elements of the quadratic potential,

$$\langle i, R^2 + m'|\, V^{(2)}\, |j, R^2 + m'\rangle \simeq$$
$$v\left[\left(R + \frac{m' + 2i + 1}{R}\right)\delta_{i,j} + \sqrt{j+1}\delta_{i,j+1} + \sqrt{j}\delta_{i,j-1}\right], \quad (A.10)$$

that can be evaluated using the wave functions (1.4) and the help of Mathematica.

We now diagonalize the approximate $H^{(2)}$ (A.7) directly. We note that a shift of the operator a by a constant, setting

$$A = a + \frac{v}{2}\left(1 - \frac{v}{R}\right), \qquad (A.11)$$

reproduces the $R \to \infty$ limit of the Bogoliubov transformation (A.4). In conclusion, the spectrum (A.5) has been recovered by using directly the approximation (A.6) in the Hamiltonian $H^{(2)}$.

We extend the previous analysis to the cases of linear and quartic confining potentials, $V^{(1)} = v_1 r$ and $V^{(4)} = v_4 r^4/R^3$. In the linear case, the Hamiltonian is:

$$H^{(1)} = 2a^\dagger a + 1 + \frac{v_1}{R}\left(a^\dagger a + b^\dagger b + 1 + a^\dagger b^\dagger + ab\right)^{1/2}. \qquad (A.12)$$

We apply the large R limit and the approximation (A.6), subtract the infinite term and find:

$$H^{(1)} = 2a^\dagger a + \frac{v_1}{2}\left(a^\dagger + a\right) + \frac{v_1}{8R}\left(6a^\dagger a + 4m'\right) - \frac{v_1}{8R}\left(a^{\dagger 2} + a^2\right) + \text{const..} \qquad (A.13)$$

The calculation of the matrix elements of $V^{(1)}$ in the edge limit agrees with the previous result:

$$\langle i, R^2 + m'|\, V^{(1)}\, |j, R^2 + m'\rangle \simeq$$
$$v_1\left[\left(\frac{6i + 4m'}{8R} + R\right)\delta_{i,j} + \frac{v_1}{2}\left(\sqrt{i-1}\delta_{i-1,j} + \sqrt{i}\delta_{i,j-1}\right)\right.$$
$$\left. + \frac{v_1}{8R}\left(\sqrt{(j+2)(j+1)}\delta_{i,j+2} + \sqrt{j(j-1)}\delta_{i,j-2}\right)\right]. \qquad (A.14)$$

The equation (A.13) involves an additional term $\left(a^{\dagger 2} + a^2\right)$ w.r.t the quadratic case (A.7) corresponding to non-vanishing matrix elements on the third diagonal. After the shift by constant of the operator a, the Hamiltonian $H^{(1)} \sim A^\dagger A + \lambda \left(A^{\dagger 2} + A^2\right)$ can be diagonalized by a change of the oscillator frequency which turns out to be $O(1/R^2)$. The diagonal form of the Hamiltonian $H^{(1)}$ is finally,

$$H^{(1)} \simeq \left(2 + \frac{3v_1}{4R}\right) A^\dagger A + v_1 \frac{m'}{2R} + \text{const.}, \tag{A.15}$$

with spectrum:

$$\epsilon_{n,m'}^{(1)} = 2n + v_1 \left(\frac{m'}{2R} + \frac{3n}{4R}\right) + \text{const.}. \tag{A.16}$$

In the case of quartic potential, the approximated Hamiltonian can be written as follows:

$$H^{(4)} = 2a^\dagger a + 1 + \frac{v_4}{R} \left(6a^\dagger a + 2m'\right) + 2v_4 \left(a^\dagger + a\right) + \frac{v_4}{R} \left(a^{\dagger 2} + a^2\right) + \text{const.}, \tag{A.17}$$

in agreement with the matrix elements,

$$\langle i, R^2 + m' | V^{(4)} | j, R^2 + m' \rangle \simeq$$
$$v_4 \left[\frac{1}{R} \left(6i + 2m' + \text{const.}\right) \delta_{i,j} + 2\sqrt{j+1}\delta_{i,j+1} + 2\sqrt{j}\delta_{i,j-1} \right.$$
$$\left. + \frac{1}{R} \left(\sqrt{(j+1)(j+2)}\delta_{i,j+2} + \sqrt{j(j-1)}\delta_{i,j-2}\right) \right]. \tag{A.18}$$

We can diagonalized (A.17) by introducing once again a constant shift in operator a and the frequency redefinition, leading to the spectrum:

$$\epsilon_{n,m'}^{(4)} = 2n + v_4 \left(\frac{2m'}{R} + \frac{6n}{R}\right) + \text{const.}. \tag{A.19}$$

Now let us discuss the generic confining potential (2.24) for $r = R + x \to \infty$:

$$V(x; R) = a_1 x + \frac{a_2}{R} x^2 + \frac{a_3}{R^2} x^3 + \dots. \tag{A.20}$$

We are interested in the relativistic conformal spectrum at the edge (2.23), which is of order $O(1/R)$. We compare the spectrum of $V^{(2)}$, $V^{(1)}$ and $V^{(4)}$ computed in this limit and obtain the following consistent result for the spectrum:

$$\epsilon_{n,m'} = a_1 \left(\frac{m'}{2R} + \frac{3n}{4R}\right) + a_2 \frac{n}{2R} + \text{const.}. \tag{A.21}$$

This comparison shows that the higher terms x^3/R^2 that appear for example in $V^{(4)}$, do not contribute to leading order $O(1/R)$. This fact can also be checked by evaluating the corresponding matrix elements in the edge limit (2.13).

In conclusion, the relativistic conformal spectrum takes values from the linear and quadratic terms in (A.20).

Appendix B

Higher-order terms in the Moyal brackets

The second-order term $O(1/B^2)$ of the Moyal brackets (2.44) for the variation of the first Landau level density takes the form:

$$\delta\widetilde{\rho}^{(0)} = \frac{2i}{B^2}\left(\bar{\partial}^2\rho^{(0)}\right)\partial^2 w + h.c. \,. \tag{B.1}$$

Remembering that $\rho = \rho^{(0)}(r)$, we rewrite it as follows:

$$\delta\widetilde{\rho}^{(0)} = \frac{2i}{B^2}\left[\left(\frac{\partial}{\partial r^2}\right)^2\rho^{(0)}\right]\left(z^2\partial^2 - \bar{z}^2\bar{\partial}^2\right)w. \tag{B.2}$$

The action of the operator,

$$D_2 = z^2\partial^2 - \bar{z}^2\bar{\partial}^2, \tag{B.3}$$

on a generic polynomial $w \sim z^n\bar{z}^m$ is given by:

$$D_2 z^n\bar{z}^m = (n-m)(n+m-1)z^n\bar{z}^m. \tag{B.4}$$

The second-order correction (B.2) to the edge current modes (2.46) can be easily computed by integrating the density in space and by taking the edge limit (2.49); we find:

$$\delta\widetilde{\rho}_k^{(0)} = \frac{1}{R}\int dx\, xe^{-2x^2}\, iD_2 w(x,\theta), \qquad (B=2). \tag{B.5}$$

This expression is different from the leading contribution $\delta\rho_k^{(0)}$ in Eq.(2.50) for two reasons. The first is the order $O(1/R)$ that is subleading w.r.t. the $O(1)$ behaviour entering the conformal current algebra (1.42). The second aspect is that the dependence on the Fourier modes (B.5) given by the operator D_2 does not appear in the conformal operators ρ_k and L_κ discussed earlier (cf. (1.39), (1.40)). Actually, this spectrum is associated to a higher-spin conserved current of the conformal theory, the dimension-three current $\hat{V}^2(\eta)$, whose expression in the fermionic conformal theory is [67]

$$\hat{V}_0^2 = \frac{1}{R^2}\sum_r\left(r - \frac{1}{2}\right)^2 : \hat{d}_r^\dagger\hat{d}_r :, \tag{B.6}$$

(note the quadratic weight in the sum w.r.t. the linear one of $\hat{L}_0$ (1.39)). Actually, the action of $\hat{V}_0^2$ on a particle-hole excitation, $\hat{d}_n^\dagger \hat{d}_m |\Omega\rangle$ is readily found to reproduce the eigenvalue of D_2 in (B.4). The operator $\hat{V}_0^2$ naturally appears as a subleading $1/R^2$ term in the Hamiltonian (2.22) of the conformal theory on the cylinder and corresponds to a non-relativistic correction to the edge dynamics [67]. In summary, the second order term in the Moyal brackets represents a non-relativistic corrections to the conformal theory of edge excitations.

We remark that such a correction is expected to express another physical effect of the orbital spin s. The work [44] presented an analysis of the $1/B$ correction to the effective theory of section 2: it involves a spin-two hydrodynamic field in the bulk $b_k = b_{\mu k} dx^\mu$, where k is a space index, and a generalized action with coupling constant proportional to s. In analogy with the discussion in section 2, this action requires a boundary term that involves the edge theory: the corresponding contribution to $\hat{H}$ is expected to be given by (B.6).

In conclusion, the $O(1/B^2)$ term in the Moyal brackets describes a non-relativistic corrections to the conformal theory that is parameterized by the orbital spin. The complete analysis of this effect is left to future developments of this work. Let us mention the related approach [126] discussing the non-relativistic correction to the Hall conductivity due to the orbital spin.

A final remark concerns the relation between the $1/B$ series in the bulk and the $1/R$ expansion at the edge defined in section 3. To leading order in $1/B$, a finite limit is found for bulk quantities in the rescaled coordinate u, with $r = Ru \sim \sqrt{N}u$. For example, the limit of the ground-state density of Laughlin states is given by the step function,

$$\rho(\sqrt{N}u) = \frac{\nu B}{2\pi}\Theta(1 - u). \tag{B.7}$$

In this limit, the magnetic length is sent to zero, owing to $\ell^2 = 2/B$, and the edge region shrinks to a point. On the contrary, in the edge limit $R \to \infty$ the relevant features take place in the shell $x = r - R = O(\ell)$, where the wavefunctions have support and the Hermite polynomial expansion takes place. This region should be kept finite. Therefore, the $1/B$ approximation is not accurate enough for the analysis of edge excitations because it is too singular in that region.

In conclusion, we identified the first subleading term that is expressed by the spin-three conserved current [67] and parameterized by the orbital spin. Being observable in the conformal theory, such correction could give physical sense to s also for single-branch excitations. The bulk-boundary correspondence for subleading corrections will involve the study of the effective theory introduced in Ref.[44] within the multipole expansion of bulk excitations.

Appendix C

Peierls argument

We evaluate the Euclidean action of the loop model (4.13) on the configuration of a monopole with minimal magnetic charge $2\pi/q_0$:

$$F_{\mu\nu} = \frac{1}{2q_0}\varepsilon_{\mu\nu\rho}\frac{x_\rho}{|x|^3}\,. \tag{C.1}$$

The integral of the nonlocal term in (4.13) reads:

$$
\begin{aligned}
S &= \frac{g}{32\pi^3 q_0^2}\int \frac{d^3x_1}{|x_1|^3}\frac{d^3x_2}{|x_2|^3}\frac{(x_1\cdot x_2)}{|x_1 - x_2|^2}\\
&= \frac{g}{4\pi q_0^2}\int_0^\infty d\alpha \int_0^\infty dr_1 \int_0^\infty dr_2 \int_{-1}^1 dy\, y\, e^{-\alpha(r_1^2 + r_2^2 - 2r_1 r_2 y)}\,,
\end{aligned}
\tag{C.2}
$$

where we have used polar coordinates, exponentiated the denominator and introduced the variable $y = \cos(\theta_1 - \theta_2)$. Upon rescaling the radii, $s_i = r_i\sqrt{\alpha}$, $i = 1, 2$, the integral factorizes into a logarithmic divergent part and a finite part, namely the integrals over α and over the others variables.

We observe that being α conjugated to r^2, we can regularize the divergent contribution as follows:

$$\int_0^{+\infty}\frac{d\alpha}{\alpha} \quad \rightarrow \quad \int_{1/L^2}^{1/a^2}\frac{d\alpha}{\alpha} = 2\ln\left(\frac{L}{a}\right), \tag{C.3}$$

where α and L are the lattice constant and the system size respectively. On the other hand the finite part can be evaluated in polar coordinates $s_1 = s\cos(\eta)$, $s_2 = s\sin(\eta)$, leading to the result (4.15).

Appendix D

Loop-model determinant on $S^2 \times \mathbb{R}$

In this appendix we give some details concerning the calculation of the oscillator spectrum and determinant of the loop model reported in Section 4.2. The first step is the spectral decomposition of the $1/x^4$ kernel in the action (4.93).

D.0.1 Kernel decomposition

As a warming up, we determine the spectral form of the propagator of scalar fields,

$$\langle \phi(x_1)\phi(x_2) \rangle_{\mathbb{R}^3} = \frac{1}{|x_1 - x_2|}. \tag{D.1}$$

The conformal map from flat space $x^\mu = (r, \theta, \varphi)$ to the cylinder $\widetilde{x}^\alpha = (u, \theta, \varphi)$ is obtained by transforming the fields, $\widetilde{\phi} = e^{u/2R}\phi$, leading to:

$$\langle \widetilde{\phi}(\widetilde{x}_1)\widetilde{\phi}(\widetilde{x}_2) \rangle_{\mathbb{R} \times S^2} = \frac{e^{(u_1+u_2)/2R}}{|x_1 - x_2|}. \tag{D.2}$$

This expression can be expanded in terms of Legendre polynomials P_ℓ and spherical harmonics Y_ℓ^m, by using [127, 128]:

$$\frac{1}{|x_1 - x_2|} = \sum_{\ell=0}^{\infty} \frac{r_1^\ell}{r_2^{\ell+1}} P_\ell(\widehat{x}_1 \cdot \widehat{x}_2), \qquad x_i = r_i \widehat{x}_i, \ \ i = 1, 2, \ \ r_1 < r_2,$$

$$P_\ell(\widehat{x}_1 \cdot \widehat{x}_2) = \frac{4\pi}{2\ell+1} \sum_{m=-\ell}^{\ell} Y_\ell^{m*}(\theta_1, \varphi_1) Y_\ell^m(\theta_2, \varphi_2). \tag{D.3}$$

Introducing the Fourier modes $e^{i\omega u}$, we obtain the spectral decomposition:

$$\langle \widetilde{\phi}(x_1)\widetilde{\phi}(x_2) \rangle_{\mathbb{R} \times S^2} = 4\pi \int_{-\infty}^{\infty} d\omega \sum_{\ell=0}^{\infty} \sum_{m=-\ell}^{\ell} e^{i\omega(u_1-u_2)} Y_\ell^{m*}(\theta_1, \varphi_1) \, \lambda_{\omega,\ell} \, Y_\ell^m(\theta_2, \varphi_2),$$

$$\lambda_{\omega,\ell} = \frac{1}{(R\omega)^2 + (\ell + 1/2)^2}. \tag{D.4}$$

This spectrum confirms that the propagator is the inverse of the conformal Laplacian in $(2+1)$ dimensions, as reported in Table 1 for the conformal scalar theory.

Let us now apply the same procedure to the $1/x^4$ kernel. We use the identity,

$$\frac{1}{|x|^4} = \frac{1}{2|x|} \int_0^{\infty} dp \, p^2 \, e^{-p|x|}, \tag{D.5}$$

and the formula:

$$\frac{e^{-p|x_1-x_2|}}{|x_1-x_2|} = \sum_{\ell=0}^{\infty} \frac{(2\ell+1)}{\sqrt{r_1 r_2}} I_{\ell+\frac{1}{2}}(pr_1) K_{\ell+\frac{1}{2}}(pr_2) P_\ell(\widehat{x}_1 \cdot \widehat{x}_2), \qquad r_1 < r_2, \qquad \text{(D.6)}$$

where I_m and K_m are modified Bessel functions of the first and second kind, respectively. The integration over p of the Bessel functions leads to the Hypergeometric function $_2F_1$; the kernel with appropriated Weyl factors is then written:

$$\frac{e^{2(u_1+u_2)/R}}{|x_1-x_2|^4} = \frac{\sqrt{\pi}}{R^4} \sum_{\ell=0}^{\infty} e^{-|u|(\ell+2)/R} \frac{\Gamma(\ell+2)}{\Gamma(\ell+\frac{1}{2})} \, _2F_1\left(\frac{3}{2}, \ell+2, \ell+\frac{3}{2}; e^{-2|u|}\right) P_\ell(\widehat{x}_2 \cdot \widehat{x}_2),$$
$$\text{(D.7)}$$

where $u = u_1 - u_2$. Finally, the series expansion of the Hypergeometric function allows one to compute the Fourier modes, leading to the spectral decomposition (4.95) with eigenvalues (4.96):

$$\lambda_{\omega,\ell} = \sum_{k=0}^{\infty} \frac{2k+\ell+2}{(\omega R)^2 + (2k+\ell+2)^2} \frac{\Gamma(k+3/2)\Gamma(k+\ell+2)}{\Gamma(k+\ell+3/2)\Gamma(k+1)}. \qquad \text{(D.8)}$$

D.0.2   Field decomposition

The spin-one field on the cylinder $\widetilde{\zeta}$ is expanded in the basis of vector spherical harmonics Y_μ^{JLSM}, with $S=1$, that can be written in terms of scalar harmonics Y_L^m and constant vectors χ_μ^m by using the addition of angular momenta [128]:

$$\widetilde{\zeta}_\mu(\widetilde{x}) = \int \frac{d\omega}{2\pi} e^{i\omega u} \sum_{J=1}^{\infty} \sum_{L=J-1}^{J+1} \sum_{M=-J}^{J} \widetilde{\zeta}_{J,L,M}(\omega) \, Y_\mu^{JL1M}(\theta,\varphi),$$
$$\text{(D.9)}$$
$$Y_\mu^{JL1M}(\theta,\varphi) = \sum_{m=-L}^{L} \sum_{m'=-1}^{1} C_{L,1}(J,M,m,m') \, Y_L^m(\theta,\varphi) \, \chi_\mu^{m'},$$

where $C_{L,1}(J,M,m,m')$ are the Clebsh-Gordan coefficients with $M = m + m'$.

Upon substituting the previous expansions in the Euclidean action (4.93) and making use of orthonormality, we obtain:

$$S[\zeta] \propto \int \frac{d\omega}{2\pi} \sum_{L=0}^{\infty} \sum_{J=L-1}^{L+1} \sum_{M=-J}^{J} \left|\widetilde{\zeta}_{J,L,M}(\omega)\right|^2 \lambda_{\omega,L}, \qquad \text{(D.10)}$$

where $\widetilde{\zeta}_{-1,L,M}(\omega) = 0$. The eigenvalues $\lambda_{\omega,L}$ (D.8) of the scalar kernel (D.7) only depends on the orbital momentum and reduce the summations in (D.10) to a single one over $L = 0, 1, \ldots$, with multiplicities $\delta(L)$. The gauge condition $\partial^\mu \zeta_\mu = 0$ imposes $\widetilde{\zeta}_{L,L,M}(\omega) = 0$, and one finds,

$$\delta(L) = 2(2L+1). \qquad \text{(D.11)}$$

D.0.3   Resummation and regularization

The sum over k in the eigenvalues $\lambda_{\omega,\ell}$ (D.8) is regularized by subtracting the asymptotic $k \to \infty$ limit of the summand, equal to $1/2$:

$$I(\ell) = \sum_{k=0}^{\infty} \left[\frac{(\ell+2+2k)}{a^2 + (\ell+2+2k)^2} \frac{\Gamma(\ell+2+k)\Gamma(k+3/2)}{\Gamma(\ell+3/2+k)\Gamma(k+1)} - \frac{1}{2} \right], \qquad \text{(D.12)}$$

where $a = \omega R$. The series (D.12) can be summed by using the Sommerfeld-Watson method and the result is expressed in terms of two finite products for even and odd ℓ values, respectively:

$$I(\ell) = \frac{\ell+1}{4} - \begin{cases} \dfrac{\pi a}{8} \displaystyle\prod_{i=0}^{(\ell-1)/2} \dfrac{(2i+1)^2 + a^2}{(2i)^2 + a^2} \tanh\left(\dfrac{a\pi}{2}\right), & \ell = 1, 3, \ldots, \\[2em] \dfrac{\pi(1+a^2)}{8a} \displaystyle\prod_{i=0}^{\ell/2} \dfrac{(2i)^2 + a^2}{(2i-1)^2 + a^2} \coth\left(\dfrac{a\pi}{2}\right), & \ell = 0, 2, \ldots. \end{cases} \tag{D.13}$$

Both products are rewritten as a ratio of complex gamma functions squared, leading to the regularized eigenvalues,

$$\lambda_{\omega,\ell}^{reg} = I(\ell) - \frac{\ell+1}{4} = -\frac{\pi}{4} \left| \frac{\Gamma((\ell+2+i\omega R)/2)}{\Gamma((\ell+1+i\omega R)/2)} \right|^2, \tag{D.14}$$

reported in (4.97). For compact time β, the Fourier modes are discretized, $\omega R = n/\tau$, with $\tau = \beta/(2\pi R)$, $n \in \mathbb{Z}$.

Next, the infinite-product representation of the gamma function [129],

$$\frac{\Gamma(a+ib)}{\Gamma(a)} = e^{-i\gamma b} \left(1 + i\frac{b}{a}\right)^{-1} \prod_{k=1}^{\infty} e^{ib/k} \left(1 + i\frac{b}{a+k}\right)^{-1}, \qquad a, b \in \mathbb{R}, \tag{D.15}$$

is used to rewrite the product of eigenvalues occurring in the determinant. Dropping inessential τ-independent factors, we obtain the expression:

$$\begin{aligned} \sum_{n,\ell} \delta(\ell) \log\left(\lambda_{n,\ell}^{reg}\right) &= \sum_{n\in\mathbb{Z}} \sum_{\ell,k=0}^{\infty} \delta(\ell) \log\left[\frac{n^2 + \tau^2(\ell+2k+1)^2}{n^2 + \tau^2(\ell+2k+2)^2}\right] \\ &= \sum_{n\in\mathbb{Z}} \sum_{L=0}^{\infty} 2L \log\left(n^2 + \tau^2 L^2\right). \end{aligned} \tag{D.16}$$

The sums in this expression simplify because the indices ℓ and k come in the combination $L = \ell + 2k$. The resulting sum over n, L, with multiplicity $\delta(L) = 2L$, can now be analytically continued by using the zeta-function method, as described in the main text.

Bibliography

[1] Andrea Cappelli and Lorenzo Maffi. Bulk-boundary correspondence in the quantum hall effect. *Journal of Physics A: Mathematical and Theoretical*, 51(36):365401, Jul 2018.

[2] Francesco Andreucci, Andrea Cappelli, and Lorenzo Maffi. Quantization of a self-dual conformal theory in $(2+1)$ dimensions. *Journal of High Energy Physics*, 2020(2), Feb 2020.

[3] Andrea Cappelli and Lorenzo Maffi. W-infinity symmetry in quantum hall effect beyond the edge approximation. *under writing*, 2021.

[4] Andrea Cappelli, Lorenzo Maffi, and Satoshi Okuda. Critical ising model in varying dimension by conformal bootstrap. *Journal of High Energy Physics*, 2019(1), Jan 2019.

[5] Horst L. Stormer, Daniel C. Tsui, and Arthur C. Gossard. The fractional quantum hall effect. *Rev. Mod. Phys.*, 71:S298–S305, Mar 1999.

[6] Frank Wilczek, editor. *Fractional statistics and anyon superconductivity*. 1990.

[7] Frank Wilczek. Magnetic flux, angular momentum, and statistics. *Phys. Rev. Lett.*, 48:1144–1146, Apr 1982.

[8] R. E. Prange and S. M. Girvin. *The Quantum Hall Effect*. Springer, Berlin, 1990.

[9] X. G. Wen. *Quantum field theory of many-body systems: From the origin of sound to an origin of light and electrons*. 2004.

[10] Eduardo Fradkin. *Field Theories of Condensed Matter Physics*. Cambridge University Press, 2 edition, 2013.

[11] J. K. Jain. Composite fermion approach for the fractional quantum Hall effect. *Phys. Rev. Lett.*, 63:199–202, 1989.

[12] R. de Picciotto, M. Reznikov, M. Heiblum, V. Umansky, G. Bunin, and D. Mahalu. Direct observation of a fractional charge. *Nature*, 389:162–164, 1997.

[13] L. Saminadayar, D. C. Glattli, Y. Jin, and B. Etienne. Observation of the e/3 Fractionally Charged Laughlin Quasiparticle. *Phys. Rev. Lett.*, 79:2526–2529, 1997.

[14] Bertrand I. Halperin, Ady Stern, Izhar Neder, and Bernd Rosenow. Theory of the Fabry-Pérot quantum Hall interferometer. *Phys. Rev.*, B83:5440–5457, 2011.

[15] B. I. Halperin. Quantized Hall conductance, current carrying edge states, and the existence of extended states in a two-dimensional disordered potential. *Phys. Rev.*, B25:2185–2190, 1982.

[16] Andrea Cappelli, Gerald V. Dunne, Carlo A. Trugenberger, and Guillermo R. Zemba. Conformal symmetry and universal properties of quantum Hall states. *Nucl. Phys.*, B398:531–567, 1993.

[17] P. Di Francesco, P. Mathieu, and D. Senechal. *Conformal Field Theory*. Graduate Texts in Contemporary Physics. Springer-Verlag, New York, 1997.

[18] Paul H. Ginsparg. APPLIED CONFORMAL FIELD THEORY. In *Les Houches Summer School in Theoretical Physics: Fields, Strings, Critical Phenomena Les Houches, France, June 28-August 5, 1988*, pages 1–168, 1988.

[19] Michael Stone. Edge Waves in the Quantum Hall Effect. *Annals Phys.*, 207:38–52, 1991.

[20] Jr. Callan, Curtis G. and Jeffrey A. Harvey. Anomalies and Fermion Zero Modes on Strings and Domain Walls. *Nucl. Phys. B*, 250:427–436, 1985.

[21] M. Nakahara. *Geometry, topology and physics*. 2003.

[22] D. J. Thouless, M. Kohmoto, M. P. Nightingale, and M. den Nijs. Quantized Hall Conductance in a Two-Dimensional Periodic Potential. *Phys. Rev. Lett.*, 49:405–408, 1982.

[23] R. B. Laughlin. Quantized Hall conductivity in two-dimensions. *Phys. Rev.*, B23:5632–5733, 1981.

[24] Edward Witten. Quantum Field Theory and the Jones Polynomial. *Commun. Math. Phys.*, 121:351–399, 1989.

[25] R. Floreanini and R. Jackiw. Self-dual fields as charge-density solitons. *Phys. Rev. Lett.*, 59:1873–1876, Oct 1987.

[26] Paul H. Ginsparg. APPLICATIONS OF TOPOLOGICAL AND DIFFERENTIAL GEOMETRIC METHODS TO ANOMALIES IN QUANTUM FIELD THEORY. In *XVI GIFT International Seminar on Theoretical Physics: New Perspectives in Quantum Field Theory Jaca (Huesca), Spain, June 3-8, 1985*, 1985.

[27] Andrea Cappelli and Guillermo R. Zemba. Modular invariant partition functions in the quantum hall effect. *Nuclear Physics B*, 490(3):595–632, Apr 1997.

[28] Gregory W. Moore and N. Read. Nonabelions in the fractional quantum Hall effect. *Nucl. Phys.*, B360:362–396, 1991.

[29] Andrea Cappelli. Composite fermion wavefunctions derived by conformal field theory. *Journal of Physics A: Mathematical and Theoretical*, 46(1):012001, Dec 2012.

[30] M. Hermanns, J. Suorsa, E. J. Bergholtz, T. H. Hansson, and A. Karlhede. Quantum hall wave functions on the torus. *Physical Review B*, 77(12), Mar 2008.

[31] Michael B. Green, John H. Schwarz, and Edward Witten. *Superstring Theory Vol. 1,2*. Cambridge University Press, 2012.

[32] L. D. Landau and E. M. Lifshitz. *Theory of Elasticity*, volume 7 of *Course of Theoretical Physics*. Elsevier Butterworth-Heinemann, New York, 1986.

[33] J. E. Avron, R. Seiler, and P. G. Zograf. Viscosity of quantum Hall fluids. *Phys. Rev. Lett.*, 75:697–700, 1995.

[34] N. Read and E. H. Rezayi. Hall viscosity, orbital spin, and geometry: paired superfluids and quantum Hall systems. *Phys. Rev.*, B84:085316, 2011.

[35] F. D. M. Haldane. "hall viscosity" and intrinsic metric of incompressible fractional hall fluids, 2009.

[36] X. G. Wen and A. Zee. Shift and spin vector: New topological quantum numbers for the Hall fluids. *Phys. Rev. Lett.*, 69:953–956, 1992. [Erratum: Phys. Rev. Lett.69,3000(1992)].

[37] Alexander G. Abanov and Andrey Gromov. Electromagnetic and gravitational responses of two-dimensional noninteracting electrons in a background magnetic field. *Phys. Rev.*, B90(1):014435, 2014.

[38] Andrey Gromov and Alexander G. Abanov. Density-curvature response and gravitational anomaly. *Phys. Rev. Lett.*, 113:266802, Dec 2014.

[39] Barry Bradlyn and N. Read. Topological central charge from berry curvature: Gravitational anomalies in trial wave functions for topological phases. *Phys. Rev. B*, 91:165306, Apr 2015.

[40] T. Can, Y. H. Chiu, M. Laskin, and P. Wiegmann. Emergent conformal symmetry and geometric transport properties of quantum hall states on singular surfaces. *Phys. Rev. Lett.*, 117:266803, Dec 2016.

[41] S. Klevtsov and P. Wiegmann. Geometric adiabatic transport in quantum hall states. *Phys. Rev. Lett.*, 115:086801, Aug 2015.

[42] P. B. Wiegmann. Hydrodynamics of euler incompressible fluid and the fractional quantum hall effect. *Phys. Rev. B*, 88:241305, Dec 2013.

[43] Paul Wiegmann and Alexander G. Abanov. Anomalous hydrodynamics of two-dimensional vortex fluids. *Phys. Rev. Lett.*, 113:034501, Jul 2014.

[44] Andrea Cappelli and Enrico Randellini. Multipole Expansion in the Quantum Hall Effect. *JHEP*, 03:105, 2016.

[45] Andrey Gromov, Scott D. Geraedts, and Barry Bradlyn. Investigating anisotropic quantum hall states with bimetric geometry. *Phys. Rev. Lett.*, 119:146602, Oct 2017.

[46] Andrey Gromov and Dam Thanh Son. Bimetric theory of fractional quantum hall states. *Phys. Rev. X*, 7:041032, Nov 2017.

[47] J. Frohlich and U. M. Studer. Gauge invariance and current algebra in nonrelativistic many body theory. *Rev. Mod. Phys.*, 65:733–802, 1993.

[48] Alexander G. Abanov and Andrey Gromov. Electromagnetic and gravitational responses of two-dimensional noninteracting electrons in a background magnetic field. *Phys. Rev. B*, 90(1):014435, 2014.

[49] Carlos Hoyos and Dam Thanh Son. Hall Viscosity and Electromagnetic Response. *Phys. Rev. Lett.*, 108:066805, 2012.

[50] N. Read. Non-Abelian adiabatic statistics and Hall viscosity in quantum Hall states and p(x) + ip(y) paired superfluids. *Phys. Rev.*, B79:045308, 2009.

[51] F. D. M. Haldane. Geometrical description of the fractional quantum hall effect. *Phys. Rev. Lett.*, 107:116801, Sep 2011.

[52] Barry Bradlyn, Moshe Goldstein, and N. Read. Kubo formulas for viscosity: Hall viscosity, ward identities, and the relation with conductivity. *Phys. Rev. B*, 86:245309, Dec 2012.

[53] Michael Stone. Gravitational Anomalies and Thermal Hall effect in Topological Insulators. *Phys. Rev.*, B85:184503, 2012.

[54] Andrea Cappelli, Marina Huerta, and Guillermo R. Zemba. Thermal transport in chiral conformal theories and hierarchical quantum Hall states. *Nucl. Phys.*, B636:568–582, 2002.

[55] Andrey Gromov and Alexander G. Abanov. Thermal hall effect and geometry with torsion. *Phys. Rev. Lett.*, 114:016802, Jan 2015.

[56] N. Read and Dmitry Green. Paired states of fermions in two-dimensions with breaking of parity and time reversal symmetries, and the fractional quantum Hall effect. *Phys. Rev.*, B61:10267, 2000.

[57] Luis Alvarez-Gaume and Edward Witten. Gravitational Anomalies. *Nucl. Phys.*, B234:269, 1984.

[58] Andrey Gromov, Kristan Jensen, and Alexander G. Abanov. Boundary effective action for quantum Hall states. *Phys. Rev. Lett.*, 116(12):126802, 2016.

[59] Gerald V. Dunne. Edge asymptotics of planar electron densities. *Int. J. Mod. Phys.*, B8:1625, 1994.

[60] Hiroo Azuma. W(infinity) algebra in the integer quantum Hall effects. *Prog. Theor. Phys.*, 92:293–308, 1994.

[61] Andrea Cappelli, Enrico Randellini, and Jacopo Sisti. Three-dimensional topological insulators and bosonization. *Journal of High Energy Physics*, 2017(5), May 2017.

[62] Andrea Cappelli, Carlo A. Trugenberger, and Guillermo R. Zemba. Infinite symmetry in the quantum Hall effect. *Nucl. Phys.*, B396:465–490, 1993.

[63] Satoshi Iso, Dimitra Karabali, and B. Sakita. Fermions in the lowest landau level. bosonization, w algebra, droplets, chiral bosons. *Physics Letters B*, 296(1):143 – 150, 1992.

[64] Satoshi Iso, Dimitra Karabali, and B. Sakita. One-dimensional fermions as two-dimensional droplets via chern-simons theory. *Nuclear Physics B*, 388(3):700 – 714, 1992.

[65] Andrea Cappelli, Carlo A. Trugenberger, and Guillermo R. Zemba. Large N limit in the quantum Hall Effect. *Phys. Lett.*, B306:100–107, 1993.

[66] S. M. Girvin, A. H. MacDonald, and P. M. Platzman. Magneto-roton theory of collective excitations in the fractional quantum hall effect. *Phys. Rev. B*, 33:2481–2494, Feb 1986.

[67] Andrea Cappelli, Carlo A. Trugenberger, and Guillermo R. Zemba. W(1+infinity) dynamics of edge excitations in the quantum Hall effect. *Annals Phys.*, 246:86–120, 1996.

[68] A. Cappelli, Carlo A. Trugenberger, and G. R. Zemba. W(1+infinity) minimal models and the hierarchy of the quantum Hall effect. *Nucl. Phys. Proc. Suppl.*, 45A:112–119, 1996. [Lect. Notes Phys.469,249(1996)].

[69] Roni Ilan, Eytan Grosfeld, and Ady Stern. Coulomb blockade as a probe for non-abelian statistics in read-rezayi states. *Phys. Rev. Lett.*, 100:086803, Feb 2008.

[70] Andrea Cappelli, Lachezar S Georgiev, and Guillermo R Zemba. Coulomb blockade in hierarchical quantum hall droplets. *Journal of Physics A: Mathematical and Theoretical*, 42(22):222001, may 2009.

[71] Oded Agam, Eldad Bettelheim, P. Wiegmann, and A. Zabrodin. Viscous fingering and the shape of an electronic droplet in the quantum hall regime. *Phys. Rev. Lett.*, 88:236801, May 2002.

[72] Siavash Golkar, Dung Xuan Nguyen, Matthew M. Roberts, and Dam Thanh Son. Higher-spin theory of the magnetorotons. *Physical Review Letters*, 117(21), Nov 2016.

[73] Alexander Altland and Martin R. Zirnbauer. Nonstandard symmetry classes in meso-scopic normal-superconducting hybrid structures. *Phys. Rev. B*, 55:1142–1161, Jan 1997.

[74] Alexei Kitaev, Vladimir Lebedev, and Mikhail Feigel'man. Periodic table for topological insulators and superconductors. *AIP Conference Proceedings*, 2009.

[75] Andreas P. Schnyder, Shinsei Ryu, Akira Furusaki, Andreas W. W. Ludwig, Vladimir Lebedev, and Mikhail Feigel'man. Classification of topological insulators and super-conductors. *AIP Conference Proceedings*, 2009.

[76] Shinsei Ryu, Andreas P Schnyder, Akira Furusaki, and Andreas W W Ludwig. Topological insulators and superconductors: tenfold way and dimensional hierarchy. *New Journal of Physics*, 12(6):065010, Jun 2010.

[77] Ching-Kai Chiu, Jeffrey C.Y. Teo, Andreas P. Schnyder, and Shinsei Ryu. Classification of topological quantum matter with symmetries. *Reviews of Modern Physics*, 88(3), Aug 2016.

[78] Qian Niu, D. J. Thouless, and Yong-Shi Wu. QUANTIZED HALL CONDUCTANCE AS A TOPOLOGICAL INVARIANT. *Phys. Rev.*, B31:3372–3377, 1985.

[79] Liang Fu and C. L. Kane. Time reversal polarization and az2adiabatic spin pump. *Physical Review B*, 74(19), Nov 2006.

[80] Liang Fu, C. L. Kane, and E. J. Mele. Topological insulators in three dimensions. *Physical Review Letters*, 98(10), Mar 2007.

[81] Michael Levin and Ady Stern. Fractional topological insulators. *Physical Review Letters*, 103(19), Nov 2009.

[82] Yuan-Ming Lu and Ashvin Vishwanath. Theory and classification of interacting integer topological phases in two dimensions: A chern-simons approach. *Physical Review B*, 86(12), Sep 2012.

[83] J. E. Moore and L. Balents. Topological invariants of time-reversal-invariant band structures. *Physical Review B*, 75(12), Mar 2007.

[84] Rahul Roy. Z2classification of quantum spin hall systems: An approach using time-reversal invariance. *Physical Review B*, 79(19), May 2009.

[85] R. Jackiw and S. Templeton. How Superrenormalizable Interactions Cure their Infrared Divergences. *Phys. Rev. D*, 23:2291, 1981.

[86] A. N. Redlich. Parity violation and gauge noninvariance of the effective gauge field action in three dimensions. *Phys. Rev. D*, 29:2366–2374, May 1984.

[87] A. J. Niemi and G. W. Semenoff. Axial-anomaly-induced fermion fractionization and effective gauge-theory actions in odd-dimensional space-times. *Phys. Rev. Lett.*, 51:2077–2080, Dec 1983.

[88] S. Deser, L. Griguolo, and D. Seminara. Effective qed actions: Representations, gauge invariance, anomalies, and mass expansions. *Physical Review D*, 57(12):7444–7459, Jun 1998.

[89] Heinrich-Gregor Zirnstein and Bernd Rosenow. Cancellation of quantum anomalies and bosonization of three-dimensional time-reversal symmetric topological insulators. *Physical Review B*, 88(8), Aug 2013.

[90] Edward Witten. Fermion path integrals and topological phases. *Reviews of Modern Physics*, 88(3), Jul 2016.

[91] T. Xia, D. Qian, D. Hsieh, L. Wray, A. Pal, H. Lin, A. Bansil, D. Grauer, Y. S. Hor, R. J. Cava, and M. Z. Hasan. Observation of a large-gap topological-insulator class with a single dirac cone on the surface. *Nature Physics*, 5:398–402, May 2009.

[92] D. Hsieh, D. Qian, L. Wray, Y. Xia, Y. S. Hor, R. J. Cava, and M. Z. Hasan. A topological dirac insulator in a quantum spin hall phase. *Nature*, 452(7190):970–974, Apr 2008.

[93] M. Z. Hasan and C. L. Kane. Colloquium: Topological insulators. *Reviews of Modern Physics*, 82(4):3045–3067, Nov 2010.

[94] R. Jackiw and C. Rebbi. Solitons with fermion number $\frac{1}{2}$. *Phys. Rev. D*, 13:3398–3409, Jun 1976.

[95] Xiao-Liang Qi, Taylor L. Hughes, and Shou-Cheng Zhang. Topological field theory of time-reversal invariant insulators. *Physical Review B*, 78(19), Nov 2008.

[96] Yang Xu, Ireneusz Miotkowski, Chang Liu, Jifa Tian, Hyoungdo Nam, Nasser Alidoust, Jiuning Hu, Chih-Kang Shih, M. Zahid Hasan, and Yong P. Chen. Observation of topological surface state quantum hall effect in an intrinsic three-dimensional topological insulator. *Nature Physics*, 10(12):956–963, Nov 2014.

[97] Gil Young Cho and Joel E. Moore. Topological bf field theory description of topological insulators. *Annals of Physics*, 326(6):1515–1535, Jun 2011.

[98] AtMa Chan, Taylor L. Hughes, Shinsei Ryu, and Eduardo Fradkin. Effective field theories for topological insulators by functional bosonization. *Physical Review B*, 87(8), Feb 2013.

[99] AtMa P. O. Chan, Thomas Kvorning, Shinsei Ryu, and Eduardo Fradkin. Effective hydrodynamic field theory and condensation picture of topological insulators. *Physical Review B*, 93(15), Apr 2016.

[100] A Amoretti, A Blasi, N Maggiore, and N Magnoli. Three-dimensional dynamics of four-dimensional topological BF theory with boundary. *New Journal of Physics*, 14(11):113014, nov 2012.

[101] Peng Ye, Meng Cheng, and Eduardo Fradkin. Fractional s -duality, classification of fractional topological insulators, and surface topological order. *Physical Review B*, 96(8), Aug 2017.

[102] Mario Bergeron, Gordon W. Semenoff, and Richard J. Szabo. Canonical bf-type topological field theory and fractional statistics of strings. *Nuclear Physics B*, 437(3):695–721, Mar 1995.

[103] Chang-Tse Hsieh, Gil Young Cho, and Shinsei Ryu. Global anomalies on the surface of fermionic symmetry-protected topological phases in (3+1) dimensions. *Physical Review B*, 93(7), Feb 2016.

[104] Xiao Chen, Apoorv Tiwari, and Shinsei Ryu. Bulk-boundary correspondence in (3+1)-dimensional topological phases. *Physical Review B*, 94(4), Jul 2016.

[105] E.C. Marino. Quantum electrodynamics of particles on a plane and the chern-simons theory. *Nuclear Physics B*, 408(3):551–564, 1993.

[106] Wei-Han Hsiao and Dam Thanh Son. Duality and universal transport in mixed-dimension electrodynamics. *Physical Review B*, 96(7), Aug 2017.

[107] Wei-Han Hsiao and Dam Thanh Son. Self-dual =1 bosonic quantum hall state in mixed-dimensional qed. *Physical Review B*, 100(23), Dec 2019.

[108] Scott D. Geraedts and Olexei I. Motrunich. Line of continuous phase transitions in a three-dimensional u(1) loop model with1/r2current-current interactions. *Physical Review B*, 85(14), Apr 2012.

[109] Max A. Metlitski and Ashvin Vishwanath. Particle-vortex duality of two-dimensional dirac fermion from electric-magnetic duality of three-dimensional topological insulators. *Physical Review B*, 93(24), Jun 2016.

[110] Eduardo Fradkin and Steven Kivelson. Modular invariance, self-duality and the phase transition between quantum hall plateaus. *Nuclear Physics B*, 474(3):543–574, Sep 1996.

[111] Hart Goldman and Eduardo Fradkin. Loop models, modular invariance, and three-dimensional bosonization. *Physical Review B*, 97(19), May 2018.

[112] John B. Kogut. An introduction to lattice gauge theory and spin systems. *Rev. Mod. Phys.*, 51:659–713, Oct 1979.

[113] A.M. Polyakov. Quark confinement and topology of gauge theories. *Nuclear Physics B*, 120(3):429 – 458, 1977.

[114] Alexander M. Polyakov. Fermi-Bose Transmutations Induced by Gauge Fields. *Mod. Phys. Lett. A*, 3:325, 1988.

[115] Eduardo Fradkin and Fidel A. Schaposnik. The fermion-boson mapping in three-dimensional quantum field theory. *Physics Letters B*, 338(2-3):253–258, Oct 1994.

[116] Nathan Seiberg, T. Senthil, Chong Wang, and Edward Witten. A duality web in 2+1 dimensions and condensed matter physics. *Annals of Physics*, 374:395–433, Nov 2016.

[117] Andreas Karch, Brandon Robinson, and David Tong. More abelian dualities in 2 + 1 dimensions. *Journal of High Energy Physics*, 2017(1), Jan 2017.

[118] T. Senthil, Dam Thanh Son, Chong Wang, and Cenke Xu. Duality between (2+1)d quantum critical points. *Physics Reports*, 827:1–48, Sep 2019.

[119] Turner Carl. Dualities in 2+1 dimensions. *Proceedings of XIV Modave Summer School in Mathematical Physics — PoS(Modave 2018)*, Jul 2019.

[120] Andreas Karch and David Tong. Particle-vortex duality from 3d bosonization. *Physical Review X*, 6(3), Sep 2016.

[121] Edward Witten. On S duality in Abelian gauge theory. *Selecta Math.*, 1:383, 1995.

[122] David Dudal, Ana Júlia Mizher, and Pablo Pais. Exact quantum scale invariance of three-dimensional reduced qed theories. *Physical Review D*, 99(4), Feb 2019.

[123] Andrea Cappelli and Antoine Coste. On the Stress Tensor of Conformal Field Theories in Higher Dimensions. *Nucl. Phys. B*, 314:707–740, 1989.

[124] Andrea Cappelli and Giuseppe D'Appollonio. On the trace anomaly as a measure of degrees of freedom. *Physics Letters B*, 487(1-2):87–95, Aug 2000.

[125] Eduardo C. Marino. *Quantum Field Theory Approach to Condensed Matter Physics.* Cambridge University Press, 2017.

[126] Sergej Moroz, Carlos Hoyos, and Leo Radzihovsky. Galilean invariance at quantum hall edge. *Phys. Rev. B*, 91:195409, May 2015.

[127] A. Messiah. *Quantum Mechanics Vol. I.* Dover Publ., 2014.

[128] J. M. Blatt and V. F. Weisskpof. *Theoretical Nuclear Physics.* Dover Publ., 2010.

[129] *Higher Transcendental Functions, Vol.I.* McGraw-Hill Book Company, 1953.